

Montclair State University

Montclair State University Digital Commons


Theses, Dissertations and Culminating Projects

1-2017

Investigation of Hsp90 Structure-Activity Relationships in Epigallocatechin Gallate

Arpita Patel

Follow this and additional works at: <https://digitalcommons.montclair.edu/etd>

 Part of the [Chemistry Commons](#)

Montclair State University

/ Investigation of Hsp90 structure-activity relationships in epigallocatechin gallate /

By

Arpita Patel

A Master's Thesis Submitted to the Faculty of

The College of Science and Mathematics

Montclair State University

In Partial Fulfillment of the Requirements

For the Degree of

Master of Science in Chemistry

January 2017

College: College of Science and Mathematics Thesis Committee:

Department: Chemistry and Biochemistry

Thesis Sponsor: David P. Rotella

Committee Member: David W. Konas

Committee Member: John Siekierka

Abstract:

(-)-Epigallocatechin gallate (EGCG) is a polyphenolic natural product that inhibits the key chaperone protein Hsp90 by binding to the carboxy terminal portion of the protein.

The natural product has modest activity as an Hsp90 inhibitor and there is little information in the literature on structure activity relationships for EGCG analogs.

Previous studies from this laboratory provided initial data on the effect of a limited range of changes associated with functional groups, substituents and stereochemistry. The focus of this research is to explore these initial results in more detail with a focus on the synthesis of EGCG analogs with more drug like features.

Investigation of Hsp90 structure-activity relationships in epigallocatechin gallate

A Thesis

Submitted in partial fulfillment of the requirement

For the degree of Master of Science in Chemistry

By

Arpita Patel

Montclair State University

Montclair, NJ

2017

Table of Contents

Section	Page
Introduction	3
Chemistry	11
Result and discussion	18
Experimental section	20
References	39
Spectral Analysis	42

Introduction

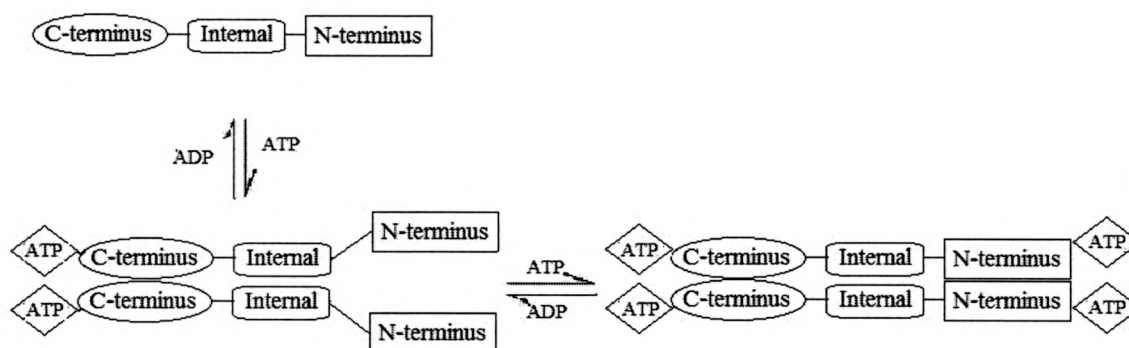
Heat shock proteins (Hsps) are proteins that act as chaperones to help regulate the structure and function of other proteins. HSPs are ubiquitously present in normal conditions in cells and produced excessively in response to stress. ^(1,2) This stress can be heat, cold, radiation, infection, inflammation, starvation, etc. ⁽³⁾ Hsps are also upregulated in transformed (cancer) cells. This may actually help the tumor cells survive regardless of any mutations the cell may have gone through. ⁽¹⁾

Hsp90 is the most abundant heat shock protein in cells. Hsp90 plays a crucial role in assembly, maturation, and degradation of many proteins in the body. The proteins that depend on Hsp90 for their functionality are referred to as client proteins. Client proteins of Hsp90 include SRC family kinases, receptor tyrosine kinases, serine/threonine kinases, cell cycle G2 checkpoint kinases, mutant fusion kinases, steroid hormone receptors, transcription factors, etc. ⁽¹⁻⁴⁾ Many of these client proteins are associated with various cancers and neurodegenerative diseases (Alzheimer's, Huntington's, and Parkinson's), infectious diseases. ^(5, 6)

There are four isoforms of Hsp90. Hsp90 α and Hsp90 β are cytosolic, Grp94 is found localized in the endoplasmic reticulum, and TRAP1 is found in mitochondria. ⁽⁷⁾ The cytosolic forms are mainly responsible for maintaining the activity, assembly, disposition and turnover of Hsp90 dependent proteins/ client proteins in the cytosol. Sidera and colleagues reported that isoforms Hsp90 α and Hsp90 β are also found on cell surface. Surface forms of Hsp90 are associated with migration of cancer cells to sites other than its origin. ⁽⁴⁾ Additionally, each of the isoforms have targeted functions.

Therefore, isoform specific inhibition may result in specific biological effects. There have been a number of studies looking into isoform specific inhibition. ⁽⁵⁾

Figure 1: Structure of Hsp90 and Hsp90 dimerization through ATP binding.



Hsp90 is a dimer (as shown in Figure 1) with each monomer made up of three regions: an N-terminal domain, a middle domain/internal domain, and C-terminal domain. Each domain is associated with ATP binding directly. The C-terminal domain controls Hsp90 dimerization necessary for functions of the protein. The C-terminus can also serve as co-chaperone interaction site. ATP binding in the N-terminal region provides the energy necessary for the interaction between Hsp90 and its client proteins as well as the energy to promote dimerization. The middle domain contains sites where substrate and co-chaperones can bind as well as ATP binding site. ^(3,5) Hsp90 inhibitors targeting each of the regions are being investigated. Most of inhibitors bind the N-terminus, some target the C-terminus, and a few target the internal region. They are discussed in more detail in a review article by Bhat and colleagues. ⁽⁵⁾

Hsp90 and its association with cancer

Hsp90 is over expressed in solid tumors and hematologic cancers. Hsp90 interacts with many oncoproteins such as Akt, BCR-ABL, EGFR, Raf-1, p53, VEGFR, HER2/ErbB2, Src, Cdk4, Cdk6, and cyclin D. ⁽²⁾ These oncoproteins are directly or indirectly linked to all six hallmarks of cancers: 1. evasion of apoptosis, 2. sustained angiogenesis, 3. limitless replicative potential, 4. tissue invasion and metastasis, 5. self sufficiency in growth signals, and 6. insensitivity to anti-growth signals. Hsp90 allows cancer cells to survive and escape apoptosis in hostile and stressful environments, thus allowing cancer cells to grow in their mutated forms. Inhibition of Hsp90 function leads to degradation of client proteins which can disrupt the survival and growth of cancerous cells. Hence, Hsp90 inhibitors can potentially be effective anti-cancer agents. ⁽³⁾

Hsp90 inhibitors

As a result of the key role Hsp90 plays in cell growth and division and cellular survival, Hsp90 inhibitors have been subject of interest in medicinal chemistry for almost 2 decades. Although there are no Hsp90 inhibitors approved for clinical use, many of them are and have been in clinical trials. A comprehensive review of Hsp90 inhibitors by Bhat and colleagues in 2014 provides a recent update on clinical and preclinical research. ⁽⁵⁾

Hsp90 inhibitors that are currently being investigated can be categorized as ⁽⁵⁾:

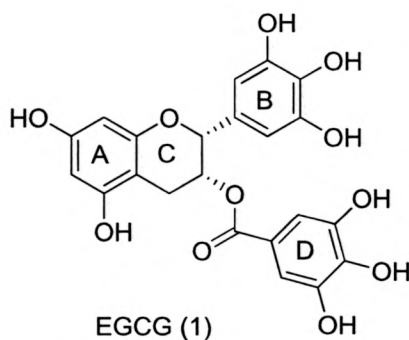
1. N-terminal inhibitors

- Natural products and derivatives (benzoquinone, radicicol)
- Synthetic small molecules and peptide derivatives
 - Purine based Inhibitors

- Isoxazole and triazole derivatives
 - Isoform selective inhibitors
2. Allosteric modulation of Hsp 90 : inhibits client proteins from binding Hsp90
 3. C-terminal inhibitors
 - Novobiocin and analogs
 - EGCG and analogs

This research project is focused on synthesis of novel EGCG derivatives. The following paragraphs provide useful background information and summarize what is known about structure activity relationships for Hsp90 inhibition in EGCG and analogs.

Figure 2: Structure of EGCG

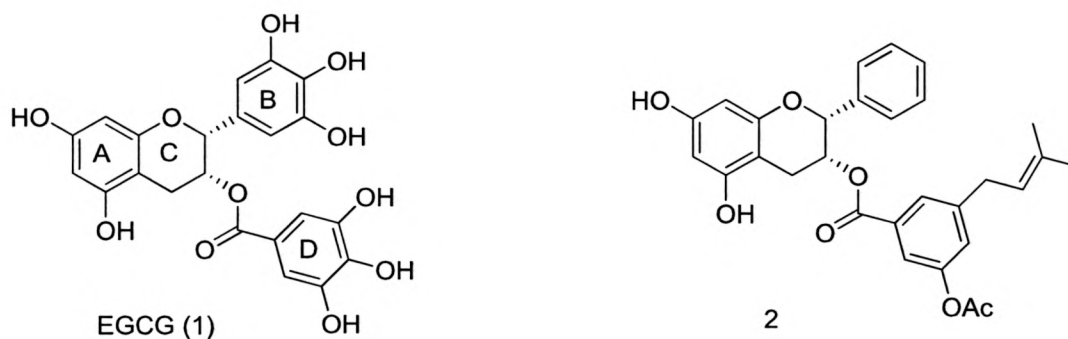


(-)-Epigallocatechin gallate (EGCG) is the most abundant polyphenol/flavanoid found in green tea. It has been the subject of wide ranging investigations related to potential utility in the treatment of inflammatory diseases, cancer, viral and neurological conditions.^(8,9) The potential of EGCG as an Hsp90 inhibitor and its mode of action by binding to the C-terminus were first reported by Gasiewicz and coworkers in 2009.⁽¹⁰⁾ Inhibition of Hsp90 leads to degradation of its client proteins; leading to downstream

signaling inhibition, and loss of client protein function.⁽⁵⁾ The precise binding site on Hsp90 for EGCG is not known however the region in the C terminus has been localized to amino acids 538-728 on Hsp90.⁽¹¹⁾

EGCG has multiple structural features that contribute to unsatisfactory drug like properties. Multiple phenolic hydroxyl groups contribute to oxidative and chemical instability in solution as well as metabolic instability. These hydroxyl groups also significantly increase the polarity of EGCG that can reduce cell permeability and oral absorption. The ester moiety is labile to hydrolysis by plasma esterases.⁽⁸⁾ As a result of these issues, our interest is focused on investigating structural modifications to EGCG that will improve one or more of these characteristics, while at the same time improving the affinity of the molecule for Hsp90. Previous work from Dr. Brian Blagg's research group and our laboratory reported initial studies toward this objective.^(5, 11)

Figure 3: EGCG (1) and EGCG analog (2) (Khandewal and coworkers)

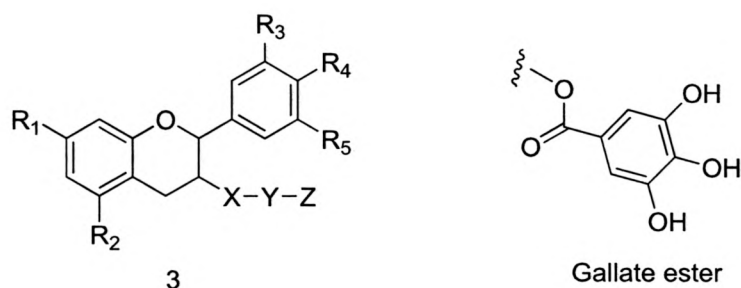


Structure activity studies on EGCG have been done on methylation and deletion of phenolic hydroxyl moieties. A study by Khandewal and group that investigated the activity of EGCG analogs against breast cancer cells showed that A-ring (shown in

Figure 3) hydroxyl groups are required and elimination of B-ring (Figure 3) hydroxyl groups can be advantageous for anti-cancer activity. Removing all hydroxyl group on the C-ring, and replacing them with different R groups in compound 2 (IC_{50} 4 μ M) improved activity by 18 fold compared to EGCG (IC_{50} 74 μ M) when tested against MCF-7 breast cancer cell lines. ⁽¹¹⁾

Previous studies on Hsp90 inhibition SAR of EGCG analogs done by our research group is summarized in Table 1. Comparison of the activity of 1 (EGCG, IC_{50} 155 μ M) to 3d (amide, IC_{50} 75 μ M) and 3e (sulfonamide, IC_{50} 44 μ M) shows that replacing the ester in EGCG with other functional groups can improve Hsp90 inhibition. These moieties are less likely to be hydrolytically cleaved which may improve compound stability. Furthermore, a number of derivatives lacking one or more phenolic hydroxyl groups including 3b (IC_{50} 24 μ M), 3h (IC_{50} 63 μ M), and 3i (IC_{50} 35 μ M) show improved potency compared to EGCG. Fluoro substitution as in 3c (IC_{50} 41 μ M) also gives more potent Hsp90 inhibition, compared to EGCG. The activity of 3a (trans, IC_{50} 34 μ M) was improved compared to EGCG suggesting that trans-orientation of substituents on the pyran ring may also improve Hsp90 inhibition. The aromatic D ring can be replaced by cyclohexane as shown in 3f (IC_{50} 81 μ M) and 3g (IC_{50} 155 μ M) to increase potency as an Hsp90 inhibitor. ⁽⁵⁾

Table 1: Summary of SAR of EGCG analogs for HSP90 inhibition by Bhat and colleagues.



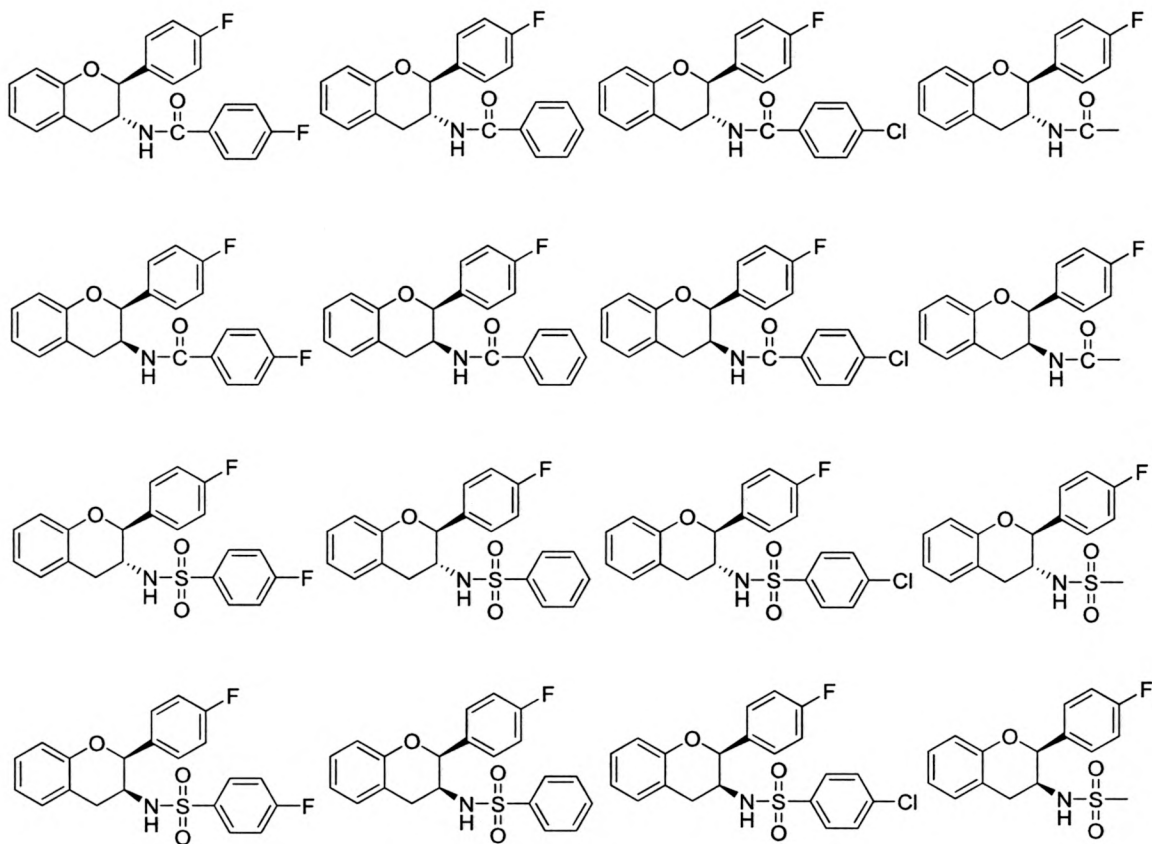
#	Cis/ trans ^a	R ₁	R ₂	R ₃	R ₄	R ₅	X	Y	Z	IC ₅₀ (μM)
1	Cis	OH	OH	OH	OH	OH	O	C=O	Gallate	155
3a	Trans	OH	OH	OH	OH	OH	O	C=O	Gallate	34
3b	Cis	OH	OH	OH	OH	OH	O	C=O	Phenyl	24
3c	Cis	OH	OH	OH	OH	OH	O	C=O	4-F-Phenyl	41
3d	Cis	OH	OH	OH	OH	OH	N	C=O	Phenyl	75
3e	Cis	OH	OH	OH	OH	OH	N	SO ₂	Phenyl	44
3f	Cis	OH	OH	OH	OH	H	O	C=O	Cyclohexane	81
3g	Cis	OH	OH	OH	OH	H	O	C=O	4-F-cyclohexane	65
3h	Cis	OH	OH	H	H	H	O	C=O	Phenyl	63
3i	Cis	H	H	H	H	H	O	C=O	Gallate	35

^a B ring/ X absolute stereochemistry for 3a-3g; and relative stereochemistry for 3h-3i

The design of new targets for this research project was based on the observations summarized above. New EGCG analogs were synthesized in which the metabolically labile ester was replaced with amide or sulfonamide, all the phenolic hydroxyl groups were removed and/or replaced by fluorine or chlorine. The D-ring was also replaced with small aliphatic methyl group in few compounds. To investigate the effect of

stereochemistry on Hsp90 inhibition, cis and trans isomers of each molecule were synthesized. All of the target molecules are shown in Figure 4.

Figure 4: All target molecules



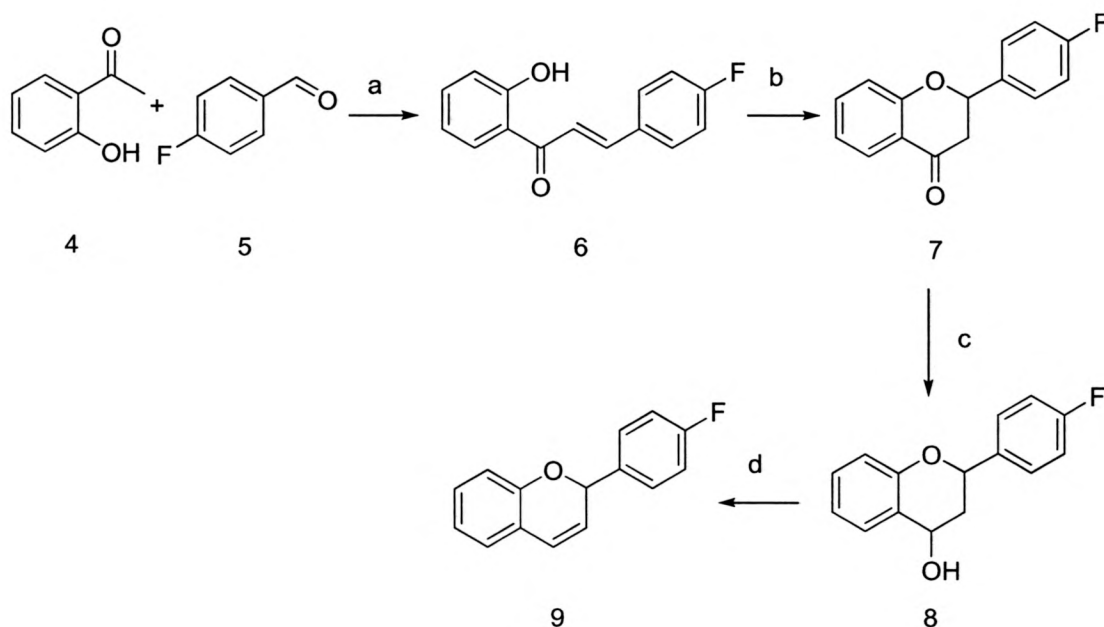
hydroxyl groups on A ring and B ring and D ring (refer to Figure 2 to see compound **1**), replacing the para hydroxyl group on B ring with fluorine, replacing ester group linking C and D ring with amides and sulfonamides, and adding halogen groups on D ring or substituting D-ring with a small aliphatic group (methyl). This sequence will also permit us to investigate the role of stereochemistry (cis/trans on the chromene ring) in potential Hsp90 inhibitor.

Amide and sulfonamide target molecules will be prepared from the corresponding amine. As indicated in Figure 4, three different routes can be investigated to the key amine (trans **19** or cis **20**). One begins with aldol condensation of ketone **4** and aldehyde **5** followed by ring closure and dehydration to furnish olefin **9**. An alternative route to **9** begins with vinyl bromide **12** and tosyl hydrazone **15**. Each of these can furnish hydroxyl chroman **9a** that can be converted to amine (**19** or **20**) by displacement or reductive amination. The third approach employs a condensation reaction between vinyl nitro compound **16** and salicaldehyde **5** to lead to nitro chromene **17**. This intermediate can be reduced to furnish key amine (**19** or **20**).

Synthesis

Route 1

Scheme 1: Reagents and conditions: a) NaOH, EtOH, rt, 24hrs; b) KF, MeOH, reflux, o/n; c) NaBH₄, EtOH, rt, 2hrs; d) R-SO₃Cl, Base*. (*The conditions for this step are described in Table 2 in more detail)



The EGCG analogs for this research were prepared synthetically. The first step was to prepare the bicyclic chromene ring system. A base catalyzed Claisen-Schmidt condensation reaction between 2-hydroxyacetophenone (5) and 4-fluorobenzaldehyde 4 in ethanol was used to synthesize chalcone 6. Attempt to make chromene 9 from 6 using NaBH₄ in different solvent systems failed. Therefore, an alternative route (shown in route 1 scheme) was chosen to synthesize chromene 9. Using KF as catalyst, 6 was isomerized/cyclized to 7 in methanol. Ketone in 7 was reduced to alcohol in 8 using NaBH₄ in ethanol.⁽¹²⁾

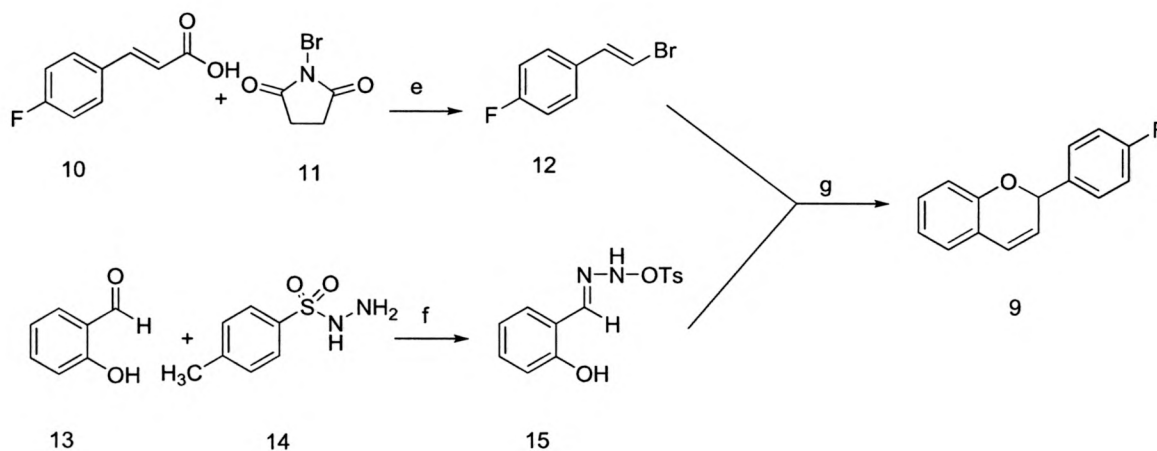
Table 2: Different reaction conditions to synthesize **9** from **8**

Trial	Base	R-SO ₂ Cl	Temperature	Time	Yield (%)
1	Et ₃ N	Me	Rt	4 hrs	16
2	Et ₃ N	Me	40°C	o/n	11
3	Diisopropylethylamine	Me	Rt	o/n	2
4	Diisopropylethylamine	Me	40°C	o/n	2.5
5	Et ₃ N	Me	Rt	o/n	6.5
6	DBU	p-toluene	Rt	3days	6

Dehydration/elimination of **8** was carried out using base and methanesulfonyl chloride. Different bases such as triethylamine, diisopropylethylamine and morpholine were investigated to optimize this reaction. However, the yield in each instance was unacceptably low. Therefore, this approach to synthesis of EGCG analogs was dropped.

Route 2

Scheme 2: Reagents and conditions: e) Mn(OAc)₂·4H₂O, H₂O:ACN, rt, 2hrs; f) MeOH, reflux, 2 hrs; g) Pd₂(dba)₃·CHCl₃, PCy₃HBF₄, K₂CO₃, Anhydrous dioxane, 100°C, o/n

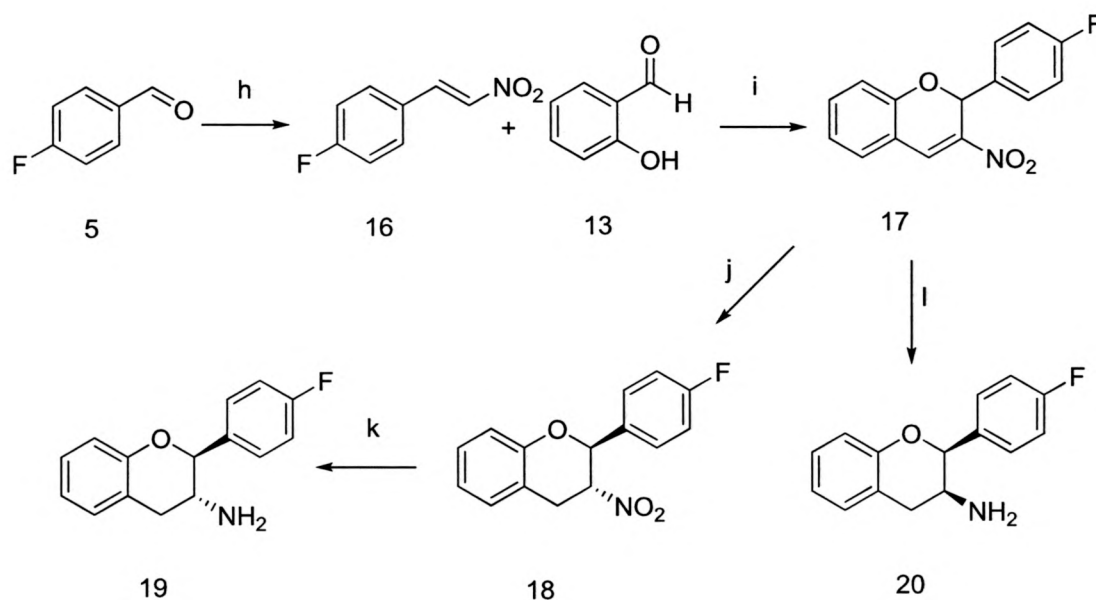


In an alternative approach to obtain chromene **9**, we needed to synthesize **12** and **15**. Hunsdiecker reaction with triethyl amine as a catalyst, 4-fluoro cinnamic acid **10** and N-bromosuccinamide **11** as starting material was not successful.⁽¹³⁾ An alternative approach that employed manganese acetate hydrate with the same starting materials furnished **12** via bromodecarboxylation.⁽¹⁴⁾ Nucleophilic addition of tosyl group from 4-methylbenzenesulfonylhydrazide **14** to salicylaldehyde **13** in methanol leads to synthesis of **15**.⁽¹⁵⁾ Palladium catalyzed coupling reaction between **12** and **15** was used to synthesize **9**.⁽¹⁶⁾ This method afforded an improved yield (52%) of chromene **9** compared to route 1. However, the reaction also produced a number of side products and the catalyst required is expensive. Therefore, this method was also eliminated.

Route 3

In another approach, base catalyzed Michael addition was used to synthesize **16** from 4-fluorobenzaldehyde **5** and nitromethane.⁽¹⁷⁾ This is similar to aldol addition. Cyclocondensation followed by Oxa-Michael addition between **16** and salicylaldehyde (**13**) was used to synthesize **17**. 4-Nitrobenzoic acid and pyrrolidine were used as catalysts.⁽¹⁸⁾ The olefin in **17** was easily reduced using NaBH₄ in methanol to form **18**.⁽¹⁹⁾ The nitro group in **18** was selectively reduced to trans amine **19** using activated Zn.⁽²⁰⁾ Synthesis of cis amine **20** was carried out using diborane in THF and sodium borohydride.⁽²¹⁾ Each of these reductions was highly stereocontrolled to provide the desired isomer in good yield. Both, cis and trans, amines were synthesized as a racemic mixture of diastereomers, since they were synthesized from non-chiral starting materials. Thus, all the compounds synthesized using these two amines acquire relative stereochemistry rather than absolute stereochemistry.

Scheme 3a: Reagents and conditions: h) I. MeNO₂, aq. NaOH, MeOH, 0°C, 1 hr; II. aq. HCl, 0°C, 10 mins; i) I. 4-nitrobenzoic acid, pyrrolidine, MeOH, rt, 1 hr; II. reflux, o/n; j) NaBH₄, THF:MeOH, 0°C, 2 hr; k) I. activated Zn, 1M HCl:IPA, 60°C, 2 hrs; II. NaHCO₃, rt, 10 mins; l) BH₃:THF, NaBH₄, 0°C- 70°C, o/n



We confirmed the stereochemistry of each amine by comparing the resonance signals and coupling constants for the methine proton alpha to the amine. The proton NMR of **19** (trans amine) shows a trans diaxial coupling constant of 8.6 Hz with the adjacent proton at alpha position to phenyl. For **20** (cis amine), the coupling constant of the same proton is 1.9 Hz, which is evident of axial-equatorial coupling. These coupling constants are consistent with the literature values for the coupling constants for similar cis and trans compounds.⁽²²⁾ Additionally, the axial proton (alpha to amine) in trans amine shows up more upfield (at 3.15 ppm) compared to the equatorial proton (alpha to amine, shows up at 3.43 ppm).

Scheme 3b: Reagents and conditions: m) R-COOH, EDCI.HCl, DMAP, DCM, rt, o/n;
n) R-SO₂Cl, Et₃NH₂, DCM, rt, o/n

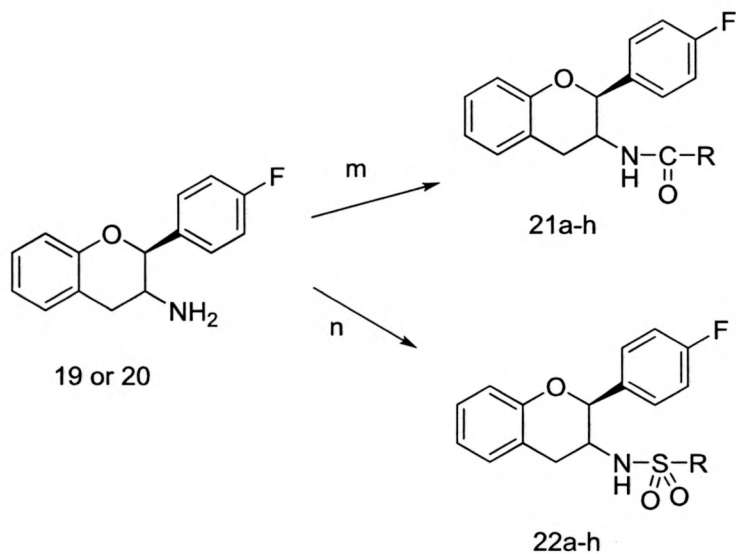
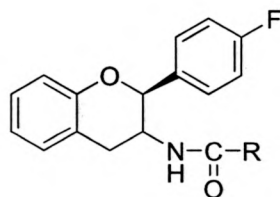


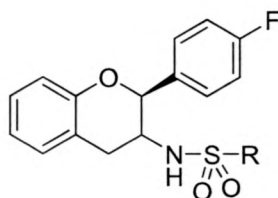
Table 3: List of amides



Compound	Stereochemistry	R	% yield
21a	Trans	4-F Phenyl	68
21b	Trans	Phenyl	66
21c	Trans	CH ₃	73
21d	Trans	4-Cl Phenyl	83
21e	Cis	4-F Phenyl	75
21f	Cis	Phenyl	56
21g	Cis	CH ₃	62
21h	Cis	4-Cl Phenyl	85

The final step is a simple coupling reaction between amine and carboxylic acid, and amine and sulfonyl chloride. Amine and carboxylic acid coupling forms amides; and amine and sulfonyl chloride coupling makes sulfonamides. All the amides and sulfonamides that were synthesized are listed in Table 3 and Table 4 respectively.

Table 4: List of sulfonamides



Compound	Stereochemistry	R	% yield
22a	Trans	4-F Phenyl	87
22b	Trans	Phenyl	52
22c	Trans	Methyl	84
22d	Trans	4-Cl Phenyl	55
22e	Cis	4-F Phenyl	72
22f	Cis	Phenyl	82
22g	Cis	Methyl	72
22h	Cis	4-Cl Phenyl	76

Results and discussion:

The synthesis of EGCG analogs (21a-h and 22a-h) with structural modifications are described in scheme 3. Selected compounds (21a, 21b, 21e, 21f, 22a, and 22e) were sent to Dr. Brian Blagg's research group at the University of Kansas to be tested for Hsp90 inhibition using standard luciferase based readout.⁽²³⁾ These compounds were

tested at concentration of 10 μ M for inhibition of Hsp90-dependent firefly luciferase refolding in PC3 cells. Preliminary results of this assay are shown in the table below. IC₅₀s values are still pending.

Table 5: Summary of the activity of the compounds tested for Hsp90 activity.

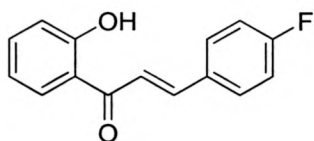
Compound	Cis/trans	Amide/ Sulfonamide	R	% refolded
21a	Trans	A	4-F Phenyl	42
21e	Cis	A	4-F Phenyl	110
22a	Trans	S	4-F Phenyl	24
22e	Cis	S	4-F Phenyl	76
21b	Trans	A	Phenyl	64
21f	Cis	A	Phenyl	97

As shown in table 5, compound 21a shows greater Hsp90 inhibition (42%) compared to 21e (110%) which indicates that compounds with trans stereochemistry shows higher inhibition compared than cis compounds. Similarly, while comparing 22a (trans, 24%) versus 22e (cis, 76%) and 21b (trans, 64%) versus 21f (cis, 97%), one can see the trend of trans molecule having higher activity. Furthermore, sulfonamide compounds 22a (24%) and 22e (76%) exhibit better Hsp90 inhibition compared to their amide analogs 21a (42%) and 21e (110%). In a very limited manner, we investigated substituent effects in the phenyl ring in which fluoro substitution was compared to hydrogen. There is insufficient information to draw a conclusion or identify trends from the compounds evaluated in this study.

Experimental section:

All reactions were monitored using thin layer chromatography using silica gel and were visualized using ultraviolet light. All extractions were performed 3 times with appropriate amounts of solvents. All reaction products were analyzed using ^1H and/or ^{13}C NMR which were obtained using a 300 MHz or 400 MHz Bruker spectrometer. All NMR samples were prepared in CDCl_3 unless stated otherwise; chemical shifts are reported in ppm. Final compounds were analyzed using Shimadzu LCMS 2020 and Acquity UPLC. Shimadzu LCMS 2020 used Shimadzu C_{18} $3\mu\text{m}$, 4.6×50 mm column, water and methanol as solvents (50% water-50% Methanol to 90% Methanol-10% water in 5 minutes) at flow rate of 0.5 mL/min, and detection wavelength 220 and 254 nm. Aquity UPLC used Acquity UPLC BEH C_8 $1.7\mu\text{m}$, 2.1×100 mm column, water and acetonitrile as solvents (90% water-10% acetonitrile to 90% acetonitrile-10% water in 6 minutes) at flow rate 0.4 mL/min, and detection wavelength 254 nm (or 230 nm when mentioned). All target compounds (amides and sulfonamides) showed at least > 97% purity by NMR and UPLC analysis.

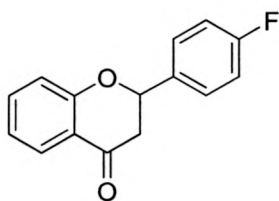
Route 1



6

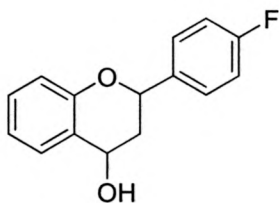
6: NaOH (7.34g, 4eq) solution (solid dissolved in 10 mL of water) was gradually added to the mixture of 2-hydroxyacetophenone **4** (10g, 1 eq) and 4-fluorobenzaldehyde **5** (9.97g, 1.1 eq) in ethanol (150 ml) at room temperature and stirred at room temperature

overnight. The reaction mixture was poured over ice to crystallize the product. 1M HCl was added to this mixture. Precipitated product was filtered and solid product was dissolved in dichloromethane, washed with brine and dried over sodium sulfate. Solvent was removed from the product by rotary evaporation; and product was purified using flash column chromatography (0-20% ethyl acetate in hexanes) to afford a yellow solid. (15.1g, 85% yield) ^1H NMR (300 MHz, CDCl_3) δ 12.80 (s, 1H), 7.96 – 7.85 (m, 2H), 7.71 – 7.64 (m, 2H), 7.60 (d, J = 15.5 Hz, 1H), 7.52 (ddd, J = 8.6, 7.2, 1.7 Hz, 1H), 7.19 – 7.10 (m, 2H), 7.05 (dd, J = 8.4, 1.2 Hz, 1H), 6.96 (ddd, J = 8.3, 7.2, 1.2 Hz, 1H).



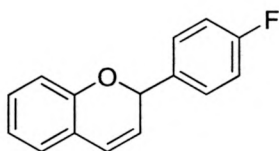
7

7: **6** (10g, 1eq) was dissolved in methanol (150 mL) with heating. KF (1.2g, 0.5 eq) was added to the mixture and the mixture was refluxed overnight. Reaction mixture was concentrated and dissolved in ethyl acetate then was washed with brine and dried over sodium sulfate.⁽¹²⁾ The light yellow solid obtained following removal of solvent by rotary evaporation was used without further purification (9.7g, 97% yield). ^1H NMR (300 MHz, CDCl_3) δ 7.98 – 7.91 (m, 1H), 7.57 – 7.45 (m, 3H), 7.14 (ddt, J = 8.7, 6.6, 2.5 Hz, 2H), 7.11 – 7.04 (m, 2H), 5.48 (dd, J = 13.2, 3.0 Hz, 1H), 3.08 (dd, J = 16.9, 13.2 Hz, 1H), 2.89 (dd, J = 16.8, 3.0 Hz, 1H); ^{13}C NMR (75 MHz, CDCl_3) δ 191.77, 164.49, 161.42, 161.21, 136.32, 134.64, 134.60, 128.12, 128.01, 127.12, 121.80, 120.92, 118.12, 115.99, 115.70, 78.96, 44.71.



8

8: NaBH₄ (1.46g, 2 eq) was added to **7** (4.7g, 1 eq) dissolved in EtOH (100 mL) at 0° C. Reaction mixture was brought to room temperature and stirred for 2 hours. 10 mL of acetone was added to the reaction mixture over 30 minutes period (2 ml at a time) to quench excess NaBH₄. The reaction mixture was concentrated and dissolved in distilled water. This solution was extracted with ethyl acetate. The collected organic extract was washed with brine and dried over sodium sulfate. The solvent was removed by rotary evaporation to provide an off white solid. ⁽¹²⁾ (4.7g, 97 % yield). ¹H NMR (300 MHz CDCl₃) δ 7.54 (dt, *J* = 7.7, 1.4 Hz, 1H), 7.48 – 7.40 (m, 2H), 7.26 – 7.19 (m, 1H), 7.14 – 7.07 (m, 2H), 7.01 (td, *J* = 7.5, 1.3 Hz, 1H), 6.90 (dd, *J* = 8.3, 1.2 Hz, 1H), 5.22 – 5.08 (m, 2H), 2.52 (ddd, *J* = 13.1, 6.3, 2.0 Hz, 1H), 2.13 (ddd, *J* = 13.1, 11.7, 10.5 Hz, 1H).

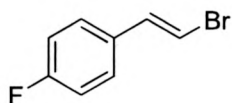


9

9: **8** (0.1g, 1 eq) was dissolved in dichloromethane (3ml) and the base (3 eq) was added to the mixture. Reaction mixture was cooled down to 0° C. Sulfonyl chloride (1.2 eq) was added to the mixture at 0° C. Reaction mixture was brought back to room temperature or 40° C (see the table 2 for clarification) and stirred. Reaction mixture was washed with ammonium chloride solution to remove excess base. Collected organic layer was diluted in distilled water. This solution was washed with brine and dried over sodium sulfate.

Organic layer was concentrated and purified using flash column chromatography (0-20 % ethyl acetate in hexanes) to afford a clear liquid. (See Table 2 for yields). ^1H NMR (300 MHz, CDCl_3) δ 7.44 (ddd, $J = 8.7, 4.9, 2.2$ Hz, 2H), 7.17 – 7.12 (m, 1H), 7.12 – 7.01 (m, 4H), 6.93 – 6.85 (m, 1H), 6.78 (dt, $J = 8.3, 1.0$ Hz, 1H), 6.57 (ddd, $J = 9.9, 1.9, 0.8$ Hz, 1H), 5.91 (dd, $J = 3.5, 1.9$ Hz, 1H), 5.79 (dt, $J = 9.9, 2.8$ Hz, 1H).

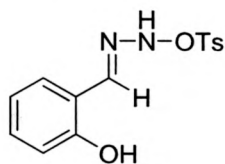
Route 2



12

12: N-Bromosuccinimide **11** (0.187g, 1.05eq) and manganese (II) acetate (0.049g, 0.2 eq) were added to 4-fluorocinnamic acid **10** (0.166g, 1 eq) in water (3 mL) and acetonitrile (3 mL) solvent mixture. Reaction mixture was stirred at room temperature for 2 hours.

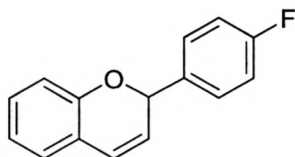
Reaction mixture was diluted in excess distilled water; and the product was extracted in ethyl acetate. The collected organic layer was washed with brine and dried over sodium sulfate. The organic layer was concentrated (using rotary evaporation); and product was purified using flash column chromatography (0-40% ethyl acetate in hexane) to afford an off white powder. ⁽¹⁴⁾ (0.129g, 64% yield). ^1H NMR (300 MHz, CDCl_3) δ 7.33 – 7.23 (m, 2H), 7.12 – 6.98 (m, 3H), 6.75 – 6.66 (m, 1H).



15

15: 4-methanebenzenesulfonylhydrazone **14** (1.22g, 1 eq) was added to salicylaldehyde **13** (1.86g, 1eq) in methanol (50 mL). Reaction mixture was refluxed for 2 hours. The

solvent was removed by rotary evaporation, and the product was washed with dichloromethane and hexanes to remove methanol from the product. All solvents were removed using rotary evaporation to afford a white solid.⁽¹⁵⁾ (2.72g, 94%). ¹H NMR (300 MHz, DMSO-*d*₆) δ 11.45 (s, 1H), 10.19 (s, 1H), 8.16 (s, 1H), 7.77 – 7.70 (m, 2H), 7.48 – 7.38 (m, 3H), 7.22 (ddd, *J* = 8.4, 7.3, 1.8 Hz, 1H), 6.87 – 6.78 (m, 2H), 2.35 (s, 3H).

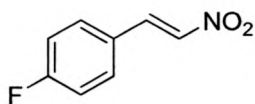


9

9: Pd₂(dba)₃·CHCl₃ (0.093g, 2.5%), PCy₃·HBF₄ (0.198g, 15%), K₂CO₃ (1.49g, 3eq) and **15** (2.08g, 2 eq) were added to an oven dried flask under anhydrous conditions.

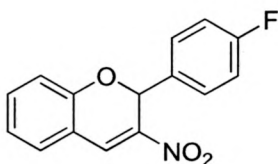
Anhydrous dioxane (10 mL) was added to the mixture. Then, **12** (0.72g, 1eq) was added to the reaction mixture. Reaction mixture was heated at 100°C and stirred overnight under anhydrous conditions. Reaction mixture was cooled to room temperature and filtered through diatomaceous earth to remove all solid side products and reagents including Pd catalyst. Reaction mixture was concentrated and then diluted in ethyl acetate. Reaction mixture was washed with water and then extracted in ethyl acetate. The collected organic layer was washed with brine and dried over sodium sulfate. The organic layer was concentrated; and flash column chromatography (0-20% ethyl acetate in hexanes) was used to purify the product to a thick cloudy orange liquid.⁽¹⁶⁾ (0.42g, 52%) ¹H NMR (400 MHz, CDCl₃) δ 7.48 – 7.43 (m, 2H), 7.14 (td, *J* = 7.7, 1.7 Hz, 1H), 7.10 – 7.03 (m, 3H), 6.90 (td, *J* = 7.4, 1.1 Hz, 1H), 6.80 (dd, *J* = 8.1, 1.1 Hz, 1H), 6.58 (dd, *J* = 9.9, 1.9 Hz, 1H), 5.92 (dd, *J* = 3.4, 1.9 Hz, 1H), 5.80 (dd, *J* = 9.8, 3.4 Hz, 1H).

Route 3



16

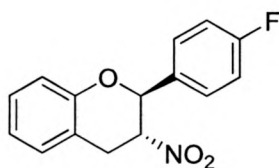
16: NaOH (7.5g, 2.5eq), dissolved in small amount of water, was gradually added to the mixture of 4-Fluorobenzaldehyde **5** (9.16g, 1 eq) and nitromethane (11.44g, 2.5 eq) in methanol (120 mL) at 0° C. Reaction mixture was stirred at 0° C for 1.5 hours. Some crushed ice was added to the mixture. Then, the reaction mixture was poured over vigorously stirring 5M HCL (100 mL) solution at 0° C. Off white colored solid product precipitates in the solution as the mixture is stirred for few minutes. Precipitated product was vacuum filtered and washed with distilled water. The product was air dried to afford an off white powder. ⁽¹⁷⁾ (5.96g, 65%). ¹H NMR (400 MHz CDCl₃) δ 7.99 (dd, *J* = 14.3, 4.9 Hz, 1H), 7.62 – 7.51 (m, 3H), 7.17 (tq, *J* = 8.2, 2.7 Hz, 2H); ¹³C NMR (101 MHz, CDCl₃) δ 166.21, 163.67, 137.85, 136.86, 131.36, 131.27, 126.35, 126.31, 116.90, 116.68.



17

17: **16**(1.67g, 0.95 eq) was added to a solution mixture of 4 nitrobenzoic acid (0.44g, 0.25 eq) and pyrrolidine (0.185g, 0.25 eq) in chloroform (20 mL) at room temperature. This mixture was stirred at room temperature for 1 hour. Then, salicylaldehyde (1.28g, 1eq) was added to the reaction mixture and the reaction mixture was refluxed overnight. Reaction mixture was cooled down to room temperature and diluted in distilled water. Product was extracted in chloroform. The collected organic layer was washed with brine

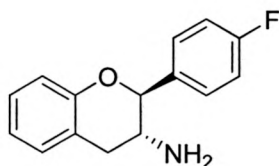
and dried over anhydrous sodium sulfate. Dry organic layer was concentrated (using rotary evaporation) and purified using flash column chromatography (0-20% ethyl acetate in hexanes) to afford a yellow solid. ⁽¹⁸⁾ (2.47g, 90%) ¹H NMR (400 MHz, CDCl₃) δ 8.08 (d, *J* = 0.9 Hz, 1H), 7.42 – 7.31 (m, 4H), 7.06 – 6.98 (m, 3H), 6.90 – 6.85 (m, 1H), 6.57 (s, 1H); ¹³C NMR (101 MHz, CDCl₃) δ 164.53, 162.05, 153.32, 141.06, 134.45, 132.76, 132.74, 130.48, 129.35, 129.04, 128.97, 122.70, 117.83, 117.31, 115.98, 115.76, 73.57.



18

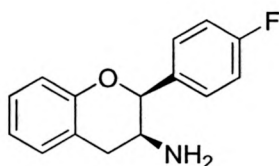
18: **17** (2.35g, 1eq) was dissolved in methanol (25 mL) and THF (15 mL) and cooled down to 0°C. NaBH₄ (0.49g, 1.5 eq) was gradually added to the mixture in fractions over 10 minutes. Reaction mixture was stirred at 0°C for 2.5 hours. The solvents were removed using rotary evaporation. The reaction mixture was diluted in ethyl acetate and washed with NH₄Cl and NaHCO₃ to remove side products. Then it was washed with water. The aqueous layer was extracted with ethyl acetate. The collected organic layers were combined, washed with brine and dried over anhydrous sodium sulfate. ⁽¹⁹⁾ The solvent was removed using rotary evaporation. Majority of the product was recrystallized in 50% ethyl acetate in hexane solvent mixture to afford a white crystals. The leftover solvent was concentrated and purified using flash column chromatography (0-30% ethyl acetate in hexanes) to afford a white solid. The products from recrystallization and chromatography were combined (1.5g, 63%). ¹H NMR (400 MHz, CDCl₃) δ 7.47 – 7.36 (m, 2H), 7.27 – 7.21 (m, 1H), 7.18 (dd, *J* = 7.6, 1.4 Hz, 1H), 7.16 – 7.07 (m, 2H), 7.02 (td, *J* = 7.4, 1.2 Hz, 1H), 6.98 (dd, *J* = 8.2, 1.2 Hz, 1H), 5.36 (d, *J* = 8.4 Hz, 1H), 5.02

(ddd, $J = 10.0, 8.4, 5.5$ Hz, 1H), 3.70 (dd, $J = 16.1, 9.9$ Hz, 1H), 3.38 (dd, $J = 16.2, 5.5$ Hz, 1H); ^{13}C NMR (75 MHz, CDCl_3) δ 164.95, 161.66, 153.18, 131.51, 131.46, 129.38, 128.96, 128.85, 128.58, 122.10, 117.63, 117.02, 116.18, 115.89, 84.21, 30.22.



19

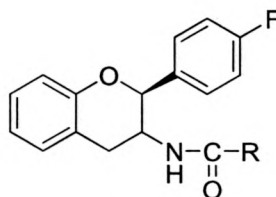
19: Fine Zn powder was activated by stirring the Zn powder in 1M HCl for 1 hour. After 1 hour activated Zn was filtered, washed with ether and placed in oven to dry for 30 minutes. Activated Zn (1-2eq) was added to **18** suspended in isopropanol (40 mL) and 1M HCL (20 mL) solvent mixture. This mixture was stirred at 60°C for 2 hours. Then, NaHCO_3 solution (25 mL) was added to the reaction mixture and the mixture was stirred for additional 20 minutes. The reaction mixture was concentrated and extracted with dichloromethane. The collected organic layer was washed with brine and dried over sodium sulfate. The solvent was removed using rotary evaporation and flash column chromatography was used to purify the product (0-100% ethyl acetate in hexanes) to afford a white solid. ⁽²⁰⁾ (0.38g, 57%) ^1H NMR (400 MHz, $\text{DMSO}-d_6$) δ 7.49 – 7.43 (m, 2H), 7.27 – 7.20 (m, 2H), 7.10 (ddd, $J = 13.3, 7.5, 1.6$ Hz, 2H), 6.86 (td, $J = 7.4, 1.2$ Hz, 1H), 6.79 (dd, $J = 8.0, 1.2$ Hz, 1H), 4.64 (d, $J = 8.6$ Hz, 1H), 3.15 (ddd, $J = 10.1, 8.5, 5.1$ Hz, 1H), 2.91 (dd, $J = 16.3, 5.2$ Hz, 1H), 2.66 (dd, $J = 16.2, 10.1$ Hz, 1H); ^{13}C NMR (101 MHz, $\text{DMSO}-d_6$) δ 163.54, 161.12, 154.61, 136.10, 130.09, 130.02, 127.63, 122.11, 120.88, 116.29, 115.68, 115.46, 83.09, 49.48, 34.23; MS (ESI+) m/z calcd 243.11, found $[\text{M} + \text{H}^+]$ 244.00.



20

20: 1 M borane (16 mL, 4 eq) in THF was slowly added to **17** dissolved in anhydrous THF at anhydrous conditions at 0°C in an oven dried flask. The reaction mixture was brought to room temperature and NaBH₄ (0.076g, 0.5eq) was added to the reaction mixture at room temperature. Reaction mixture was stirred at room temperature for 10 minutes. Then it was heated up to 65-70 °C and stirred overnight at that temperature. Reaction mix was cooled down to room temperature and some ice water was added to it. 1M HCL was added to the reaction mixture to make pH approximately 2. Reaction mixture was stirred at 65°C for 2 hours. Reaction mixture was cooled to room temperature and the acidified solution was extracted with ether. The aqueous layer was basified to pH ~12 by adding some 6M NaOH solution. Basified aqueous layer was extracted with ethyl acetate. Ethyl acetate layer was washed with brine and dried over sodium sulfate. Ethyl acetate layer was concentrated and flash column chromatography was used to purify the product (0-100% ethyl acetate in hexanes) to afford clear liquid product.⁽²¹⁾ (0.67g, 61%). ¹H NMR (400 MHz, DMSO-*d*₆) δ 7.53 – 7.46 (m, 2H), 7.26 – 7.20 (m, 2H), 7.13 (t, *J* = 7.0 Hz, 2H), 6.89 (dd, *J* = 7.8, 6.5 Hz, 2H), 5.20 (d, *J* = 1.8 Hz, 1H), 3.43 (ddd, *J* = 5.0, 3.1, 1.9 Hz, 1H), 3.22 (dd, *J* = 16.4, 4.9 Hz, 1H), 2.65 (dd, *J* = 16.4, 3.2 Hz, 1H); ¹H NMR (400 MHz, MeOD) δ 7.52 (ddd, *J* = 9.9, 5.4, 2.5 Hz, 2H), 7.16 (ddt, *J* = 12.6, 10.4, 4.4 Hz, 4H), 6.98 – 6.86 (m, 2H), 5.18 (s, 1H), 3.49 – 3.39 (m, 1H), 3.39 – 3.30 (m, 1H), 2.78 (dt, *J* = 15.3, 4.0 Hz, 1H); ¹³C NMR (101 MHz, MeOD) δ

153.97, 130.09, 127.62, 127.62, 127.16, 120.91, 119.26, 116.22, 114.85, 114.63, 78.09, 32.73; MS (ESI+) m/z calcd 243.11, found $[M + H^+]$ 244.00



Amide (**21**)

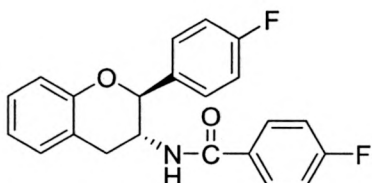
Table 6: List of Amides and their yields. (* Carboxylic acid was not used for this experiment. Acetic anhydride was used as a source of methyl ester)

Compound	Stereochemistry	Carboxylic acid	% yield
21a	Trans	4-F Phenyl	68
21b	Trans	Phenyl	66
21c	Trans	Acetic anhydride*	73
21d	Trans	4-Cl Phenyl	83
21e	Cis	4-F Phenyl	75
21f	Cis	Phenyl	56
21g	Cis	Acetic anhydride*	62
21h	Cis	4-Cl Phenyl	85

General procedure to synthesize amides:

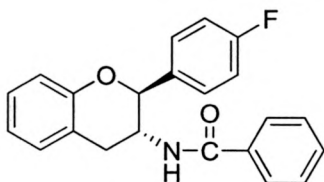
Amine (**19** or **20**) (1eq), Carboxylic acid (2 eq), EDCI.HCl (2.1 eq), dimethylaminopyridine (0.4 eq) and dichloromethane were mixed in an RBF and stirred overnight at room temperature. The reaction mixture was diluted in dichloromethane and washed with 1M HCl. The collected organic layer was first washed with distilled water, then with brine and then dried over anhydrous sodium sulfate. The organic layer was concentrated and purified using flash column chromatography (0-60 % gradient of ethyl

acetate in hexanes) to afford a white powder. (Refer to Table 6 for yields of all the amides that were synthesized)



21a

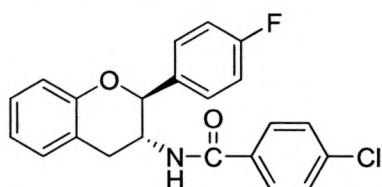
21a: ^1H NMR (400 MHz, CDCl_3) δ 7.75 – 7.69 (m, 2H), 7.43 – 7.37 (m, 2H), 7.32 – 7.27 (m, 1H), 7.15 – 7.06 (m, 6H), 7.00 (td, J = 7.4, 1.4 Hz, 1H), 6.37 (d, J = 8.3 Hz, 1H), 5.47 (d, J = 3.9 Hz, 1H), 4.88 (dq, J = 8.6, 4.4 Hz, 1H), 2.98 (dd, J = 16.7, 4.9 Hz, 1H), 2.86 (dd, J = 16.7, 4.5 Hz, 1H); ^{13}C NMR (101 MHz, CDCl_3) δ 166.24, 166.10, 163.59, 161.14, 153.05, 134.73, 134.69, 130.40, 130.31, 129.35, 129.26, 128.42, 127.44, 127.35, 121.41, 118.70, 116.82, 115.80, 115.77, 115.58, 115.55, 47.23, 27.41; MS (ESI+) m/z calcd 365.12, found $[\text{M} + \text{H}^+]$ 366.20; UPLC retention time: 4.487 min.



21b

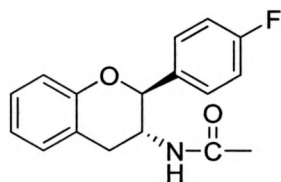
21b: ^1H NMR (400 MHz, Acetone- d_6) δ 7.90 (d, J = 8.8 Hz, 1H), 7.80 – 7.67 (m, 2H), 7.60 (ddd, J = 10.9, 6.6, 3.8 Hz, 2H), 7.51 (dd, J = 8.4, 6.1 Hz, 1H), 7.43 (dd, J = 8.3, 6.7 Hz, 2H), 7.29 – 7.06 (m, 4H), 7.02 – 6.85 (m, 2H), 5.28 (d, J = 8.5 Hz, 1H), 4.74 (qd, J = 8.9, 5.8 Hz, 1H), 3.21 (dd, J = 16.3, 9.4 Hz, 1H), 3.13 (dd, J = 16.5, 5.9 Hz, 1H); ^{13}C NMR (101 MHz, Acetone- d_6) δ 205.25, 166.08, 163.67, 161.26, 154.27, 135.33, 135.30,

134.88, 131.08, 129.77, 129.37, 129.28, 128.17, 127.56, 127.01, 120.82, 116.35, 114.89, 79.49, 48.03, 30.91; MS (ESI+) m/z calcd 347.13, found $[M + H]^+$ 348.15; UPLC retention time: 3.509 min.



21c

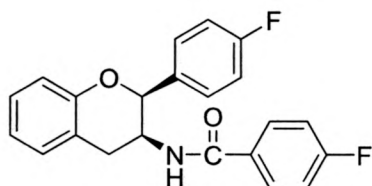
21c: ^1H NMR (400 MHz, CDCl_3) δ 7.65 (d, $J = 8.4$ Hz, 2H), 7.45 – 7.36 (m, 4H), 7.31 – 7.25 (m, 1H), 7.13 – 7.04 (m, 4H), 7.00 (t, $J = 7.4$ Hz, 1H), 6.39 (d, $J = 8.3$ Hz, 1H), 5.46 (d, $J = 4.0$ Hz, 1H), 4.88 (dq, $J = 8.8, 4.5$ Hz, 1H), 2.98 (dd, $J = 16.7, 4.9$ Hz, 1H), 2.86 (dd, $J = 16.6, 4.4$ Hz, 1H); ^{13}C NMR (101 MHz, CDCl_3) δ 166.25, 163.60, 161.15, 153.05, 138.02, 134.67, 134.64, 132.47, 130.39, 128.88, 128.43, 128.39, 127.46, 127.37, 121.42, 118.67, 116.82, 115.77, 115.56, 47.29, 27.43; MS (ESI+) m/z calcd 381.09, found $[M + H]^+$ 381.10; UPLC retention time: 3.831 min.



21d

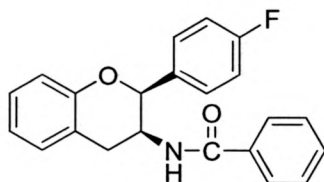
21d: ^1H NMR (400 MHz, CDCl_3) δ 7.35 (dd, $J = 8.7, 5.3$ Hz, 2H), 7.31 – 7.25 (m, 1H), 7.14 – 7.02 (m, 4H), 6.98 (t, $J = 7.4$ Hz, 1H), 5.91 (d, $J = 8.2$ Hz, 1H), 5.36 (d, $J = 3.9$ Hz, 1H), 4.70 (dq, $J = 8.2, 4.1$ Hz, 1H), 2.86 (dd, $J = 16.7, 4.7$ Hz, 1H), 2.72 (dd, $J = 16.7, 4.0$ Hz, 1H), 2.01 (s, 3H); ^{13}C NMR (101 MHz, CDCl_3) δ 169.87, 163.51, 161.07, 153.04, 134.84, 130.41, 128.35, 127.34, 127.27, 121.28, 118.77, 116.74, 115.68, 115.47,

46.55, 27.15, 23.43; MS (ESI+) m/z calcd 285.12, found $[M + H^+]$ 286.05; UPLC retention time: 3.631 min (detected at 230 nm)



21e

21e: ^1H NMR (400 MHz, CDCl_3) δ 7.57 (tdd, $J = 9.2, 5.0, 2.3$ Hz, 4H), 7.30 – 7.24 (m, 1H), 7.21 (d, $J = 7.3$ Hz, 1H), 7.17 – 7.02 (m, 6H), 6.33 (d, $J = 8.7$ Hz, 1H), 5.33 (s, 1H), 5.00 (ddt, $J = 8.7, 4.8, 2.1$ Hz, 1H), 3.46 (dd, $J = 17.0, 5.1$ Hz, 1H), 3.14 (dd, $J = 17.0, 2.2$ Hz, 1H); ^{13}C NMR (101 MHz, CDCl_3) δ 166.26, 165.98, 163.66, 163.47, 161.21, 153.84, 133.52, 133.49, 130.58, 130.33, 129.20, 129.12, 127.92, 127.41, 127.32, 122.08, 119.38, 117.15, 115.71, 115.64, 115.49, 115.42, 46.52, 32.10; MS (ESI+) m/z calcd 365.12, found $[M + H^+]$ 366.15; UPLC retention time: 3.640 min.

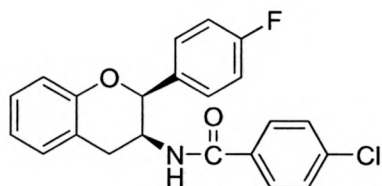


21f

21f: ^1H NMR (400 MHz, CDCl_3) δ 7.57 (dd, $J = 8.2, 5.7$ Hz, 4H), 7.49 (t, $J = 7.3$ Hz, 1H), 7.40 (t, $J = 7.5$ Hz, 2H), 7.30 – 7.24 (m, 1H), 7.21 (d, $J = 7.6$ Hz, 1H), 7.15 (t, $J = 8.5$ Hz, 2H), 7.10 (d, $J = 8.1$ Hz, 1H), 7.04 (t, $J = 7.4$ Hz, 1H), 6.40 (d, $J = 8.4$ Hz, 1H), 5.34 (s, 1H), 5.08 – 4.97 (m, 1H), 3.46 (dd, $J = 16.9, 4.9$ Hz, 1H), 3.16 (dd, $J = 17.1, 2.0$ Hz, 1H); ^{13}C NMR (101 MHz, CDCl_3) δ 167.32, 163.66, 161.21, 153.87, 134.22, 133.59, 133.55, 131.60, 130.57, 128.55, 127.89, 127.47, 127.40, 126.81, 122.02, 119.44, 117.12,

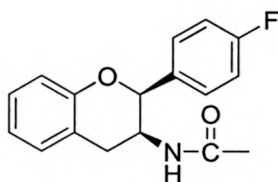
115.61, 115.39, 46.45, 32.13; MS (ESI+) m/z calcd 347.13, found $[M + H]^+$ 348.15;

UPLC retention time: 3.291 min.



21g

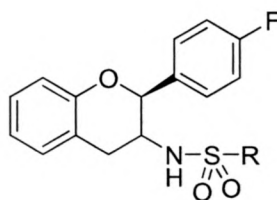
21g: ^1H NMR (400 MHz, CDCl_3) δ 7.57 – 7.52 (m, 2H), 7.52 – 7.48 (m, 2H), 7.39 – 7.33 (m, 2H), 7.30 – 7.24 (m, 1H), 7.20 (dd, $J = 7.5, 1.6$ Hz, 1H), 7.17 – 7.11 (m, 2H), 7.10 (dd, $J = 8.3, 1.2$ Hz, 1H), 7.05 (td, $J = 7.4, 7.4, 1.4$ Hz, 1H), 6.34 (d, $J = 8.5$ Hz, 1H), 5.33 (s, 1H), 5.00 (ddt, $J = 8.8, 5.3, 2.0, 2.0$ Hz, 1H), 3.47 (dd, $J = 17.0, 5.1$ Hz, 1H), 3.14 (dd, $J = 17.1, 2.2$ Hz, 1H); ^{13}C NMR (101 MHz, CDCl_3) δ 166.25, 163.66, 161.21, 153.82, 137.85, 133.47, 133.45, 132.51, 130.56, 128.80, 128.26, 127.94, 127.40, 127.31, 122.11, 119.32, 117.17, 115.64, 115.64, 46.56, 32.06; MS (ESI+) m/z calcd 381.09, found $[M + H]^+$ 382.15; UPLC retention time: 3.815 min.



21h

21h: ^1H NMR (400 MHz, CDCl_3) δ 7.50 (dd, $J = 8.7, 5.4$ Hz, 2H), 7.26 (t, $J = 7.7$ Hz, 1H), 7.19 (d, $J = 7.4$ Hz, 1H), 7.17 – 7.12 (m, 2H), 7.05 (td, $J = 8.3, 1.9$ Hz, 2H), 5.77 (d, $J = 8.8$ Hz, 1H), 5.23 (s, 1H), 4.84 (ddt, $J = 8.8, 4.7, 1.9$ Hz, 1H), 3.37 (dd, $J = 16.9, 5.1$ Hz, 1H), 3.00 (dd, $J = 17.1, 2.2$ Hz, 1H), 1.86 (s, 3H); ^{13}C NMR (101 MHz, CDCl_3) δ

169.84, 163.63, 161.18, 153.87, 133.53, 133.50, 130.59, 127.85, 127.46, 127.37, 121.93, 119.45, 117.09, 115.52, 115.30, 45.78, 32.21, 23.21; MS (ESI+) m/z calcd 285.12, found $[M + H]^+$ 286.05; UPLC retention time: 2.375 min.



Sulfonamide (**22**)

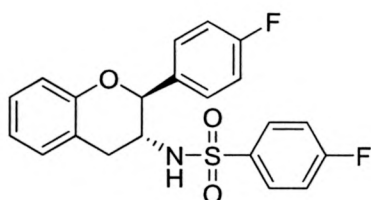
Table 7: List of sulfonamides and their yields.

Compound	Stereochemistry	Sulfonyl chloride	% yield
22a	Trans	4-F Phenyl	87
22b	Trans	Phenyl	52
22c	Trans	Me	84
22d	Trans	4-Cl Phenyl	55
22e	Cis	4-F Phenyl	72
22f	Cis	Phenyl	82
22g	Cis	Me	72
22h	Cis	4-Cl Phenyl	76

General procedure to synthesize sulfonamides:

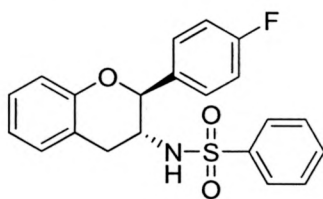
Amine (**19** or **20**) (1eq), Sulfonyl Chloride (1.25 eq), triethyl amine (2eq), and dichloromethane were mixed together in a RBF and stirred overnight at room temperature. The reaction mixture was diluted in dichloromethane and washed with saturated NH_4Cl solution. The collected organic layer was washed with distilled water, then with brine and then dried over anhydrous sodium sulfate. The organic layer was concentrated and purified using flash column chromatography (0-60 % gradient of ethyl

acetate in hexanes) to afford a white powder. (Refer to Table 7 for yields of all the amides that were synthesized)



22a

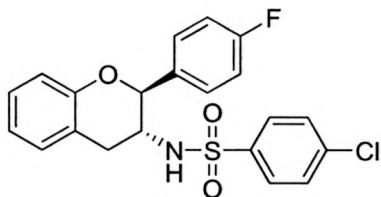
22a: ^1H NMR (400 MHz, CDCl_3) δ 7.83 – 7.72 (m, 2H), 7.30 – 7.13 (m, 5H), 6.99 (td, J = 8.1, 7.5, 4.8 Hz, 5H), 5.03 (d, J = 5.9 Hz, 1H), 4.89 (d, J = 8.1 Hz, 1H), 3.90 (dq, J = 8.2, 5.8 Hz, 1H), 3.01 (dd, J = 16.6, 4.9 Hz, 1H), 2.73 (dd, J = 16.5, 6.4 Hz, 1H); ^{13}C NMR (101 MHz, CDCl_3) δ 166.36, 163.82, 161.12, 153.06, 136.45, 133.87, 130.08, 129.66, 129.55, 128.45, 127.76, 127.67, 121.55, 118.35, 116.65, 116.50, 116.28, 115.83, 115.62, 51.36, 30.21; MS (ESI+) m/z calcd 401.09, found $[\text{M} + \text{H}^+]$ 402.15, $[\text{M} + \text{NH}_4^+]$ 419.20; UPLC retention time: 3.417 min.



22b

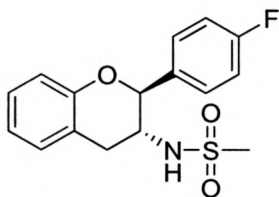
22b: ^1H NMR (400 MHz, CDCl_3) δ 7.79 – 7.73 (m, 2H), 7.67 – 7.61 (m, 1H), 7.52 (dd, J = 8.3, 7.0 Hz, 2H), 7.27 – 7.20 (m, 1H), 7.18 – 7.12 (m, 2H), 7.02 – 6.93 (m, 5H), 5.01 (d, J = 5.6 Hz, 1H), 4.90 (d, J = 8.3 Hz, 1H), 3.94 – 3.85 (m, 1H), 3.00 (dd, J = 16.5, 4.9 Hz, 1H), 2.73 (dd, J = 16.5, 6.4 Hz, 1H); ^{13}C NMR (101 MHz, CDCl_3) δ 163.75, 161.28, 153.09, 140.31, 133.90, 132.79, 130.12, 129.21, 128.37, 127.75, 127.66, 126.87, 121.50,

118.45, 116.61, 115.82, 115.61, 51.26, 30.11; MS (ESI+) m/z calcd 383.10, found $[M + H^+]$ 384.15, $[M + NH_4^+]$ 401.25; UPLC retention time: 3.397 min.



22c

22c: 1H NMR (400 MHz, $CDCl_3$) δ 7.71 – 7.63 (m, 2H), 7.51 – 7.43 (m, 2H), 7.24 (td, J = 7.5, 2.0 Hz, 1H), 7.21 – 7.14 (m, 2H), 6.99 (dtd, J = 13.1, 6.8, 6.0, 3.2 Hz, 5H), 5.02 (d, J = 5.9 Hz, 1H), 4.92 (d, J = 8.3 Hz, 1H), 3.90 (dq, J = 8.3, 5.8 Hz, 1H), 3.02 (dd, J = 16.5, 4.9 Hz, 1H), 2.74 (dd, J = 16.5, 6.4 Hz, 1H); ^{13}C NMR (101 MHz, $CDCl_3$) δ 163.82, 161.37, 153.06, 139.34, 138.85, 133.81, 133.78, 130.05, 129.44, 128.45, 128.27, 127.78, 127.69, 121.55, 118.36, 116.65, 115.82, 115.61, 51.42, 30.35; MS (ESI+) m/z calcd 417.06, found $[M + H^+]$ 418.15, $[M + NH_4^+]$ 435.25; UPLC retention time: 3.894 min.

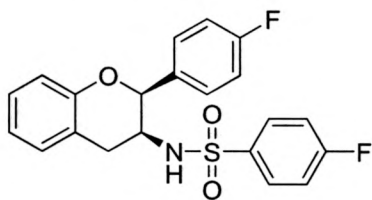


22d

22d: 1H NMR (400 MHz, $CDCl_3$) δ 7.46 – 7.39 (m, 2H), 7.28 – 7.22 (m, 1H), 7.17 – 7.09 (m, 3H), 7.04 – 6.97 (m, 2H), 5.12 (d, J = 6.4 Hz, 1H), 4.69 (d, J = 8.5 Hz, 1H), 4.09 (dtd, J = 8.8, 6.9, 5.1 Hz, 1H), 3.14 (dd, J = 16.4, 5.1 Hz, 1H), 2.89 (dd, J = 16.4, 7.1 Hz, 1H), 2.66 (s, 3H); ^{13}C NMR (101 MHz, $CDCl_3$) δ 163.94, 161.47, 153.22, 134.48, 134.44, 129.96, 128.42, 128.32, 128.23, 121.54, 118.64, 116.71, 115.91, 115.71, 51.98,

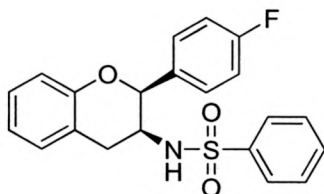
41.78, 31.39; MS (ESI+) m/z calcd 321.08, found $[M + H]^+$ 322.05, $[M + NH_4]^+$ 339.10;

UPLC retention time: 2.689 min.



22e

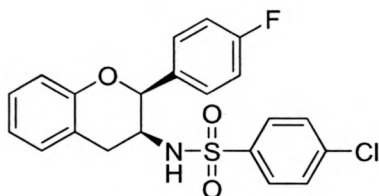
22e: 1H NMR (400 MHz, $CDCl_3$) δ 7.51 – 7.43 (m, 2H), 7.29 – 7.21 (m, 3H), 7.14 (d, J = 7.4 Hz, 1H), 7.00 (tt, J = 14.9, 8.1 Hz, 6H), 5.11 (s, 1H), 4.88 (d, J = 8.5 Hz, 1H), 3.94 (ddt, J = 8.6, 4.4, 2.0 Hz, 1H), 3.34 (dd, J = 16.8, 4.5 Hz, 1H), 3.13 (dd, J = 16.9, 2.4 Hz, 1H); ^{13}C NMR (101 MHz, $CDCl_3$) δ 166.08, 163.54, 161.17, 153.53, 136.00, 133.07, 130.63, 129.36, 129.28, 128.14, 127.15, 127.06, 122.18, 118.29, 116.96, 116.06, 115.84, 115.40, 115.20, 51.24, 33.39; MS (ESI+) m/z calcd 401.09, found $[M + H]^+$ 402.20, $[M + NH_4]^+$ 419.20; UPLC retention time: 3.341 min.



22f

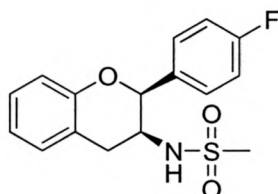
22f: 1H NMR (400 MHz, $CDCl_3$) δ 7.57 – 7.46 (m, 3H), 7.35 (d, J = 7.5 Hz, 2H), 7.24 (ddd, J = 8.9, 5.6, 2.6 Hz, 3H), 7.13 (dd, J = 7.5, 1.6 Hz, 1H), 7.06 – 6.98 (m, 2H), 6.95 – 6.87 (m, 2H), 5.11 (s, 1H), 4.84 (d, J = 8.4 Hz, 1H), 3.97 (ddt, J = 8.6, 4.4, 2.1 Hz, 1H), 3.32 (dd, J = 16.7, 4.5 Hz, 1H), 3.12 (dd, J = 16.7, 2.4 Hz, 1H); ^{13}C NMR (101 MHz, $CDCl_3$) δ 163.53, 161.08, 153.59, 139.91, 133.01, 132.25, 130.63, 128.84, 128.08, 127.14, 127.06, 126.61, 122.09, 118.40, 116.92, 115.42, 115.20, 51.11, 33.33; MS (ESI+)

m/z calcd 383.10, found $[M + H]^+$ 384.15, $[M + NH_4]^+$ 401.15; UPLC retention time: 3.295 min.



22g

22g: 1H NMR (400 MHz, $CDCl_3$) δ 7.41 – 7.36 (m, 2H), 7.30 – 7.27 (m, 2H), 7.26 – 7.20 (m, 3H), 7.14 (dd, $J = 7.6, 1.5$ Hz, 1H), 7.07 – 6.98 (m, 2H), 6.98 – 6.91 (m, 2H), 5.10 (s, 1H), 4.92 (d, $J = 8.4$ Hz, 1H), 3.94 (ddt, $J = 8.4, 4.3, 2.1$ Hz, 1H), 3.35 (dd, $J = 16.7, 4.5$ Hz, 1H), 3.14 (dd, $J = 16.9, 2.2$ Hz, 1H); ^{13}C NMR (101 MHz, $CDCl_3$) δ 163.68, 161.23, 153.52, 138.87, 138.37, 133.02, 132.98, 130.62, 129.03, 128.14, 128.01, 127.06, 126.99, 122.19, 118.29, 116.96, 115.40, 115.20, 51.30, 33.49; MS (ESI+) m/z calcd 417.06, found $[M + H]^+$ 418.15, $[M + NH_4]^+$ 435.20; UPLC retention time: 5.055 min.



22h

22h: 1H NMR (400 MHz, $CDCl_3$) δ 7.58 – 7.52 (m, 2H), 7.29 – 7.23 (m, 1H), 7.23 – 7.17 (m, 3H), 7.07 – 7.01 (m, 2H), 5.23 (s, 1H), 4.68 (d, $J = 9.5$ Hz, 1H), 3.47 (dd, $J = 16.7, 4.8$ Hz, 1H), 3.11 (dd, $J = 16.7, 2.3$ Hz, 1H), 2.28 (s, 3H); ^{13}C NMR (101 MHz, $CDCl_3$) δ 163.79, 161.33, 153.53, 134.07, 134.04, 130.72, 128.26, 127.69, 127.62, 122.20, 118.01, 116.99, 115.71, 115.49, 51.97, 40.99, 34.16; MS (ESI+) m/z calcd 321.08, found $[M + H]^+$ 322.05, $[M + NH_4]^+$ 339.10; UPLC retention time: 2.628 min.

References:

1. Bagatell, R.; Whitesell, L.; Altered Hsp90 function in cancer: A unique therapeutic opportunity. *Mol. Cancer Ther.* **2004**, 3(8), 1021-1030.
2. Hall, J. A.; Forsberg, L. K.; Blagg, B. S. Alternative approaches to Hsp90 modulation for the treatment of cancer. *Future Med Chem.* **2014**, 6 (14), 1587–1605.
3. Sidera, K.; Patsavoudi, E. Hsp90inhibitors: Current Development and Potential in Cancer Therapy. *Recent Pat. Anti-Cancer Drug Discovery PRA.* **2013**, 9 (1), 1–20.
4. Sidera, K.; Gaitanou, M.; Stellas, D.; Matsas, R.; Patsavoudi, E. J. A critical Role for Hsp90 in Cancer Cell Invasion Involves Interaction with the Extracellular Domain of HER-2. *Biol. Chem.* **2007**, 283 (4), 2031–2041.
5. Bhat, R.; Tummalapalli, S. R.; Rotella, D. P. Progress in the discovery and development of Heat Shock Protein 90 (Hsp90) inhibition. *J. Med. Chem.* **2014**, 57 (21), 8718–8728.
6. Steinmann, J.; Buer, J.; Pietschmann, T.; Steinmann, E. Anti-infective properties of epigallocatechin-3-gallate (EGCG), a component of green tea. *Br. J. Pharmacol.* **2013**, 168 (5), 1059–1073.
7. Buchner, J.; Li, J. Structure, Function and Regulation of Hsp90 Machinery. *Biomed J.* **2013**, 36 (3), 106–117.
8. Bhat, R.; Adam, A. T.; Lee, J. J.; Gasiewicz, T. A.; Henry, E. C.; Rotella, D. P. Towards the discovery of drug-like epigallocatechin gallate analogs as Hsp90 inhibitors. *Bioorg. & Med. Chem. Lett.* **2014**, 24 (10), 2263–2266.

9. Mereles, D.; Hunstein, W. Epigallocatechin-3-gallate (EGCG) for Clinical Trials. *Int. J. Mol. Sci.* **2011**, *12* (12), 5592–5603.
10. Yin, Z.; Henry, E. C.; Gasiewicz, T. A. (-)-Epigallocatechin-3-gallate is a Novel Hsp90 Inhibitor. *Biochem.* **2009**, *48* (2), 336–345.
11. Khandelwal, A.; Hall, J. A.; Blagg, B. S. Synthesis and Structure –Activity Relationships of EGCG Analogues, a Recently Identified Hsp90 Inhibitor. *J. Org. Chem.* **2013**, *78* (16), 7859–7884.
12. Fraley, M. E.; Hungate, R. W.; Naylor-Olsen, A. M.; Vacca, J. P.; Thrombin Inhibitors. PCT/US1997/014019, Feb 19, **1998**.
13. Das, J. P.; Roy, S. Catalytic Hunsdiecker Reaction of α,β -Unsaturated Carboxylic acids: How Efficient is the Catalyst? *J. Org. Chem.* **2002**, *67*, 7861–7864.
14. Cheung, C. W.; Buchwald, S. L. Room Temperature Copper (II)- Catalyzed Oxidative Cyclization of Enamides to 2,5- Disubstituted Oxazoles via Vinylic C-H Functionalization. *J. Org. Chem.* **2012**, *77* (17), 7526–7537.
15. Backes, G. L.; Neumann, D. M.; Jursic, B. S. Synthesis and antifungal activity of substituted salicylaldehyde hydrazones, hydrazides and sulfohydrazides. *Bioorg. Med. Chem.* **2014**, *22* (17), 4629–4636.
16. Xia, Y.; Xia, Y.; Zhang, Y.; Wang, J. Palladium-catalyzed coupling of N-tosyl-hydrazones and β -bromostyrene derivatives: new approach to 2H-chromenes. *Org. Biomol. Chem.* **2014**, *12* (46), 9333–9336.
17. Simpson, A. J.; Lam, H. W. Enantioselective Nickel-Catalyzed Michael Additions of 2-Acetylazarenes to Nitroalkenes. *Org. Lett.* **2013**, *15* (11), 2586–2589.

18. Wang, P.; Zhang, D.; Lui, X. Facile access to 2-aryl-3-nitro-2H-chromenes and 2,3,4-trisubstituted chromanes. *Arkivoc* **2014**, 2014 (5), 408–419.
19. Varma, R. S.; Kadkhodayan, M.; Kabalka, G. W. Synthesis of 2-phenyl-3-nitro-3,4-dihydro-2H-1-benzopyrans. *Heterocycles* **1986**, 24 (6), 1647–1652.
20. Kusuma, B. R.; Zhang, L.; Sundstrom, T.; Peterson, L. B.; Dobrowsky, R. T.; Blagg, B. S. J. Synthesis and Evaluation of Novologues as C-Terminal Hsp90 Inhibitors with Cytoprotective Activity against Sensory Neuron Glucotoxicity. *J. Med. Chem.* **2012**, 55 (12), 5797–5812.
21. Das, B. C.; Mohapatra, S.; Campbell, P. D.; Nayak, S.; Mahalingam, S. M.; Evans, T. Synthesis of function-oriented 2-phenyl-2H-chromene derivatives using L-pipecolinic acid and substituted guanidine organocatalysts. *Tetrahedron Lett.* **2010**, 51 (19), 2567–2570.
22. Varma, R. S.; Gai, Y.-Z.; Kabalka, G. W. Reduction of α,β -unsaturated nitroalkenes with borane and borohydrides. A convenient route to 3-nitro, 3-hydroxylamin, and 3-amino-2H-1-benzopyran derivatives. *J. Heterocycl. Chem.* **1987**, 24 (3), 767–772.
23. Sadikot, T.; Swink, M.; Eskew, J. D.; Brown, D.; Zhao, H.; Kusuma, B. R.; Rajewski, R. A.; Blagg, B. S. J.; Matts, R. L.; Holzbeierlein, J. M.; Vielhauer, G. A. Development of a high-throughput screening cancer cell-based luciferase refolding assay for identifying Hsp90 inhibitors. *ASSAY Drug Dev. Technol.* October **2013**, 11 (8), 478–488.

Spectral Analysis:

Figure 6: ^1H NMR of 6

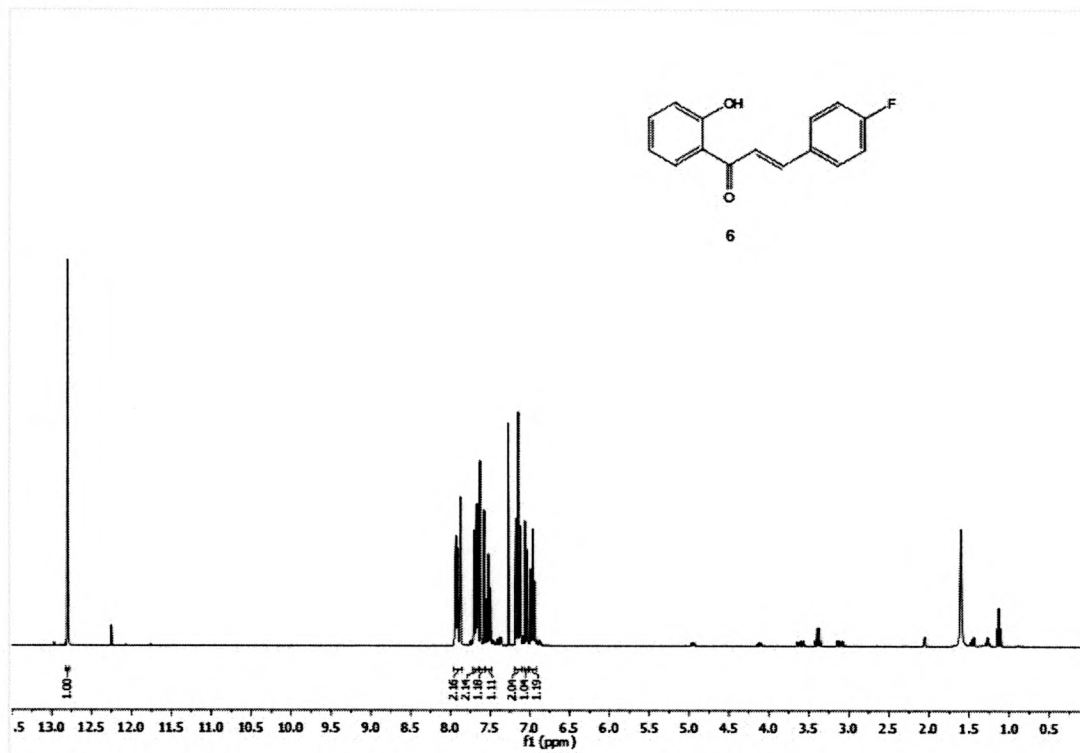


Figure 7: ^1H NMR of 7

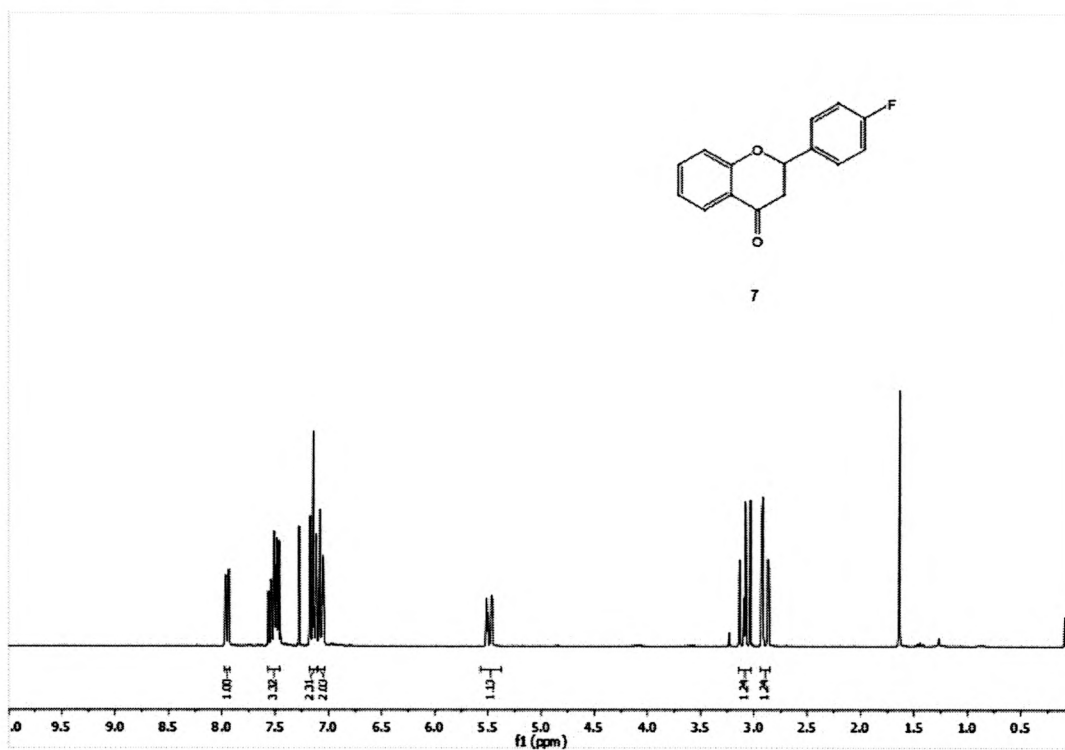


Figure 8: ^{13}C NMR of 7

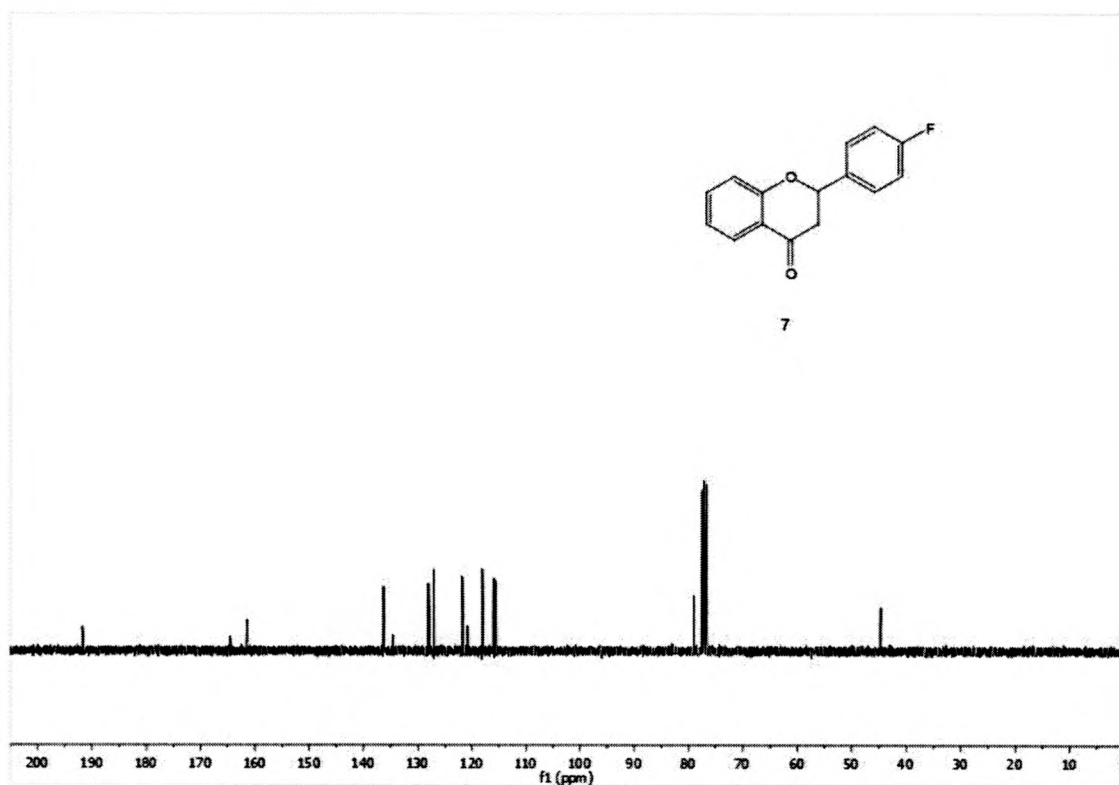


Figure 9: ^1H NMR of 8

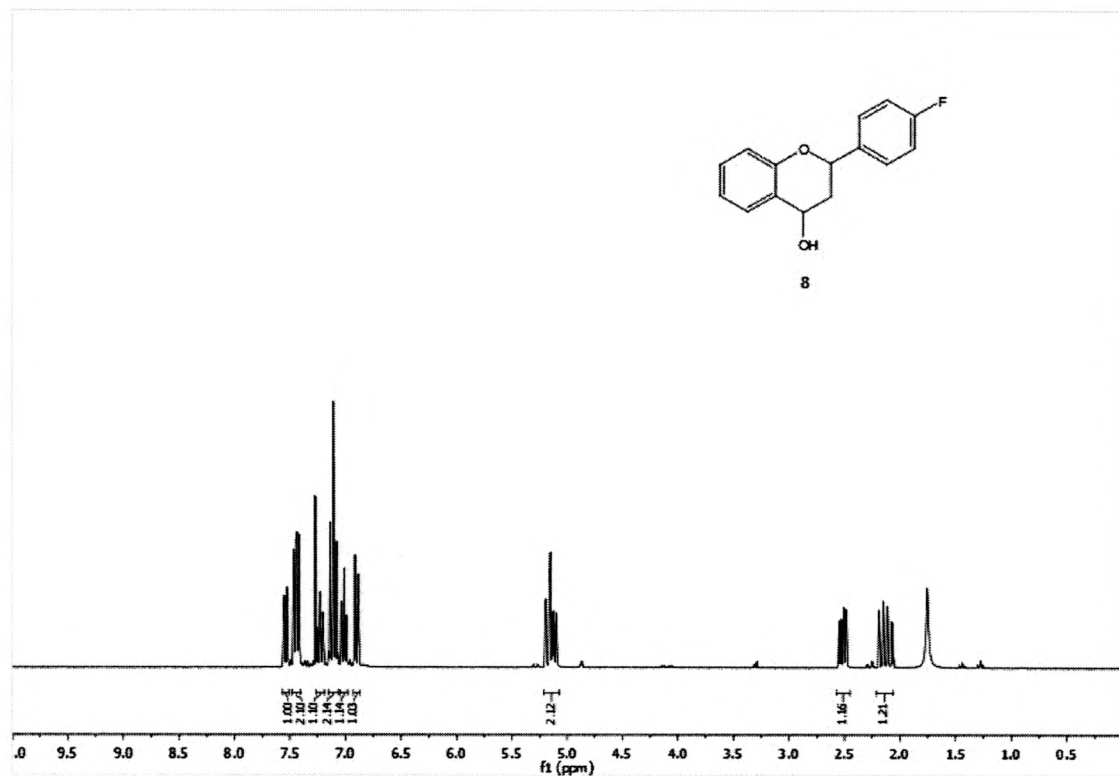


Figure 10: ^1H NMR of **9** (Route 1)

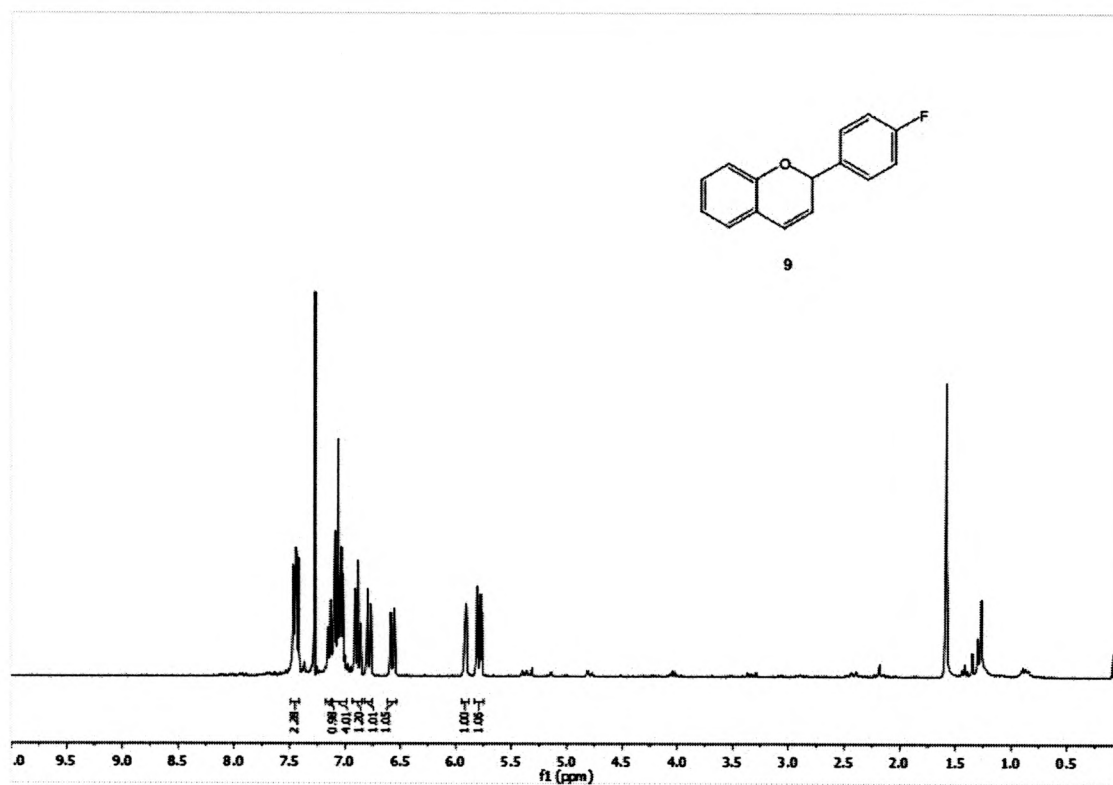


Figure 11: ^1H NMR of **12**

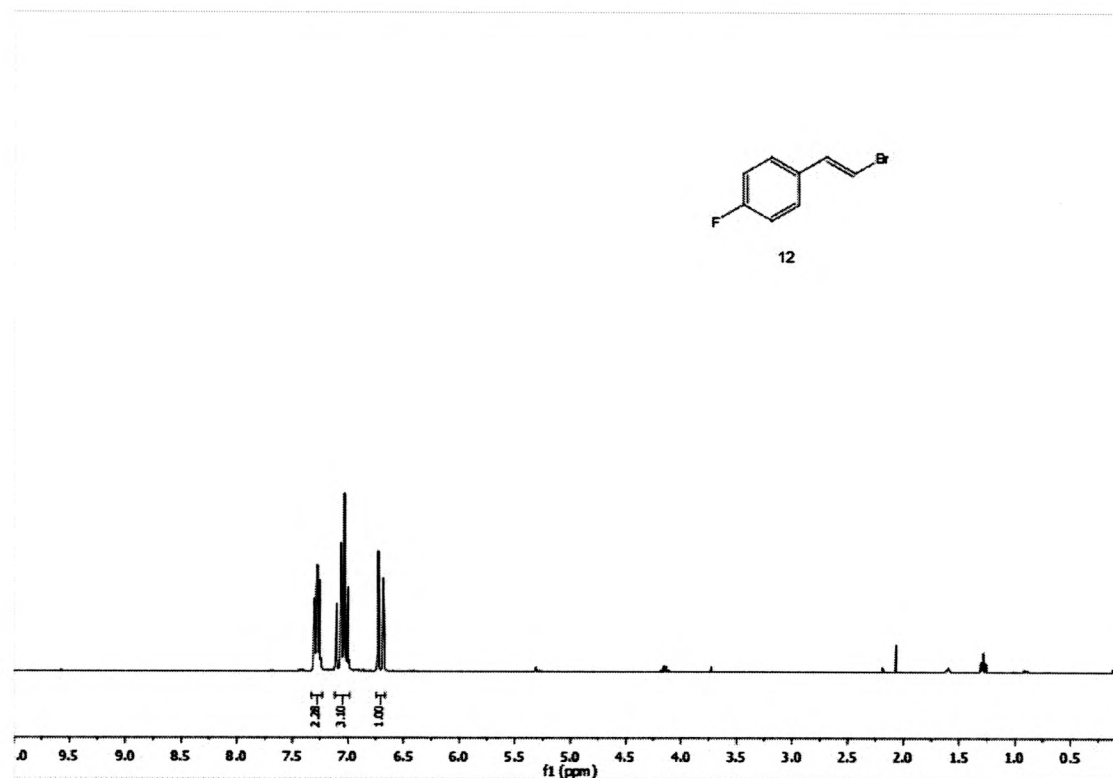


Figure 12: ^1H NMR of 15

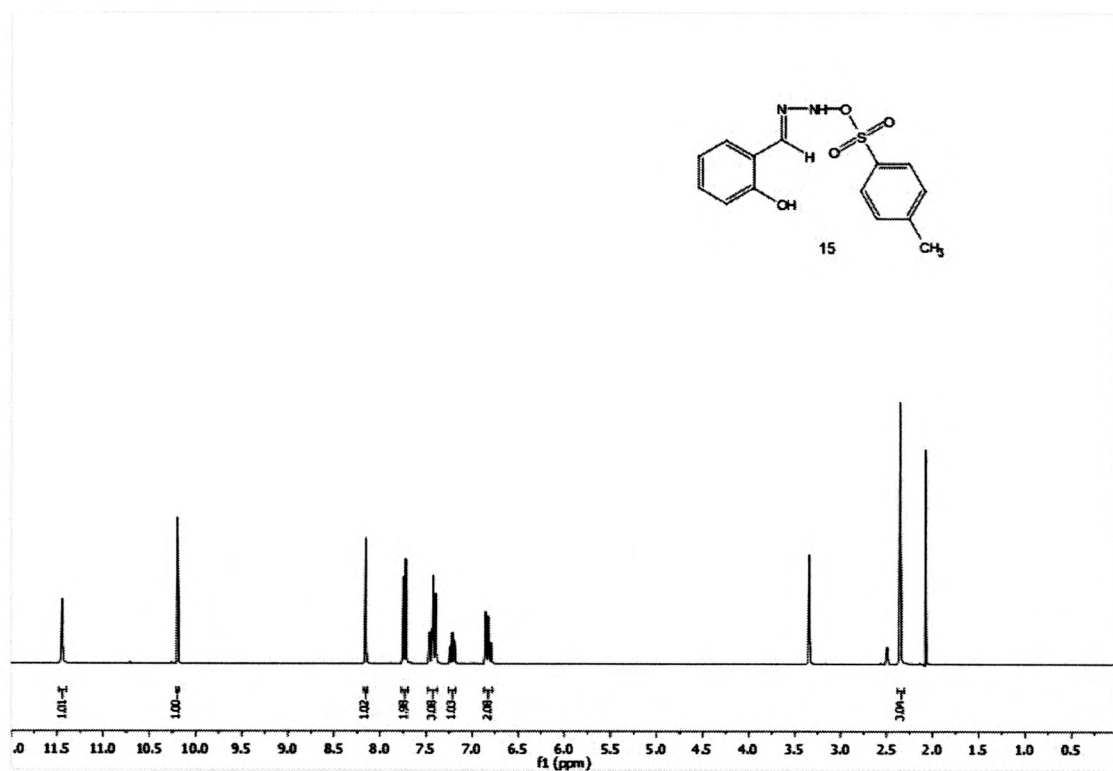


Figure 13: ^1H NMR of 9 (Route 2)

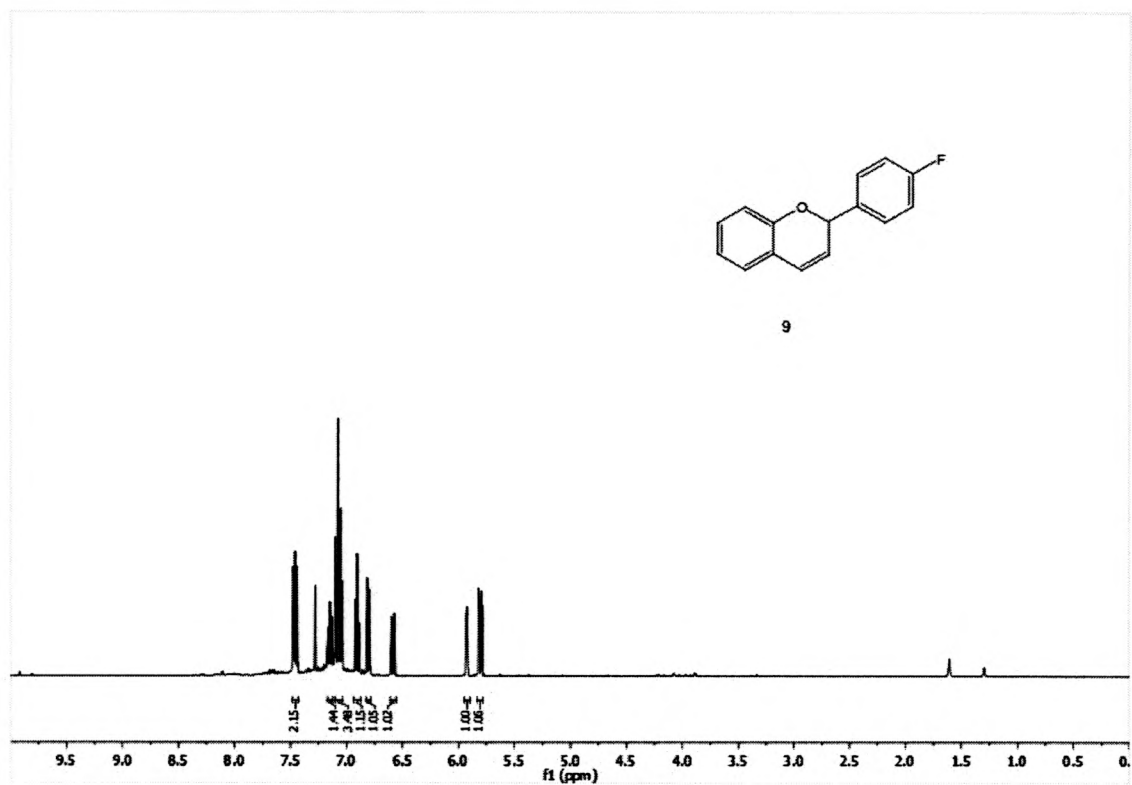


Figure 14: ^1H NMR of 16

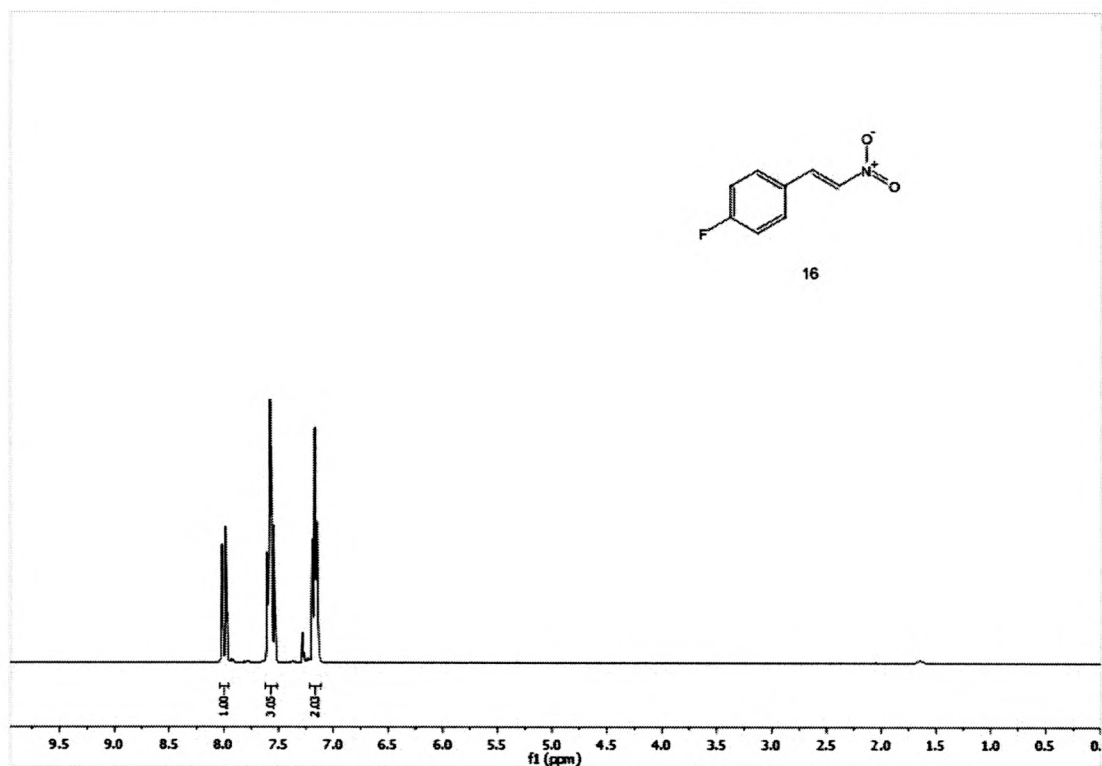


Figure 15: ^{13}C NMR of 16

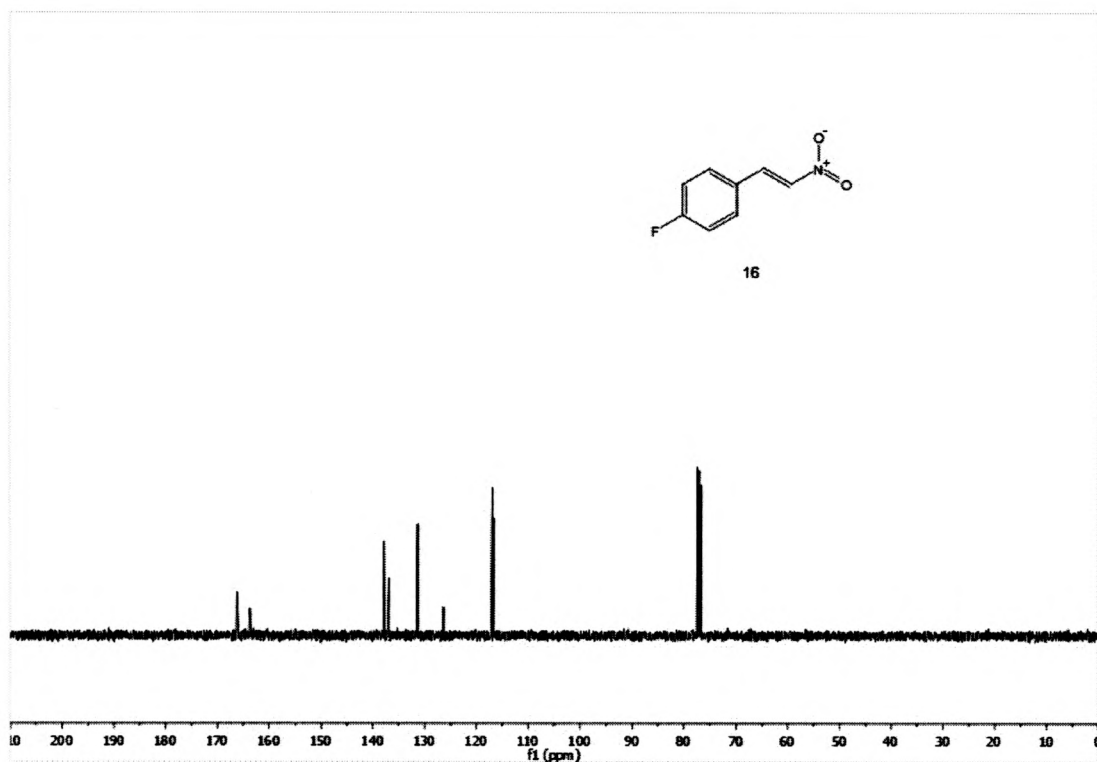


Figure 16: ^1H NMR of 17

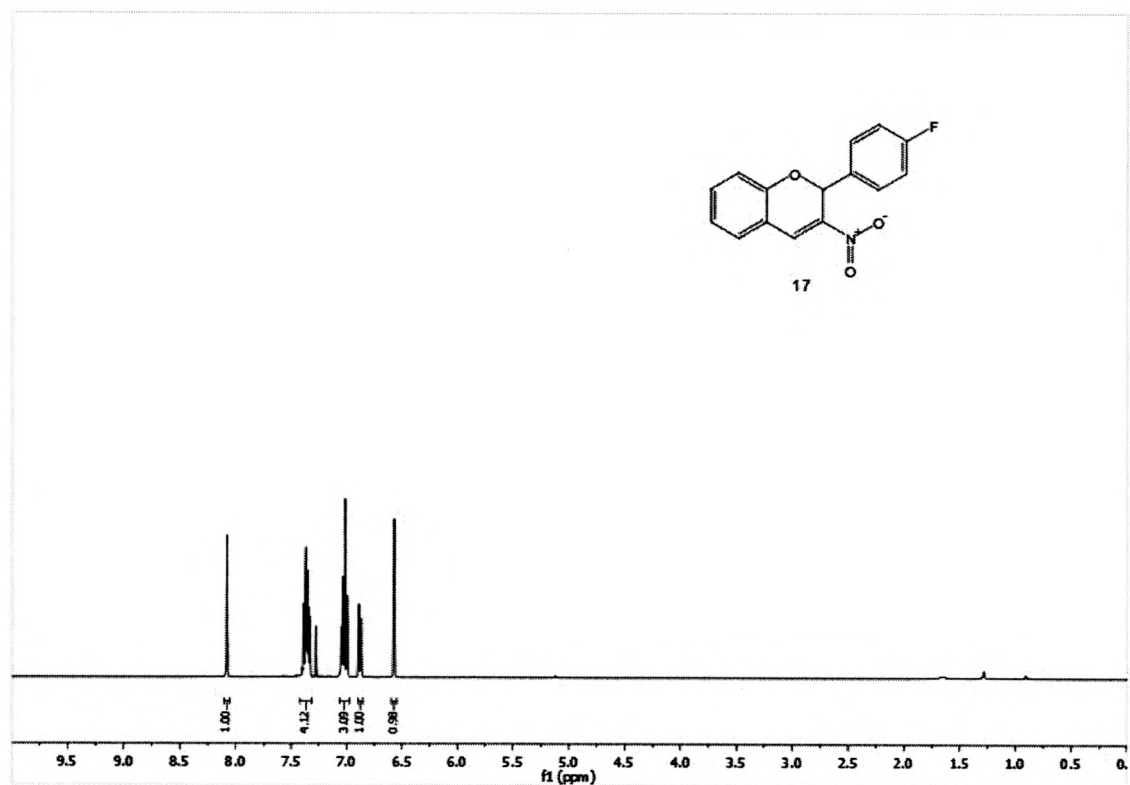


Figure 17: ^{13}C NMR of 17

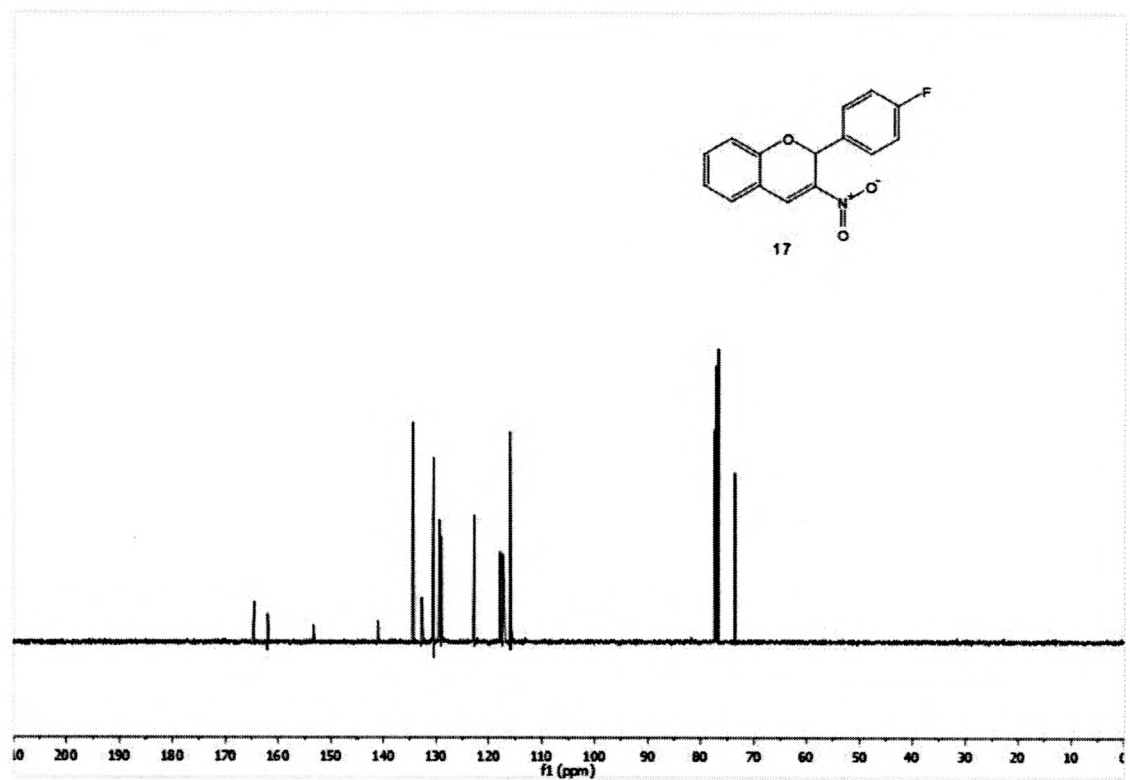


Figure 18: ^1H NMR of **18**

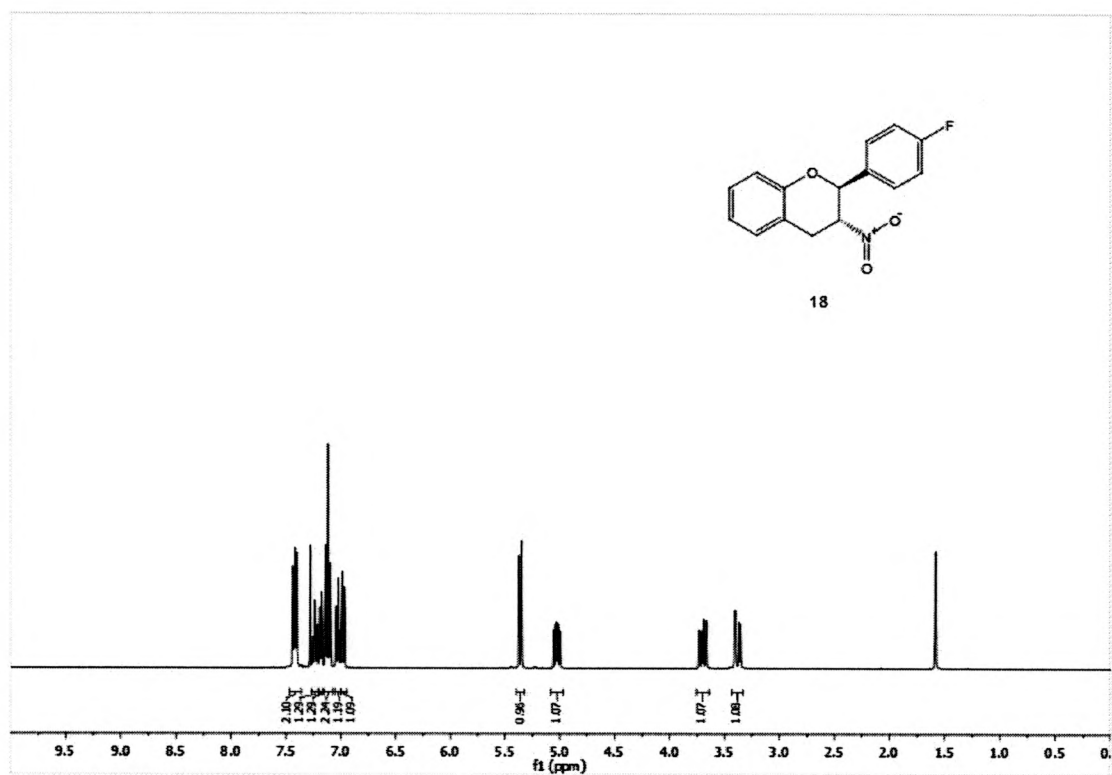


Figure 19: ^{13}C NMR of **18**

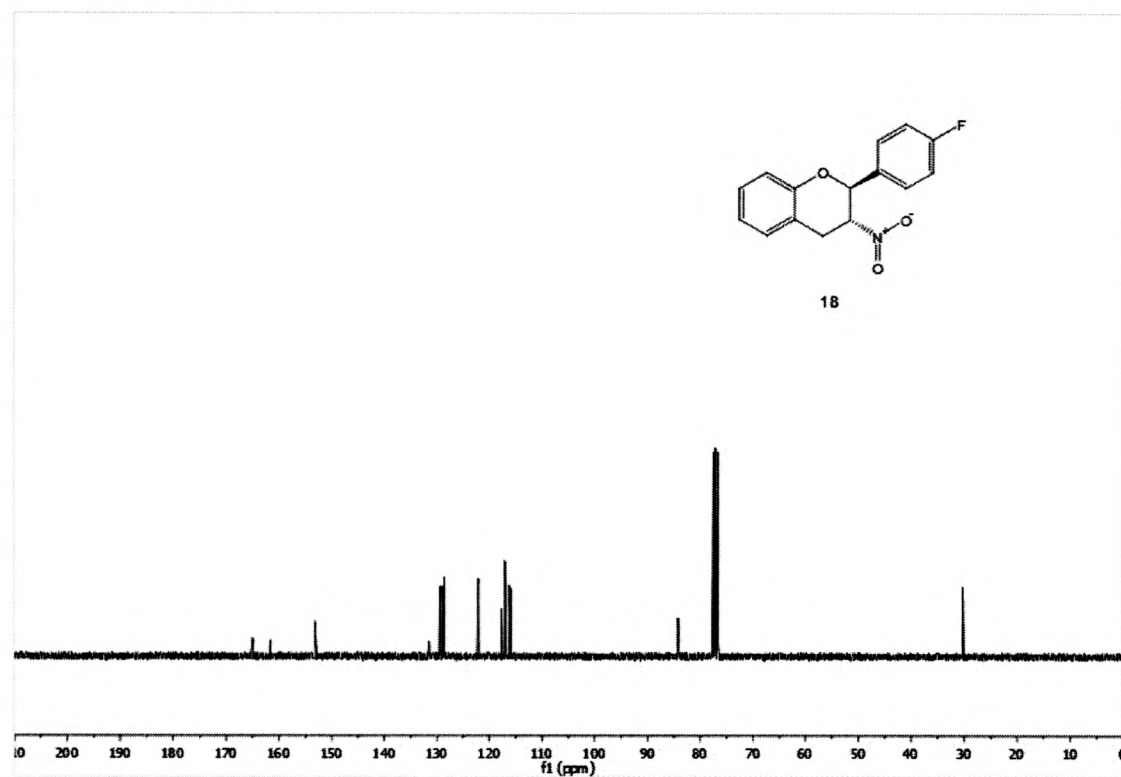


Figure 20: ^1H NMR of **19** (in DMSO)

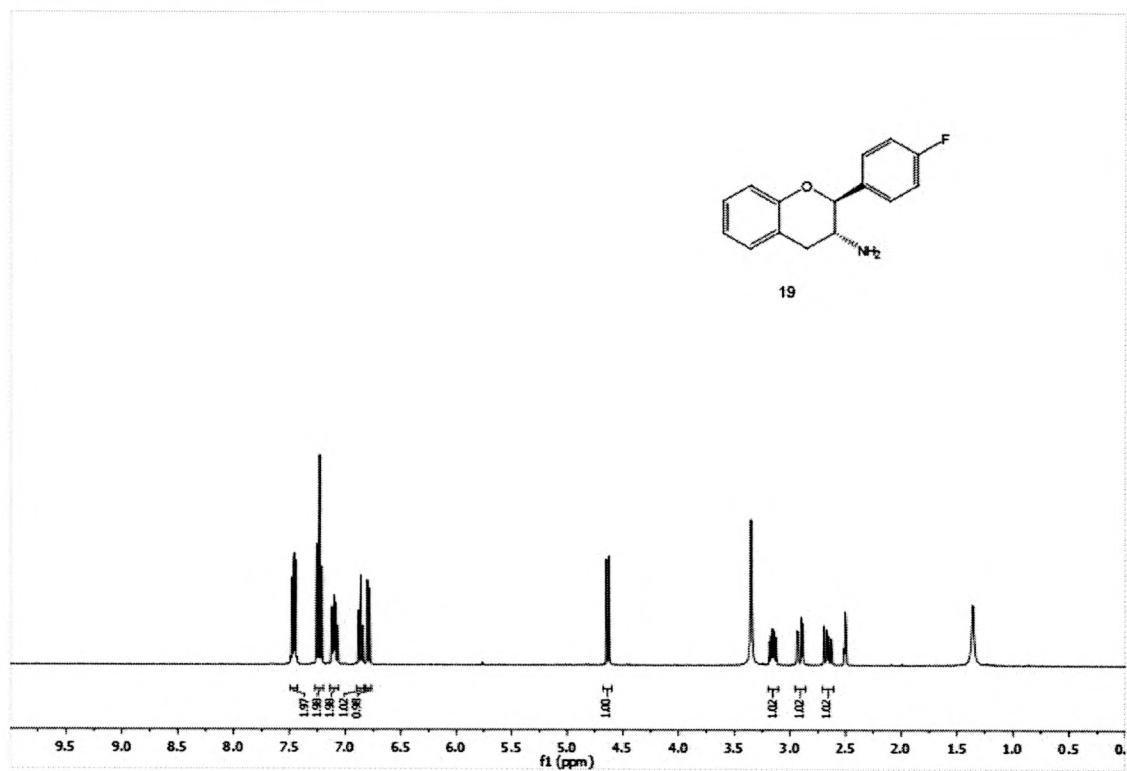


Figure 21: ^{13}C NMR of **19** (in DMSO)

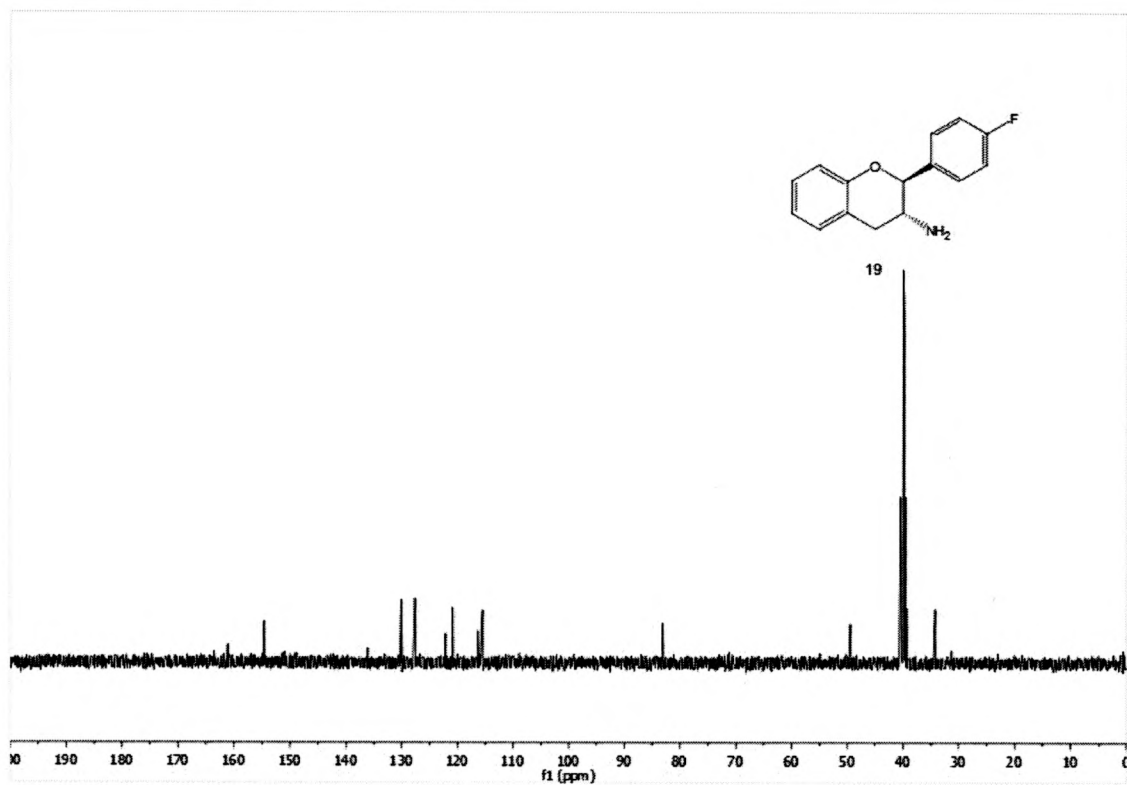


Figure 22: ^1H NMR of **20** (in MeOD)

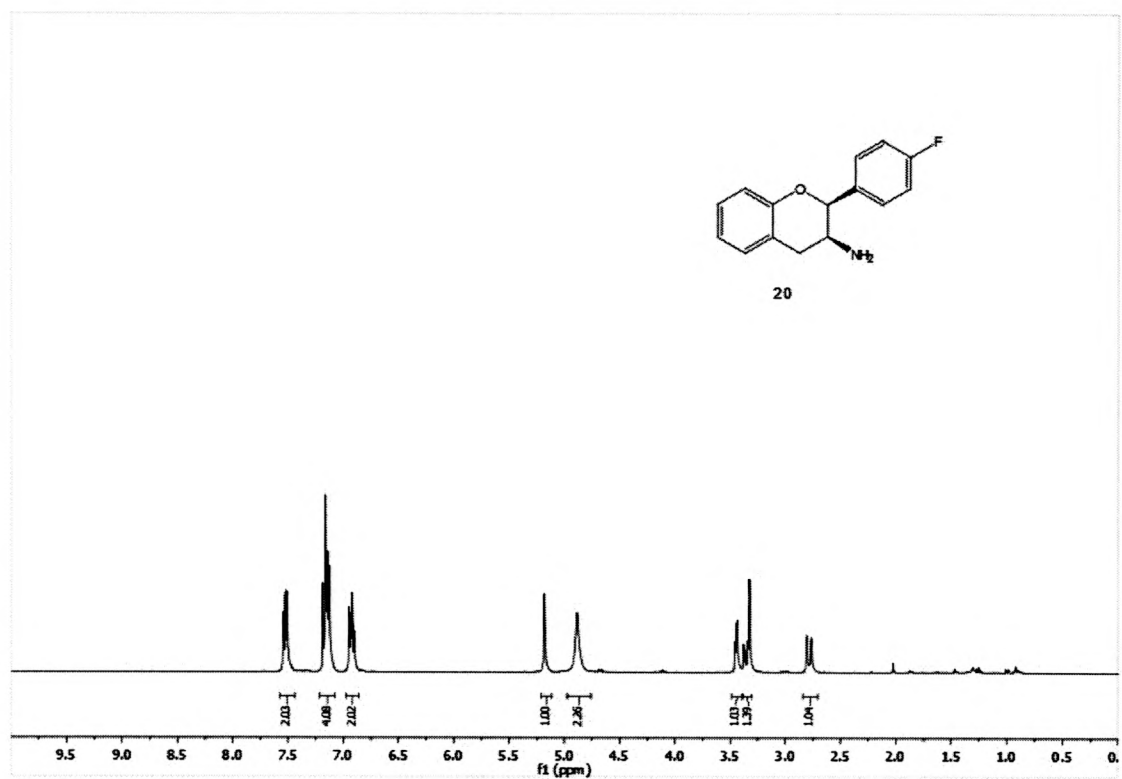


Figure 23: ^{13}C NMR of **20** (in MeOD)

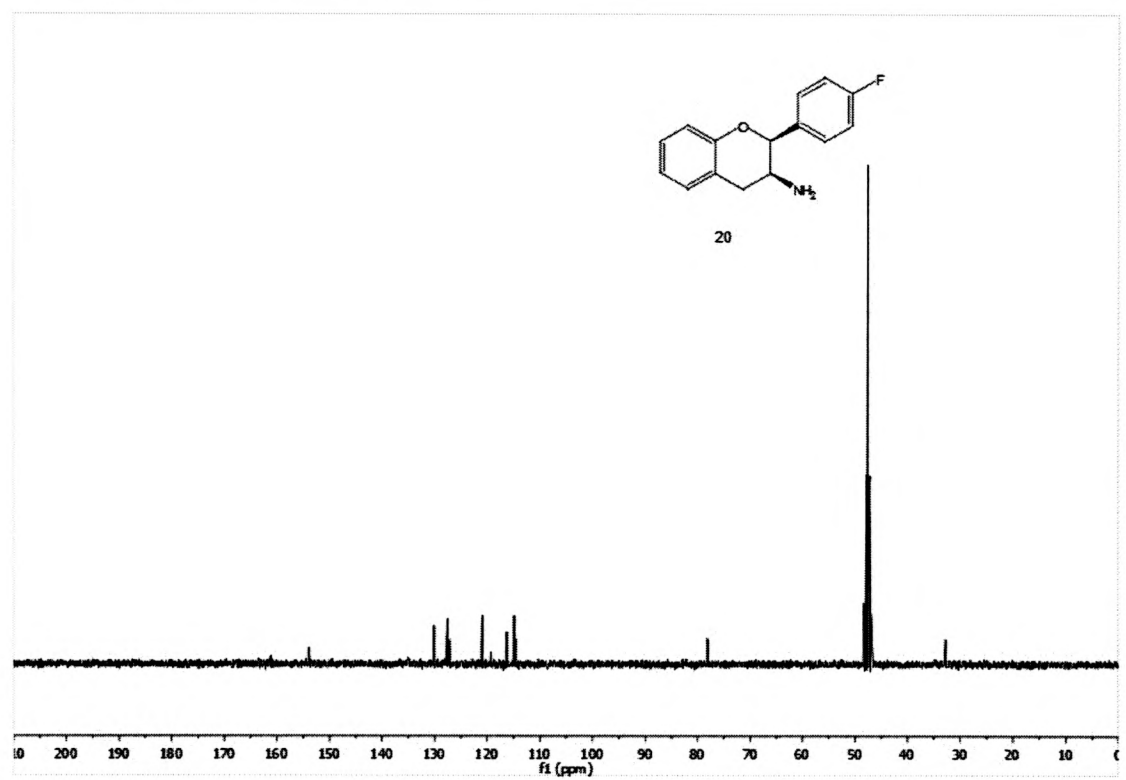


Figure 24: ^1H NMR of **20** (in DMSO)

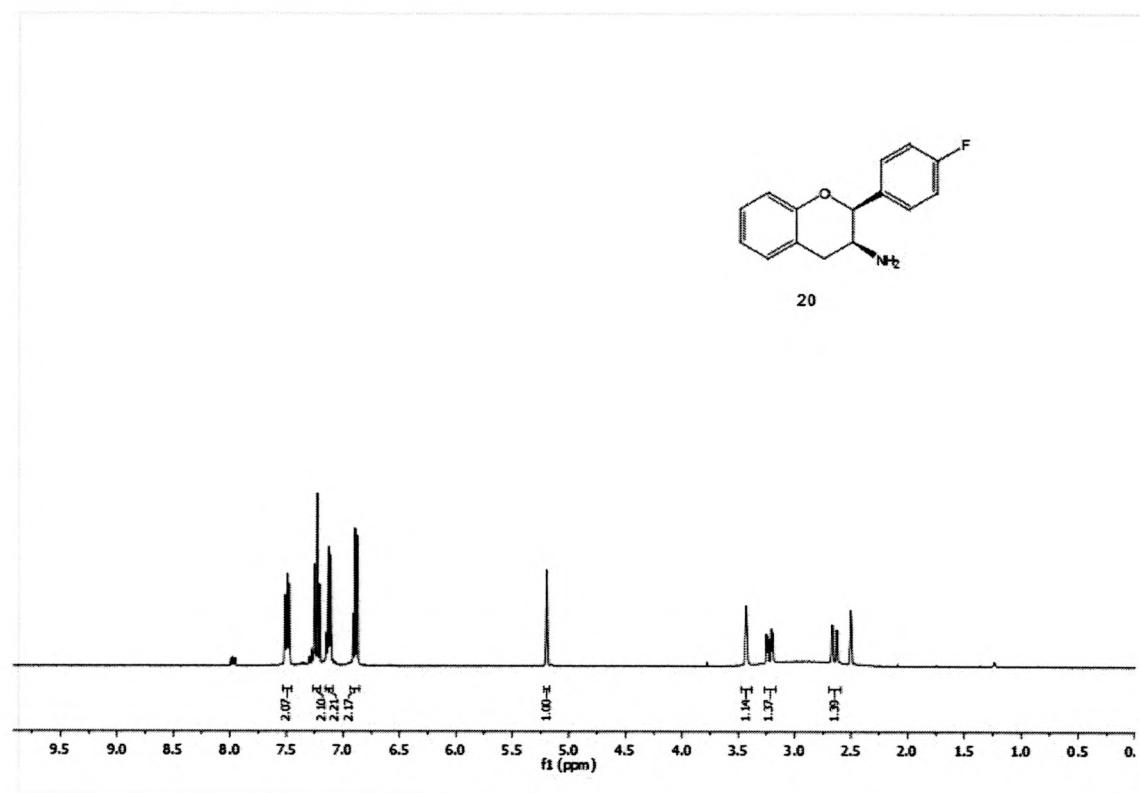


Figure 25: ^1H NMR of **21a**

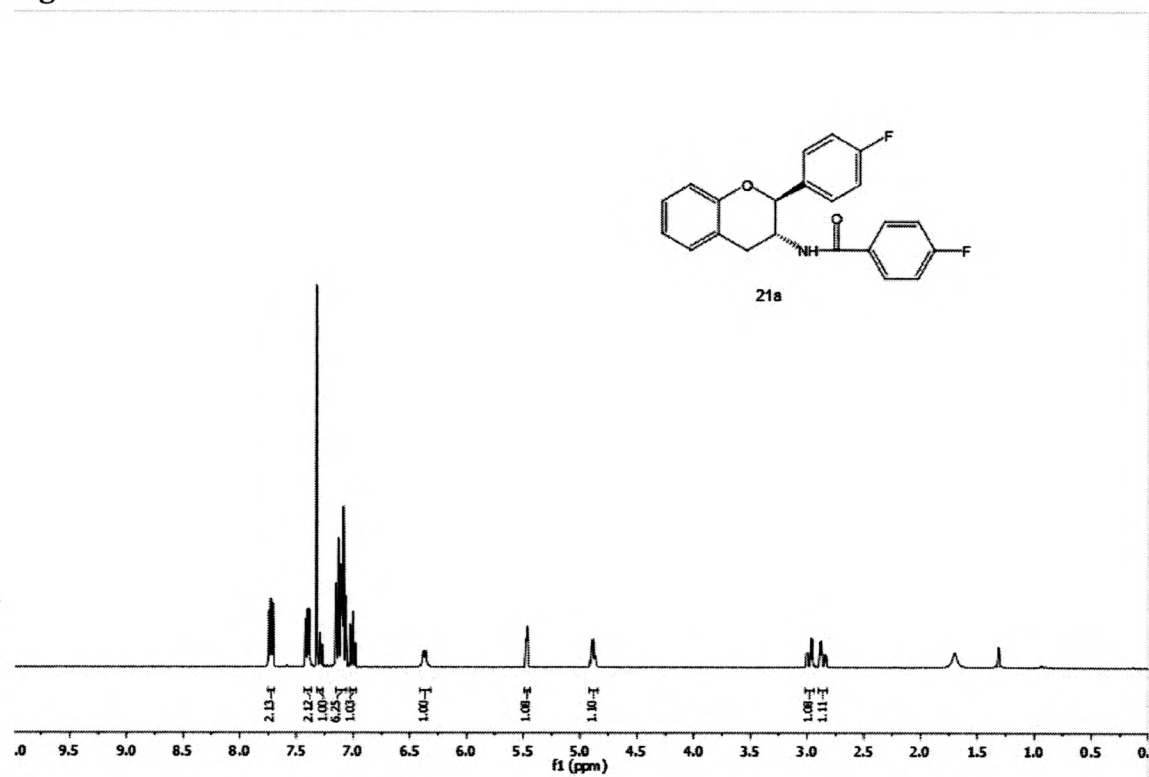


Figure 26: ^{13}C NMR of **21a**

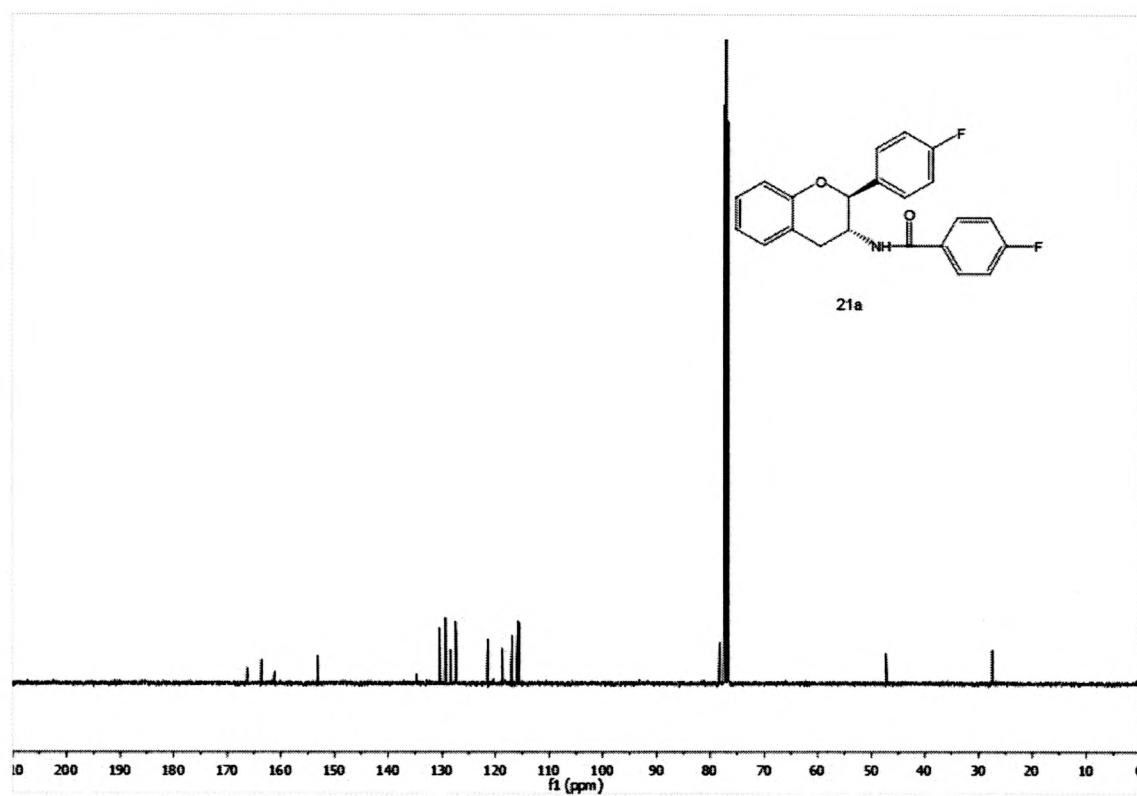


Figure 27: ^1H NMR of **21b** (in Acetone- d_6)

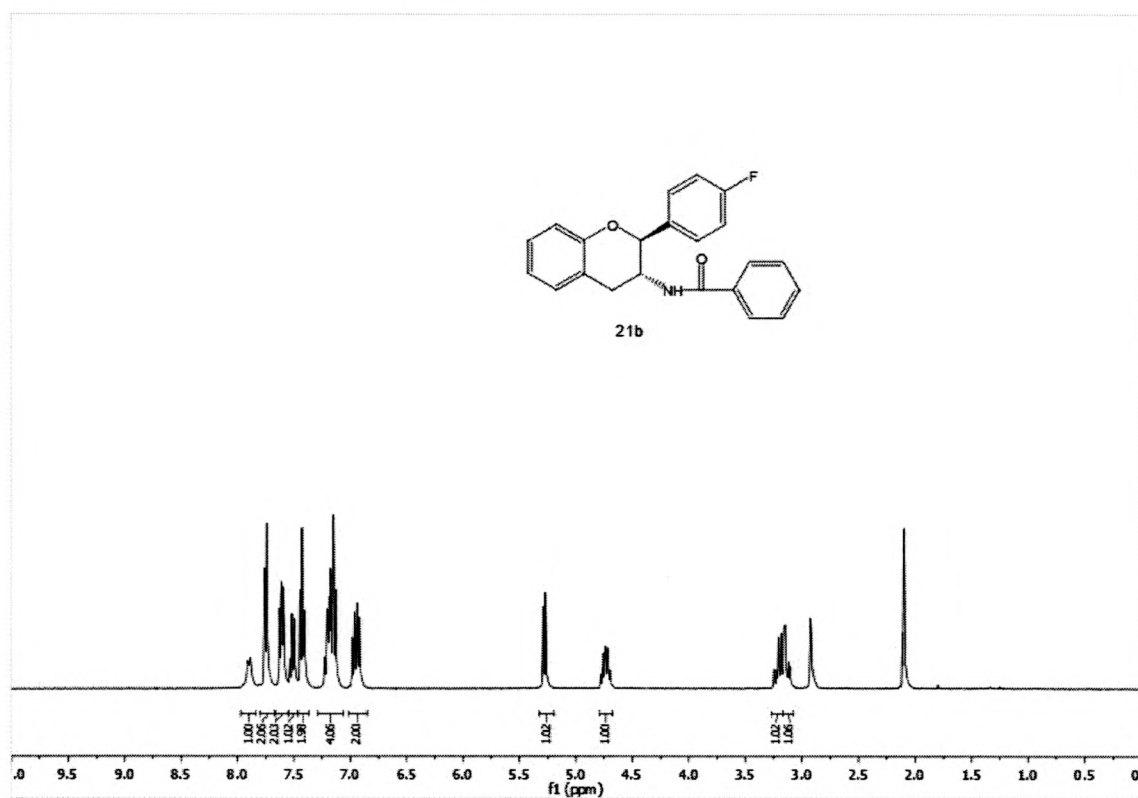


Figure 28: ^{13}C NMR of **21b** (in Acetone- d_6)

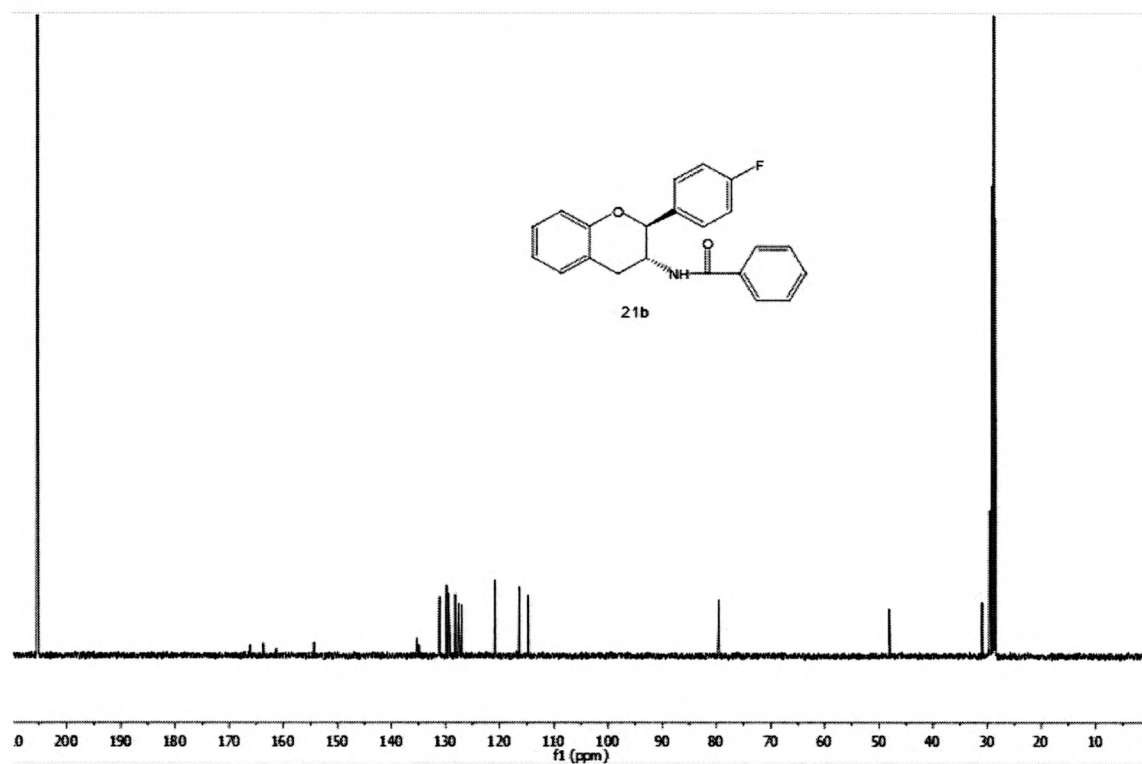


Figure 29: ^1H NMR of **21c**

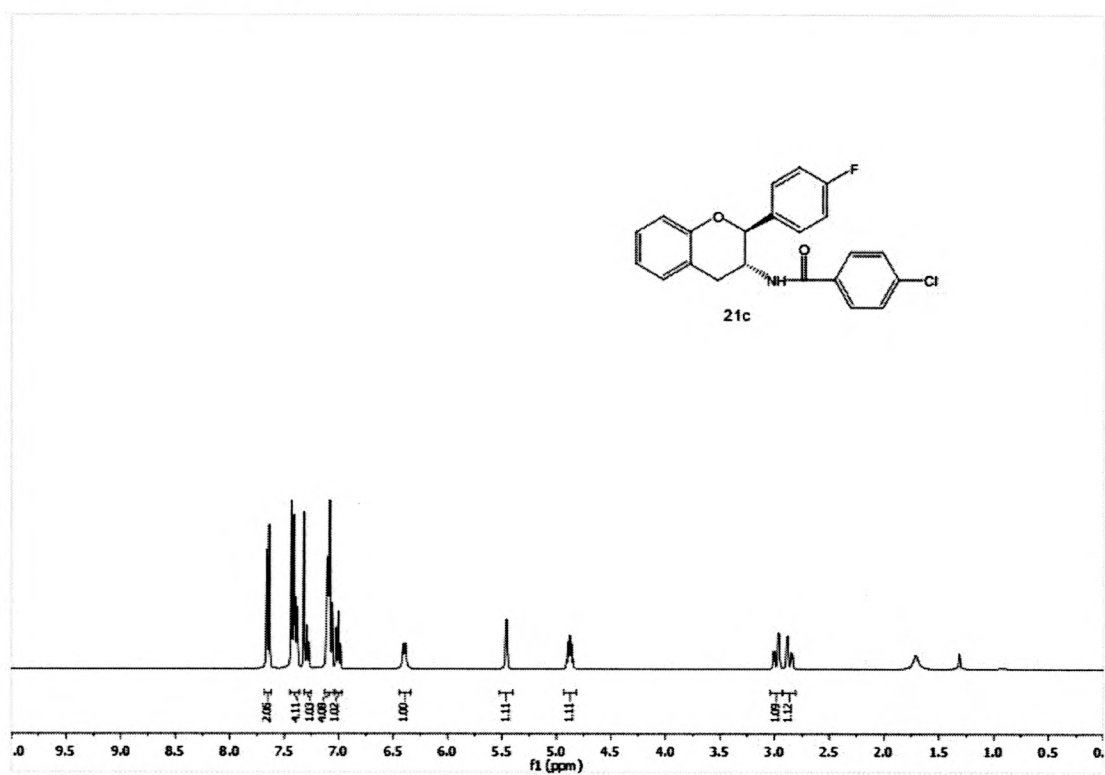


Figure 30: ^{13}C NMR of **21c**

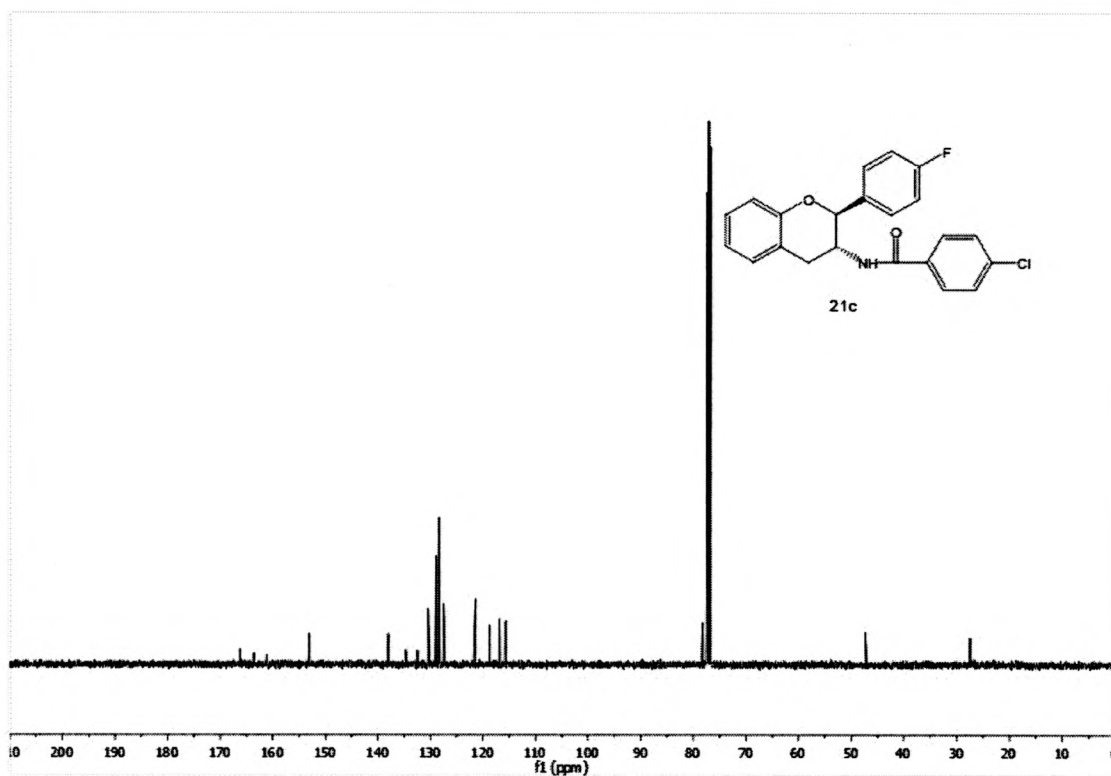


Figure 31: ^1H NMR of **21d**

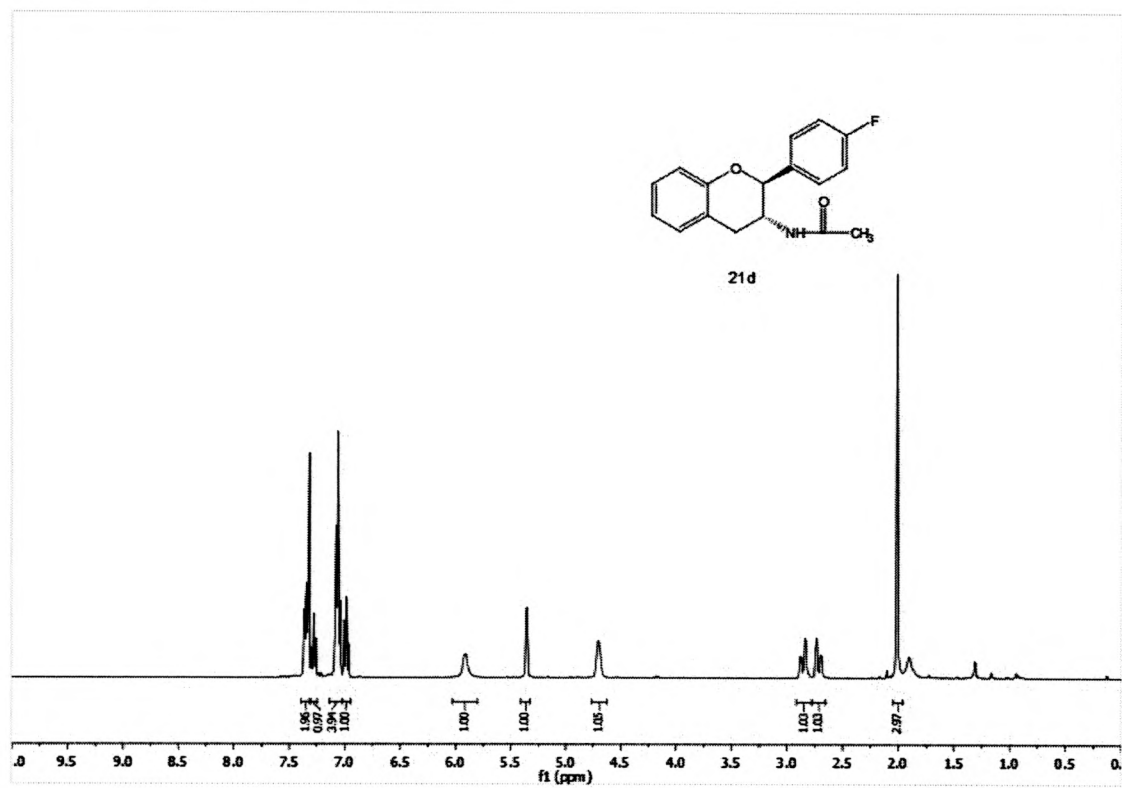


Figure 32: ^{13}C NMR of **21d**

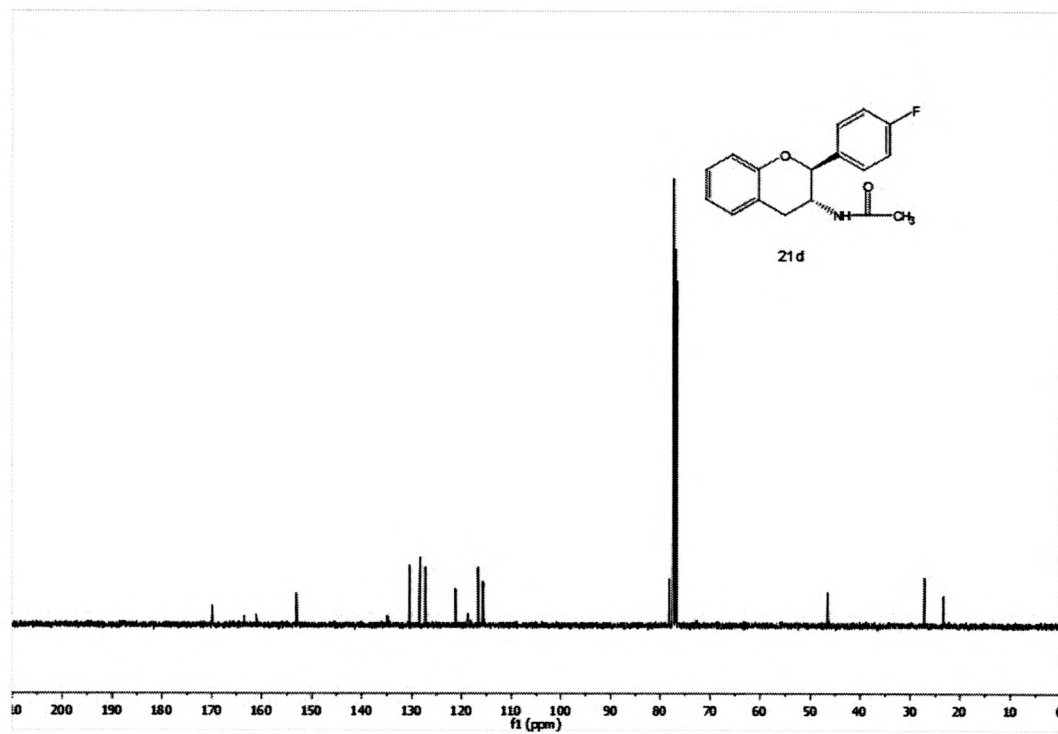


Figure 33: ^1H NMR of **21e**

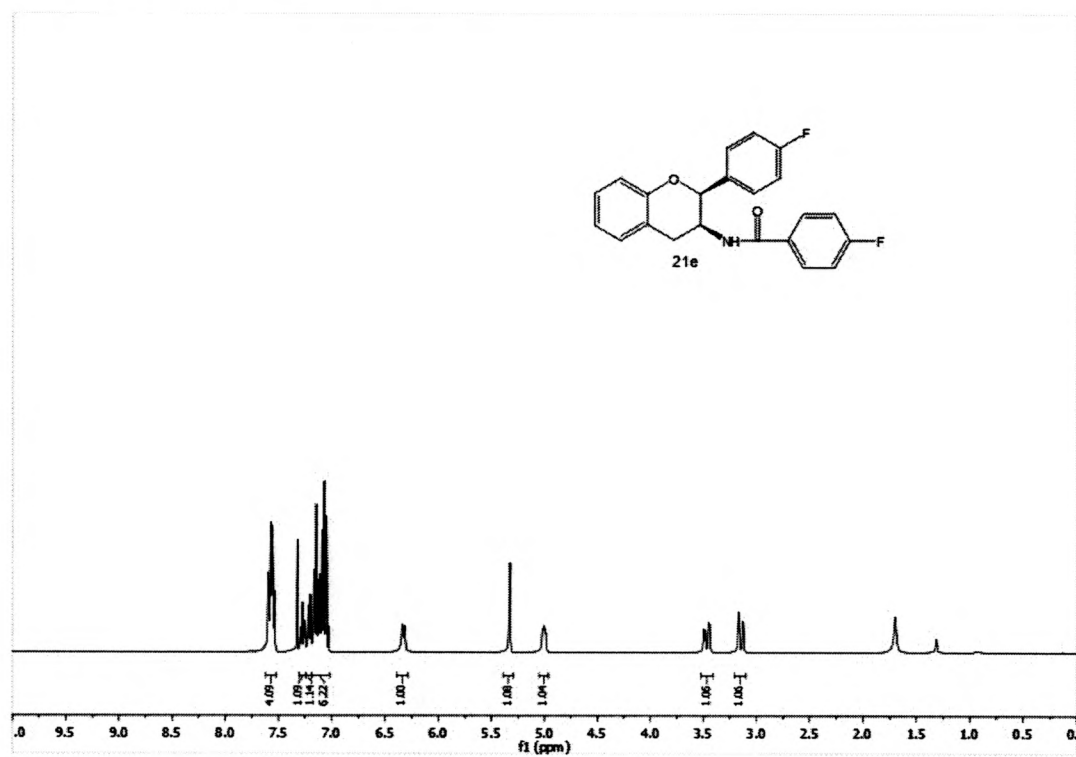


Figure 34: ^{13}C NMR of **21e**

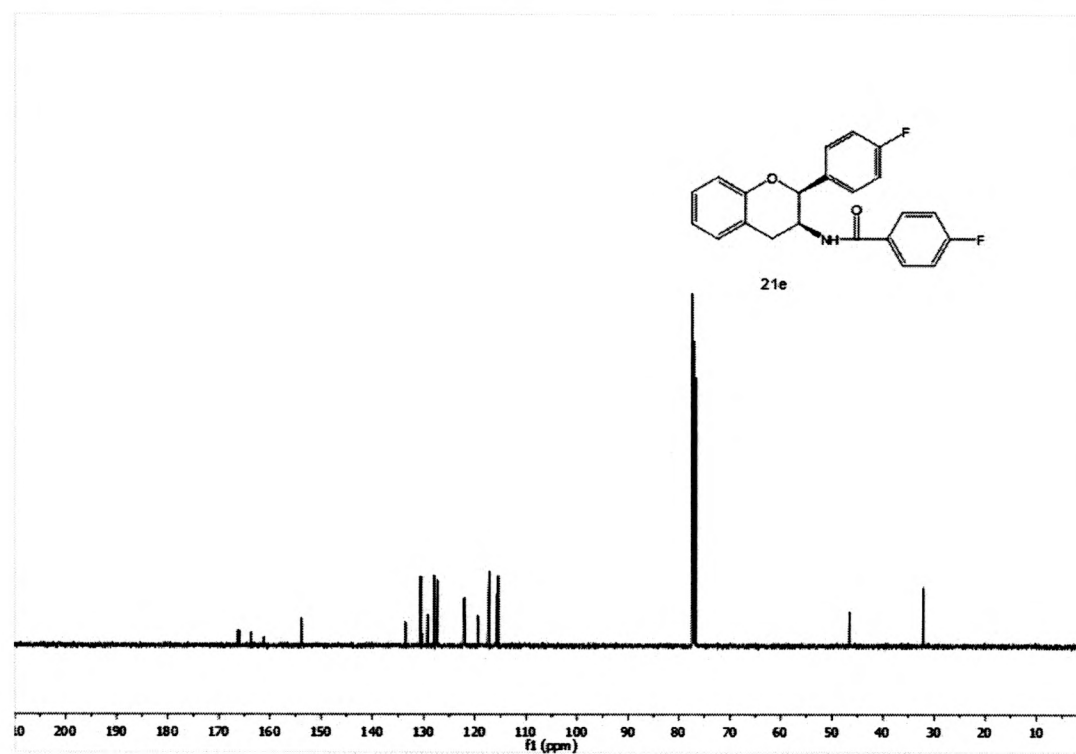


Figure 35: ^1H NMR of **21f**

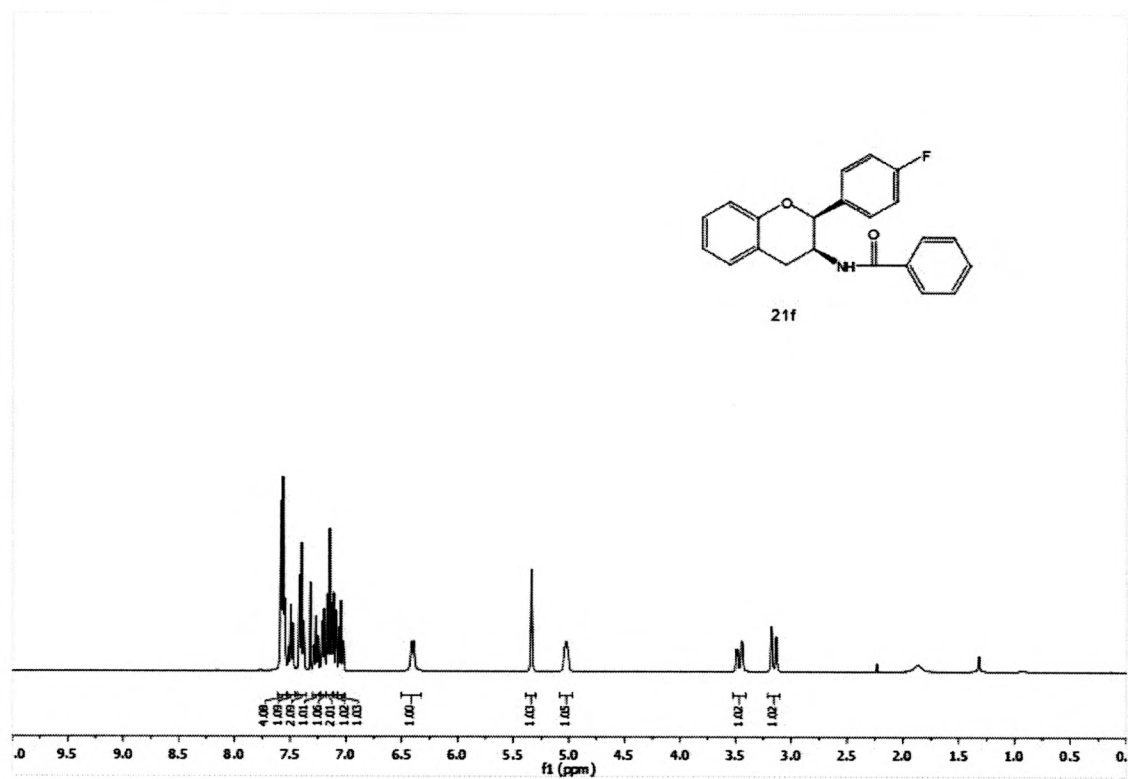


Figure 36: ^{13}C NMR of **21f**

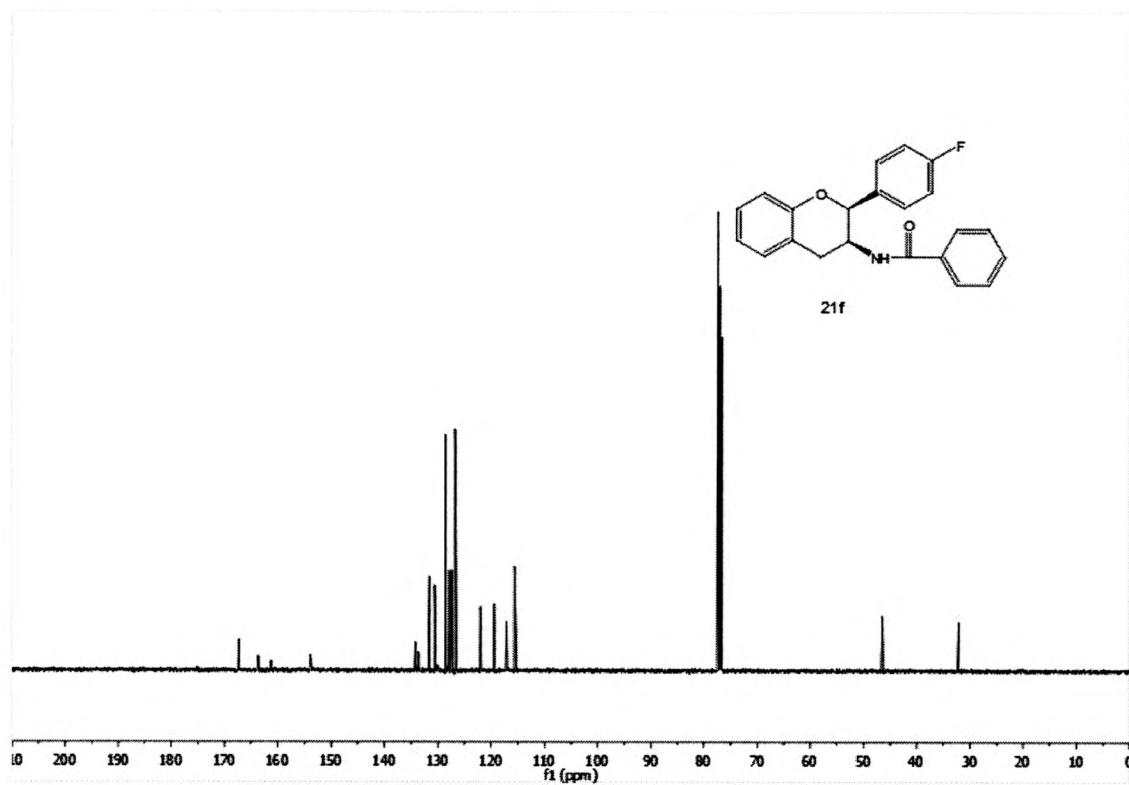


Figure 39: ^1H NMR of **21h**

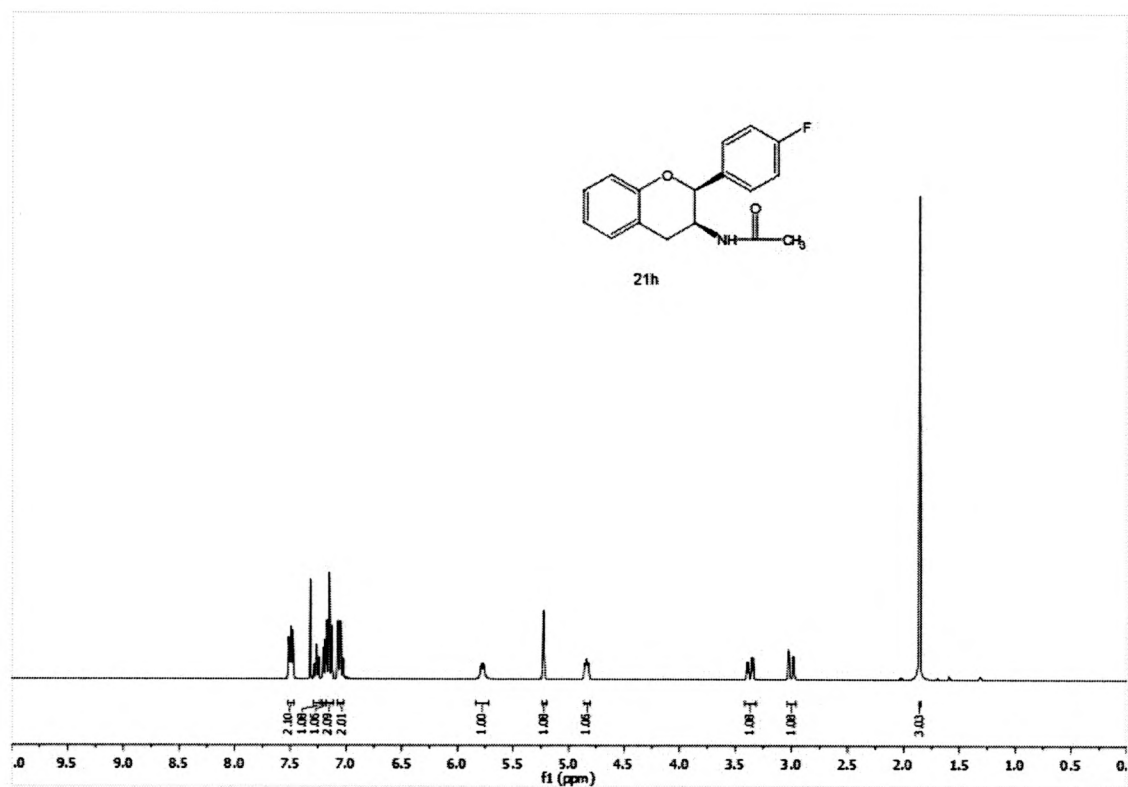


Figure 40: ^{13}C NMR of **21h**

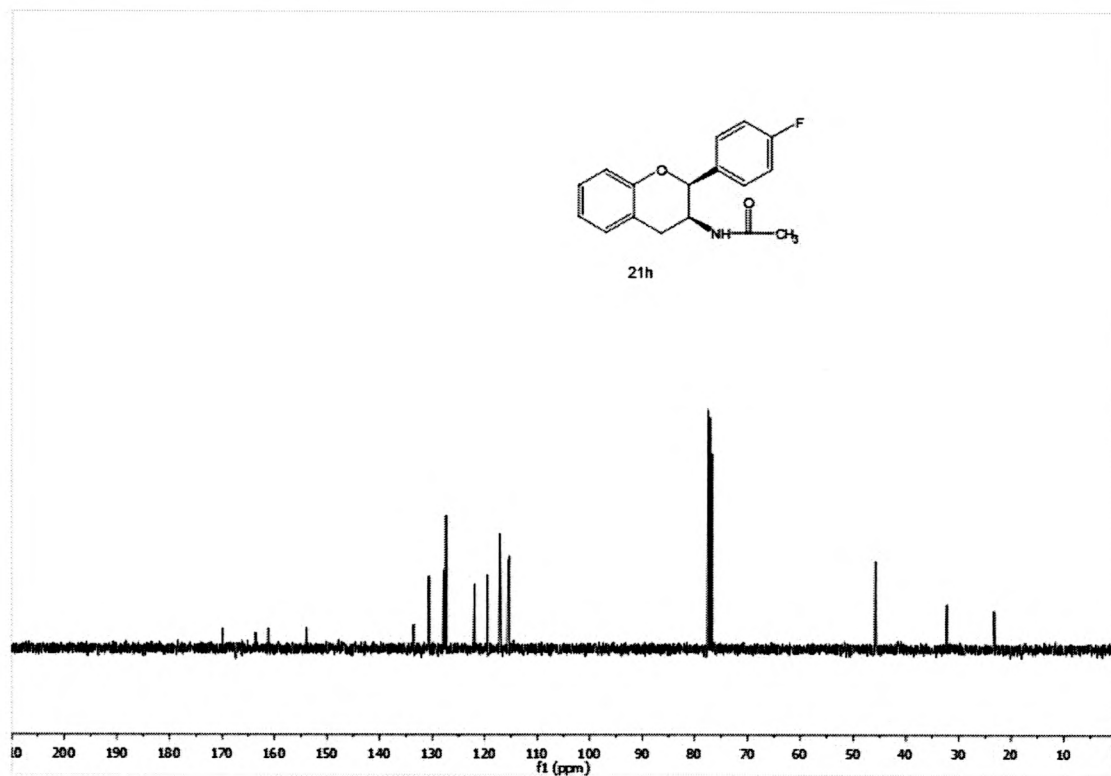


Figure 41: ^1H NMR of **22a**

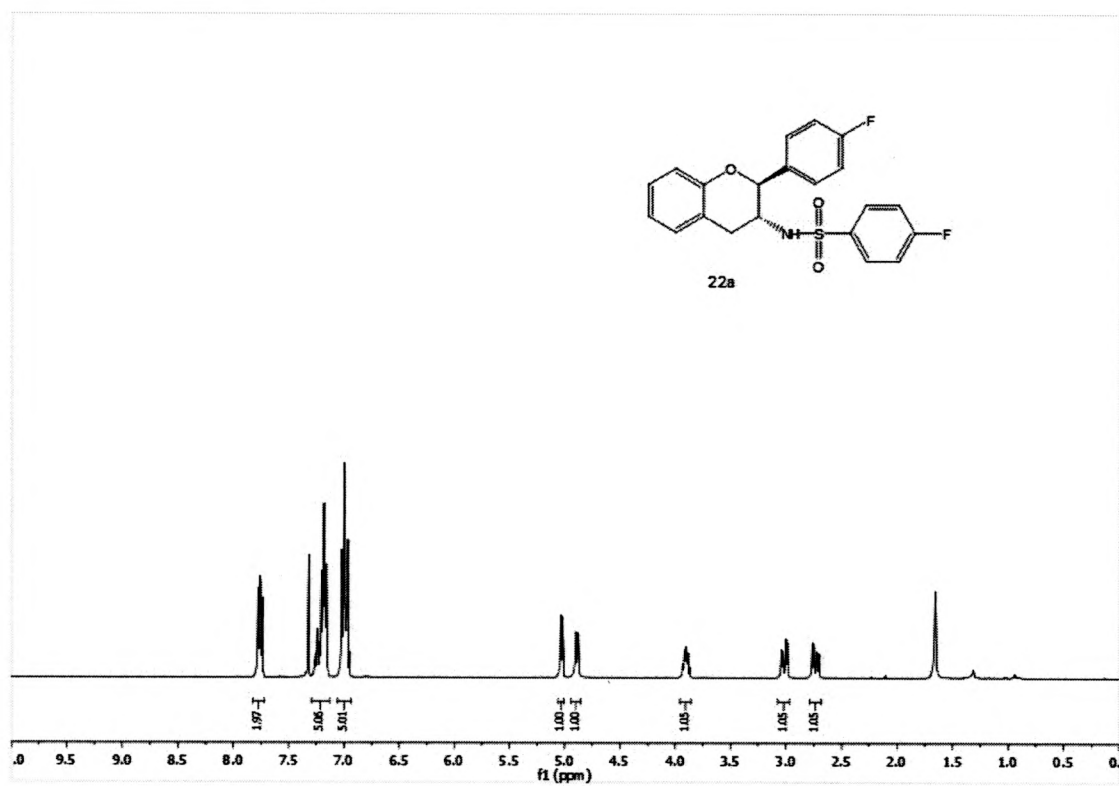


Figure 42: ^{13}C NMR of **22a**

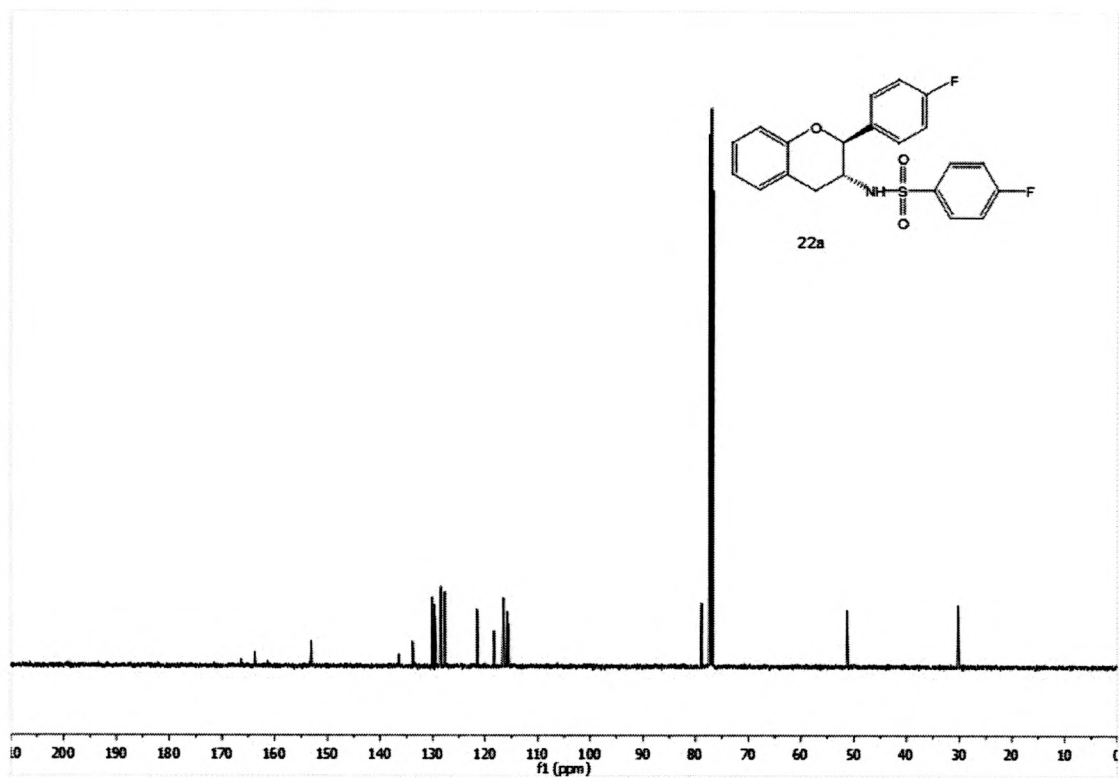


Figure 43: ^1H NMR of **22b**

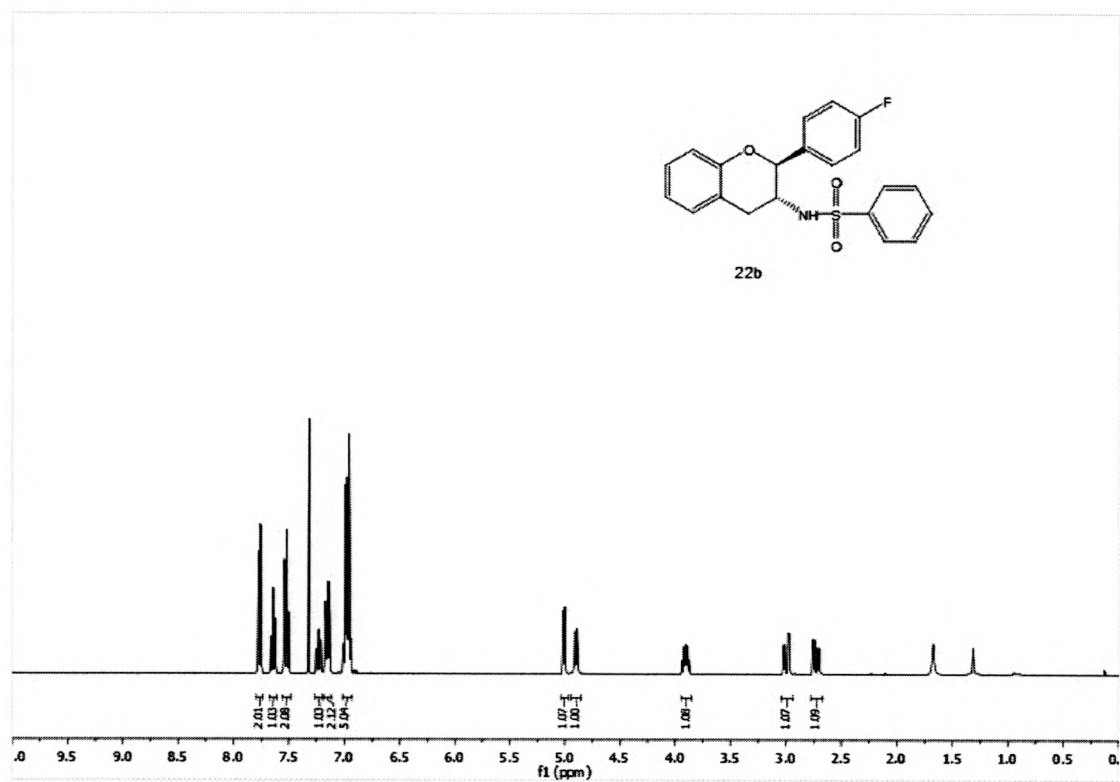


Figure 44: ^{13}C NMR of **22b**

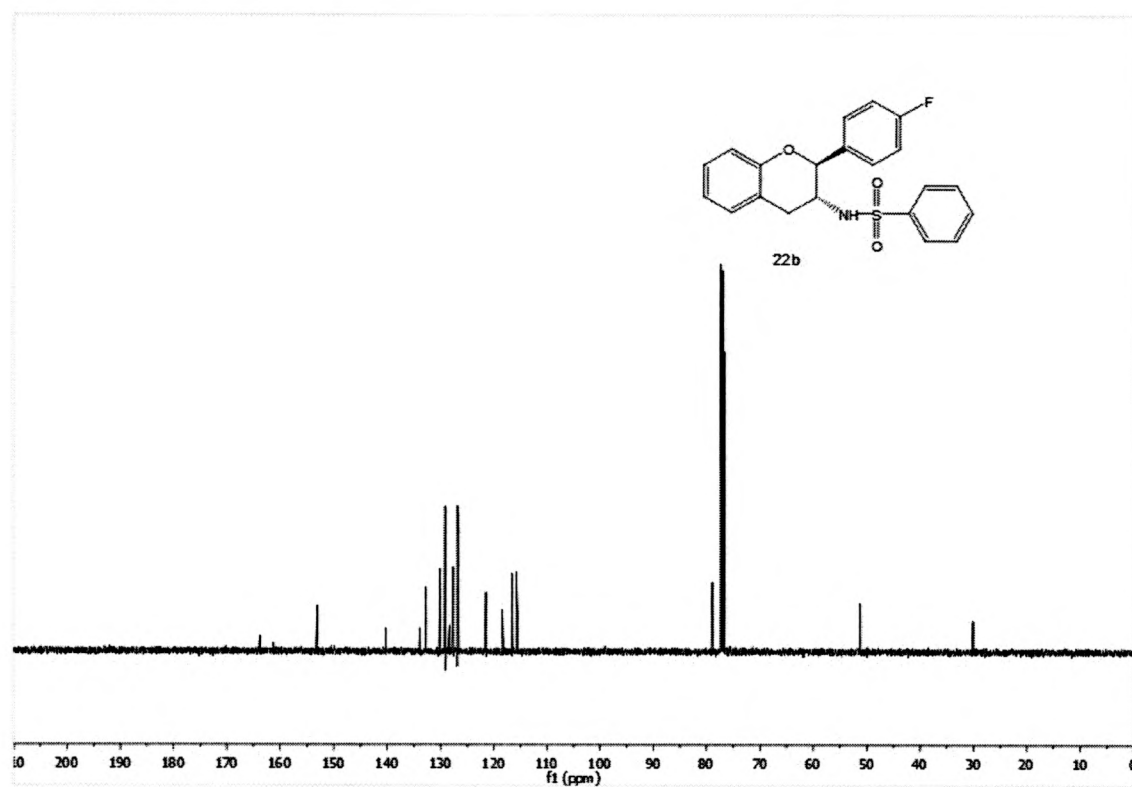


Figure 45: ^1H NMR of **22c**

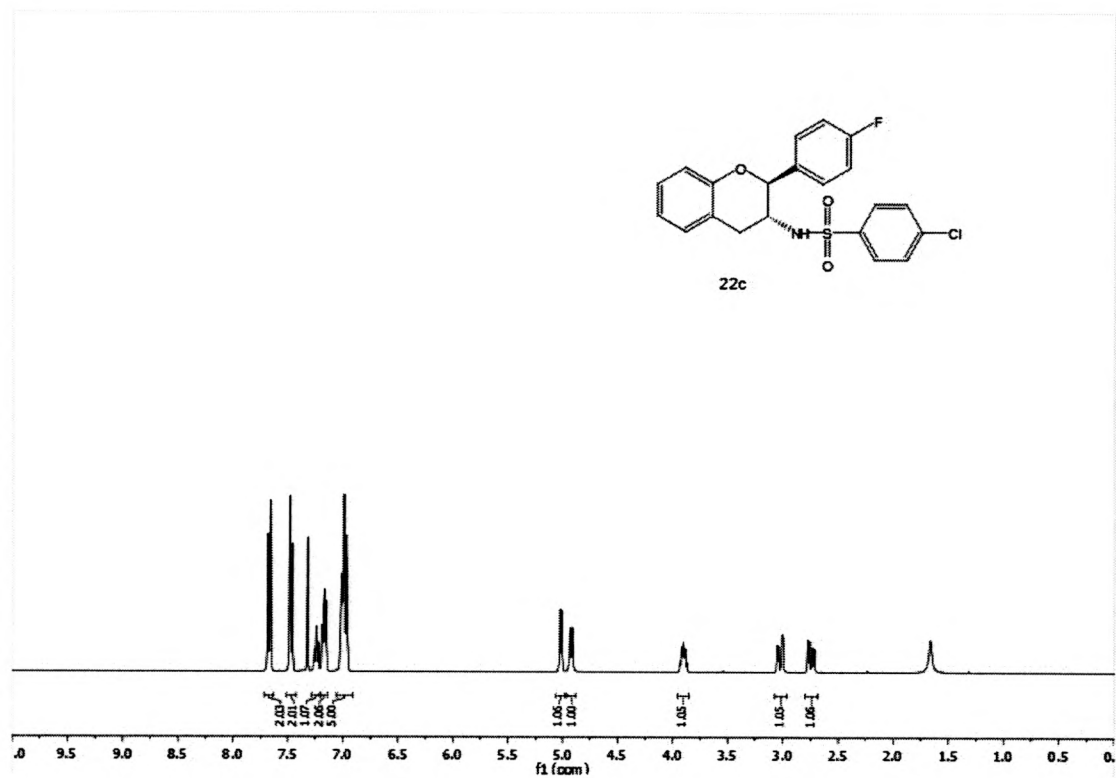


Figure 46: ^{13}C NMR of **22c**

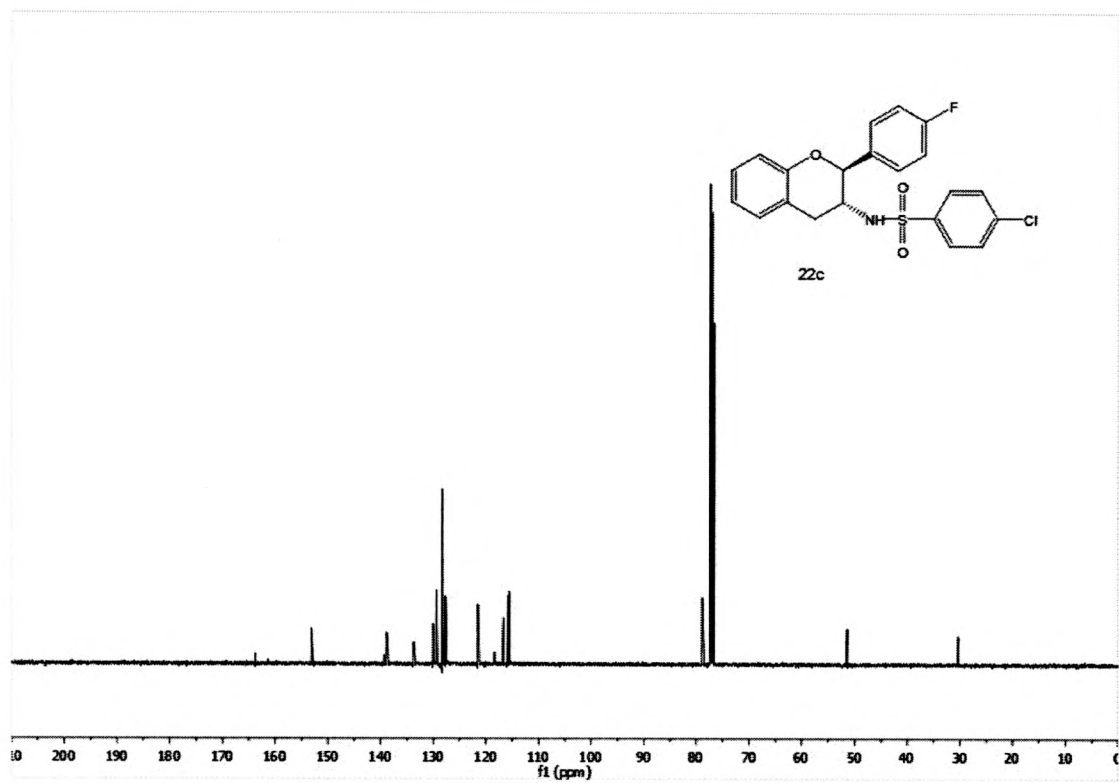


Figure 47: ^1H NMR of **22d**

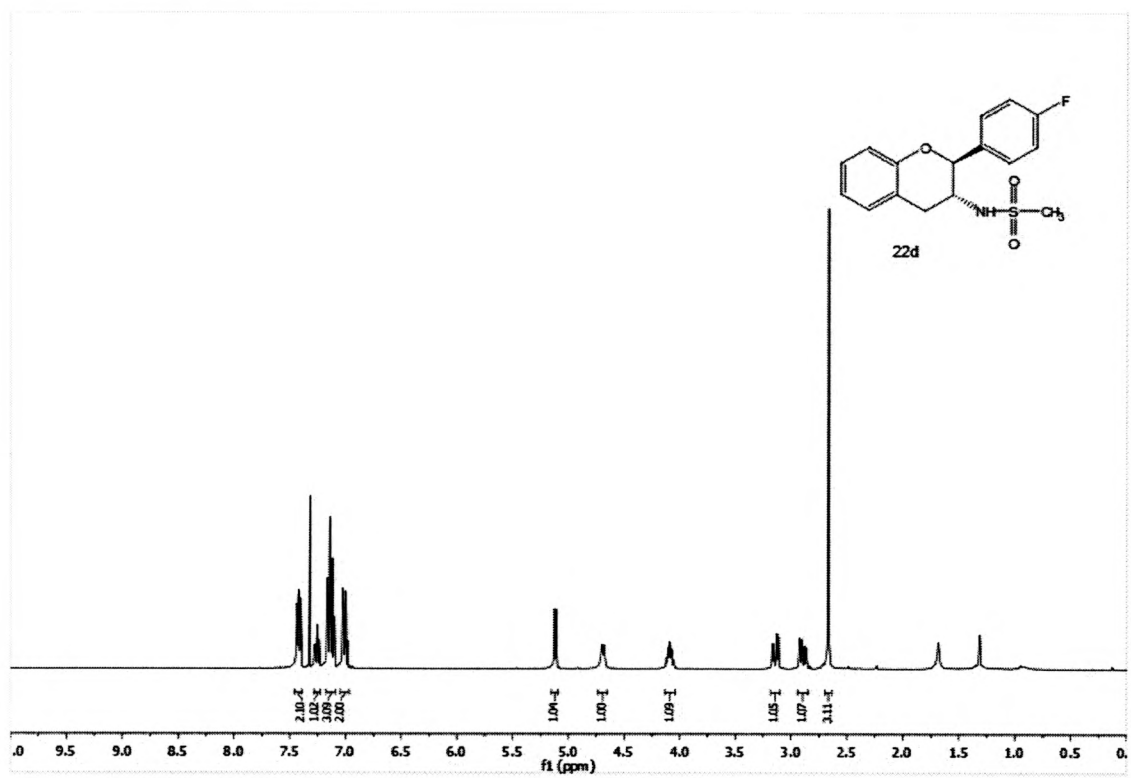


Figure 48: ^{13}C NMR of **22d**

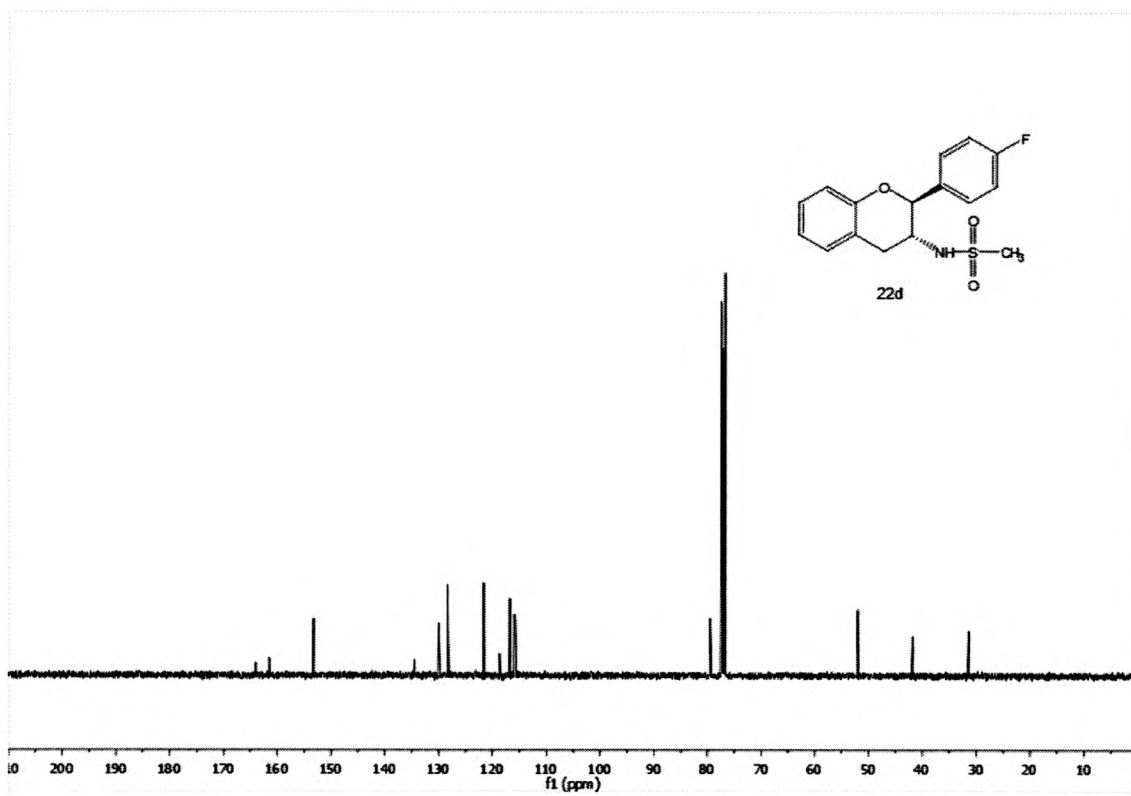


Figure 49: ^1H NMR of **22e**

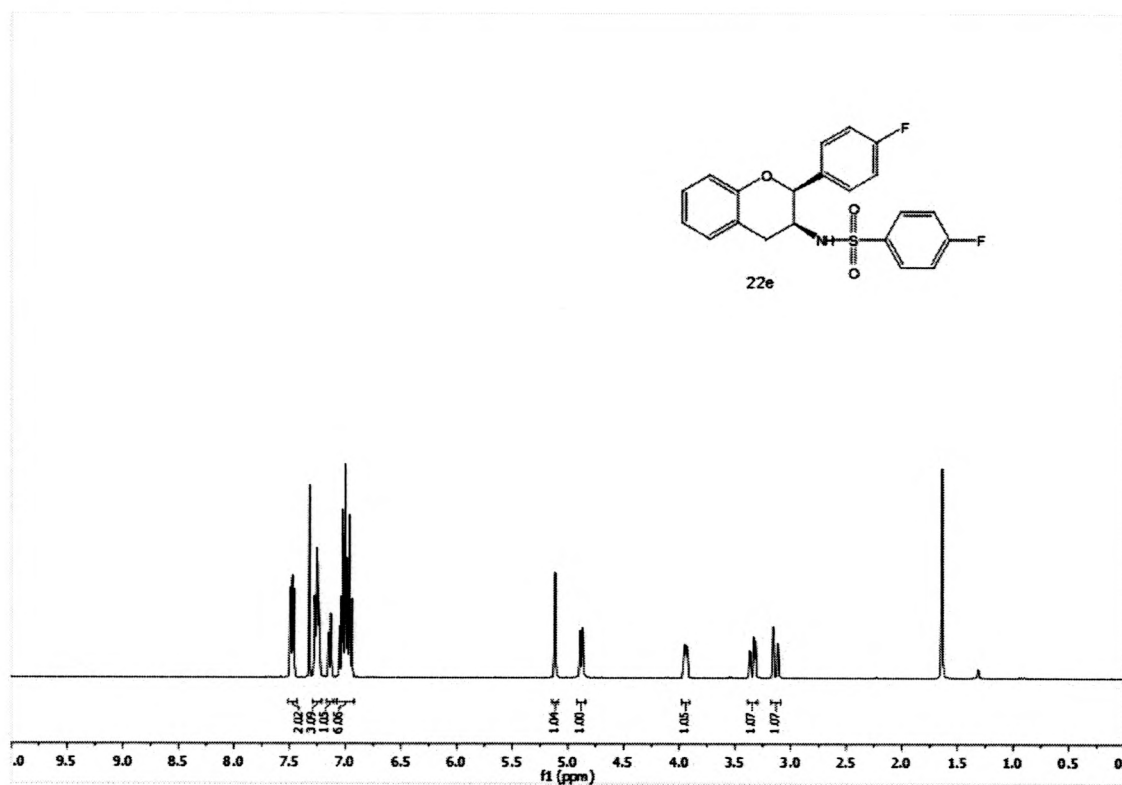


Figure 50: ^{13}C NMR of **22e**

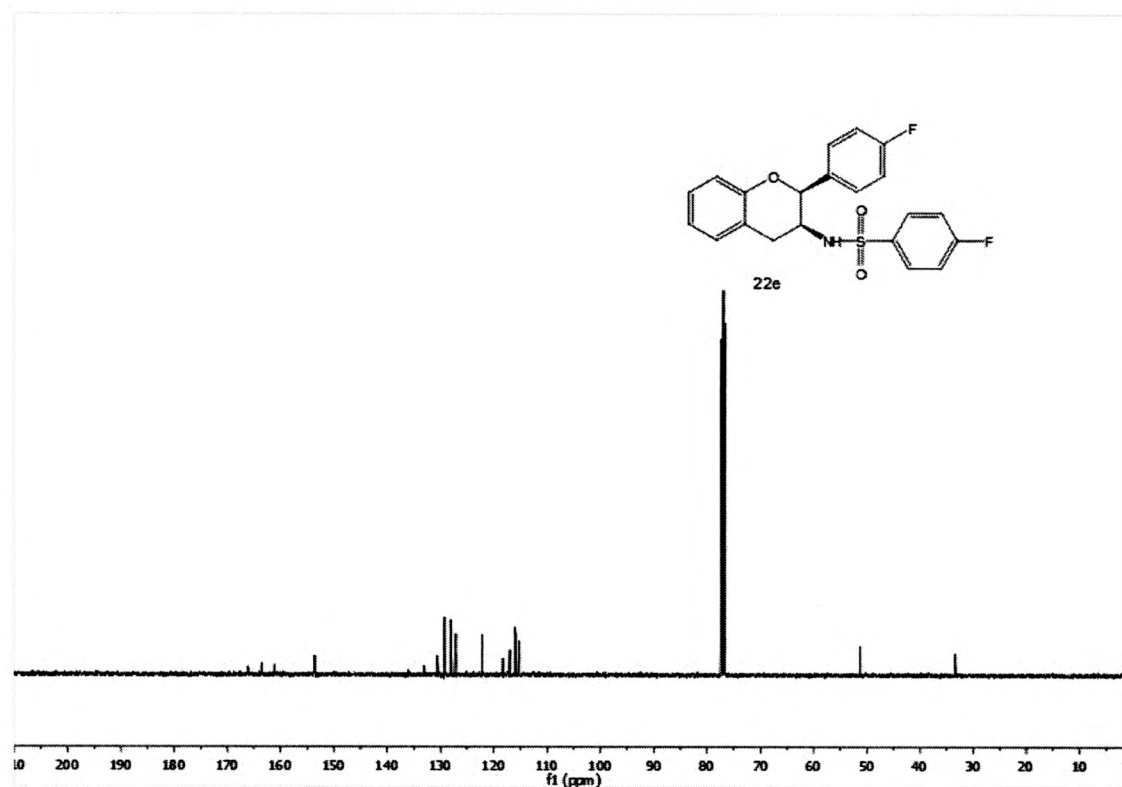


Figure 51: ^1H NMR of **22f**

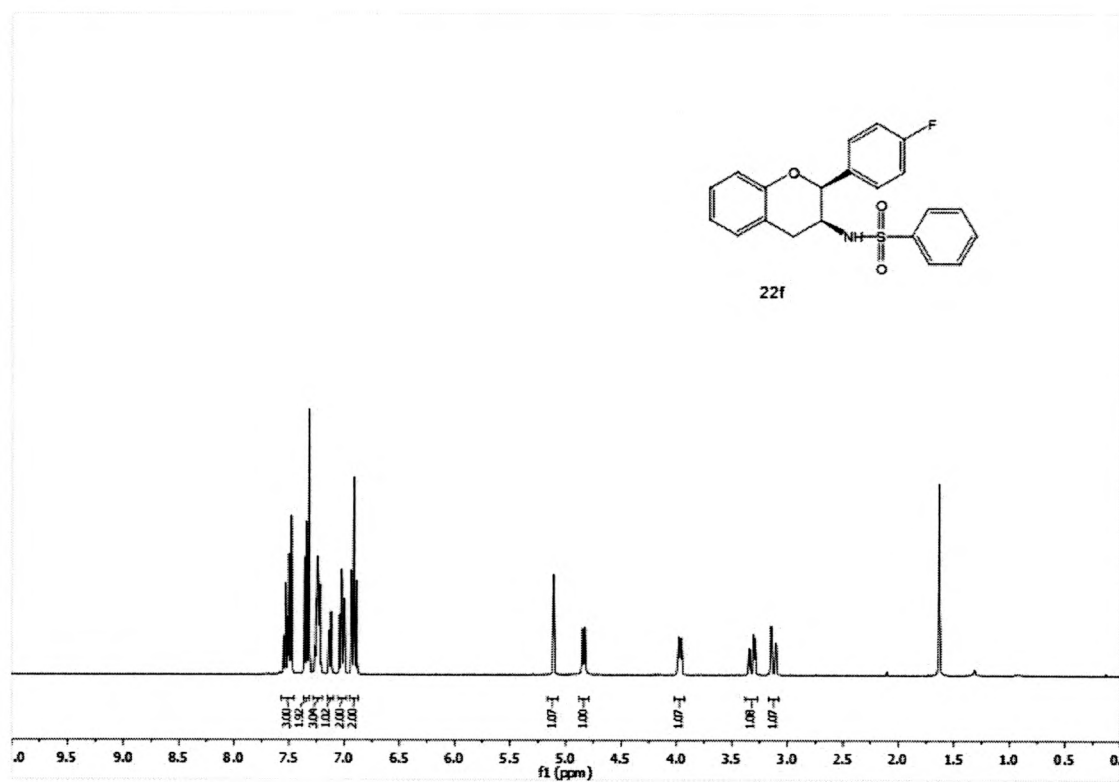


Figure 52: ^{13}C NMR of **22f**

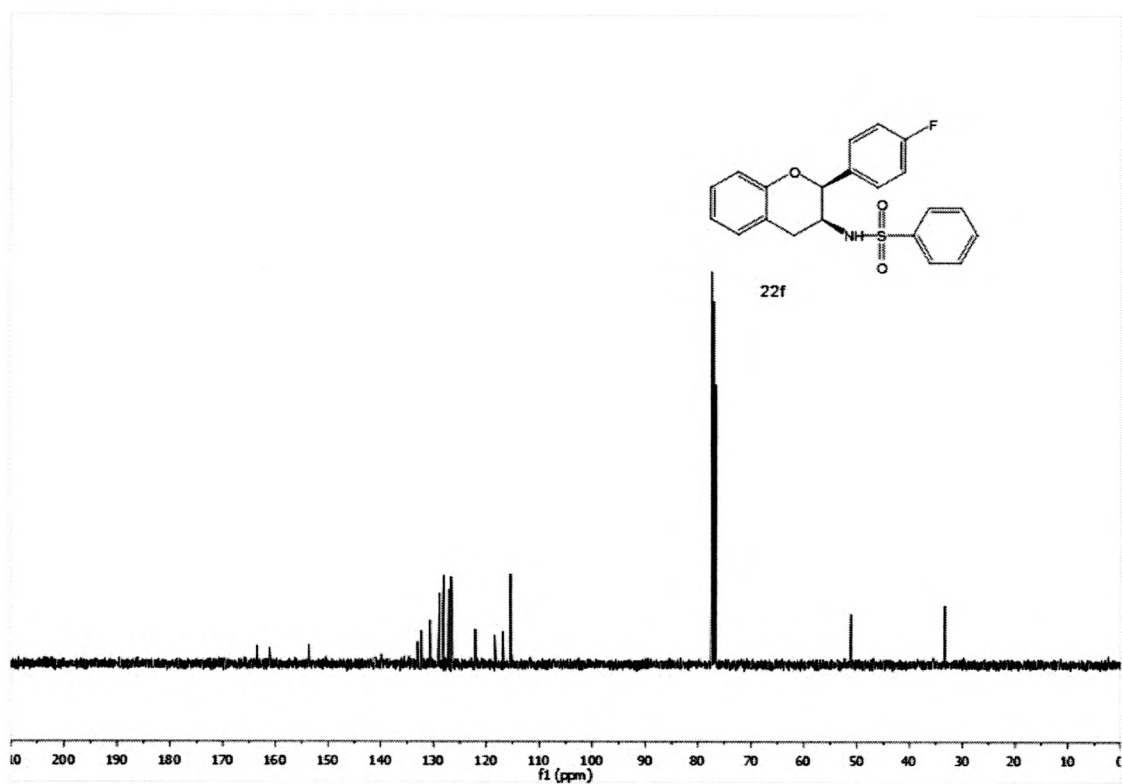


Figure 53: ^1H NMR of **22g**

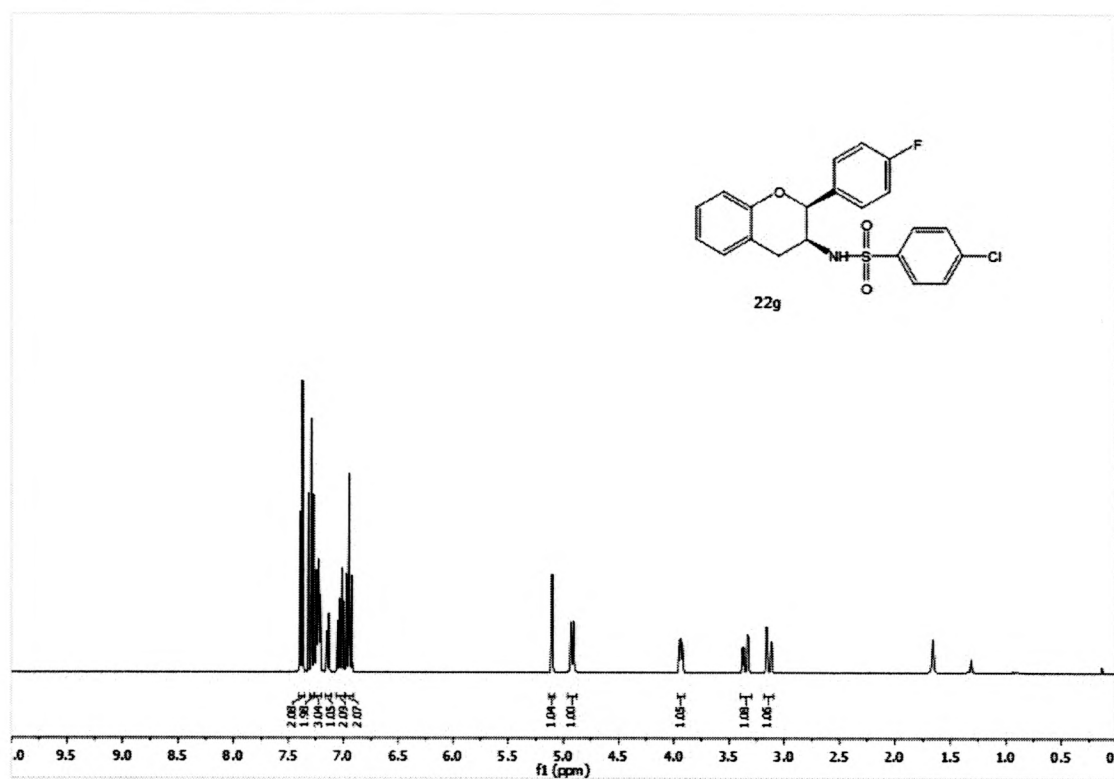


Figure 54: ^{13}C NMR of **22g**

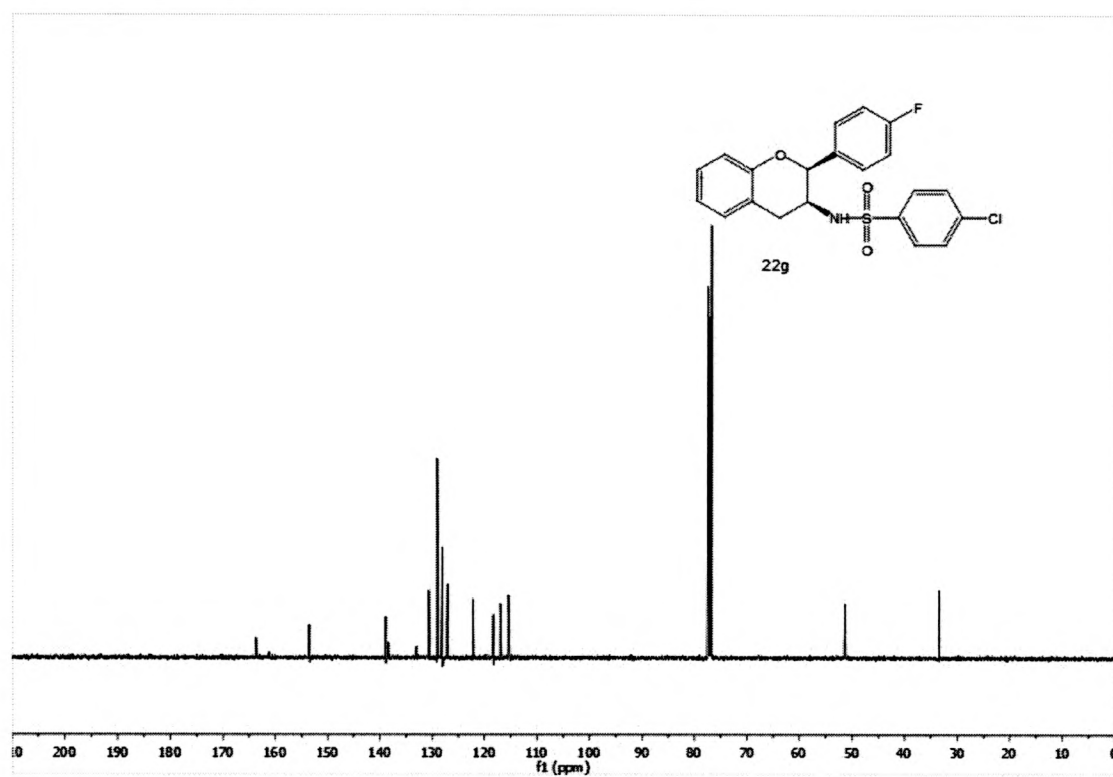


Figure 55: ^1H NMR of **22h**

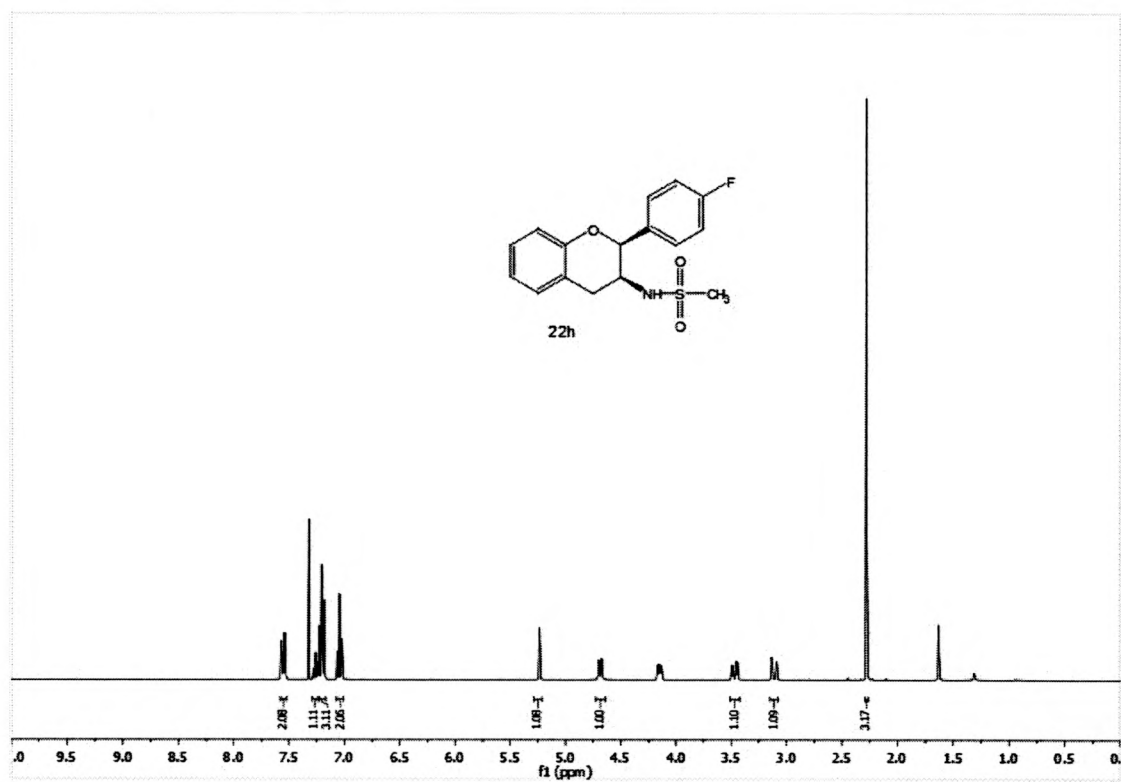


Figure 56: ^{13}C NMR of **22h**

